CELLULAR RESPONSES TO INORGANIC PHOSPHATE IN PHYSIOLOGICAL AND PATHOLOGICAL PROCESSES

APPROVED BY SUPERVISORY COMMITTEE

Orson Moe, M.D.

Makoto Kuro-o, M.D., Ph.D.

Thomas Carroll, Ph.D.

Chou-Long Huang, M.D., Ph.D.

DEDICATION

To my parents,

Charles and Rhonda

CELLULAR RESPONSES TO INORGANIC PHOSPHATE IN PHYSIOLOGICAL AND PATHOLOGICAL PROCESSES

by

JOEL SCHWARTZ-MORETTI

DISSERTATION

Presented to the Faculty of the Graduate School of Biomedical Sciences

The University of Texas Southwestern Medical Center at Dallas

In Partial Fulfillment of the Requirements

For the Degree of

DOCTOR OF PHILOSOPHY

The University of Texas Southwestern Medical Center at Dallas

Dallas, Texas

May, 2013

Acknowledgements

I would like to thank all the members of the Kuro-o Laboratory, past and present. Particular thanks are owed to: Lei Wang, who gave me my first introduction to many of the molecular biology techniques used in the research presented here; my fellow graduate student Addie Dickson, who gave advice and walked this road before me; and to Kazuhiro Shiizaki, who contributed experimental data presented in Chapter 5. I thank my mentor, Makoto Kuro-o, who always thoughtfully considered our opinions and gave us extraordinary freedom to pursue our hypotheses. I also thank the members of my dissertation committee for their oversight and guidance.

CELLULAR RESPONSES TO INORGANIC PHOSPHATE IN PHYSIOLOGICAL AND PATHOLOGICAL PROCESSES

Joel Schwartz-Moretti, Ph.D.

The University of Texas Southwestern Medical Center at Dallas, 2013

Supervising Professor: Makoto Kuro-o, M.D., Ph.D.

Phosphate is an essential chemical component of all known living organisms and is present in a variety of biological molecules such as nucleic acids and phospholipids. In vertebrates, phosphate is one of the primary ionic constituents of bone mineral. Phosphate homeostasis is maintained by a balance of absorption in the intestine, storage in pools such as bone and soft tissue, and excretion in the kidney. The flow of phosphate through these sites is controlled by several interacting hormone systems, including parathyroid hormone, vitamin D and the recently discovered endocrine hormone fibroblast growth factor 23.

Loss of appropriate control of phosphate homeostasis can result in structural defects in bone if phosphate supply is inadequate, or can lead to mineralization of soft tissues if phosphate is present in excess. In human diseases or animal models characterized by impaired function of fibroblast growth factor 23 or its co-receptor Klotho, phosphate is not sufficiently eliminated by the kidney and excess phosphate accumulates. This results in ectopic mineralization in soft tissues and a variety of other pathological consequences, ultimately increasing risk of death.

Previous research in the areas of osteoblast development and pathological mineralization in vascular tissue has indicated that excess extracellular phosphate causes changes in cellular behavior. We performed a series of experiments to examine in detail what effects excessive extracellular phosphate might have both on individual cells and on the organism as a whole. We found that treatment with elevated extracellular phosphate caused acute activation of cellular signaling pathways and induced expression of the mineral binding protein osteopontin in osteoblasts and fibroblasts. We found evidence that these responses are likely not the result of interaction of cells with phosphate *per se* but with calcium phosphate precipitates that form in the experimental conditions used. We found that diets containing higher than normal phosphate had adverse effects on mice, such as weight loss and kidney fibrosis. There is accumulating clinical evidence that such insoluble calcium phosphate particles arise in conditions of phosphate excess such as chronic kidney disease. Greater understanding of the formation and clearance of such particles may aid in the management of pathologies caused by phosphate excess.

Table of Contents

List of Figures

List of Abbreviations

α-SMA	smooth muscle actin-α
ATP	adenosine triphosphate
bFGF	basic fibroblast growth factor
CA	citric acid
cAMP	cyclic adenosine monophosphate
CaSR	calcium-sensing receptor
cDNA	complementary DNA
CKD	chronic kidney disease
CPP	calciprotein particle
CREB	cyclic-AMP response element binding protein
DMEM	Dulbecco's modified Eagle's medium
DNA	deoxyribonucleic acid
EDTA	ethylenediaminetetraacetic acid
ERK1/2	extracellular signal-regulated kinase
FBS	fetal bovine serum
FCS	fetal calf serum
FGF	fibroblast growth factor
FGF23	fibroblast growth factor 23
FGFR	fibroblast growth factor receptor
FRS2α	FGF receptor substrate 2 α
Gd^{3+}	gadolinium ion
HUVEC	human vascular endothelial cell
IP_6	inositol hexakisphosphate
IP_7	inositol heptakisphosphate
JNK	c-Jun N-terminal kinase

KDIGO	Kidney Disease: Improving Global Outcomes
kD	kilodalton
KO	knock-out
KP_i	potassium phosphate
MAPK	mitogen-activated protein kinase
MCP-1	monocyte chemotactic protein-1
MGP	matrix GLA protein
Na^+	sodium ion
NAC	N-acetylcysteine
NaP_i	sodium phosphate
Npt2	type II Na^+-dependent cotransporter
NT	no treatment
OPN	osteopontin
P_i	inorganic phosphate
PFA	phosphonoformic acid
PP_i	inorganic pyrophosphate
PTH	parathyroid hormone
RNA	ribonucleic acid
ROS	reactive oxygen species
RTK	receptor tyrosine kinase
RT-PCR	revers transcription- polymerase chain reaction
SDS-PAGE	sodium dodecyl sulfate-polyacrylamide gel electrophoresis
TBS	tris-buffered saline
TGF-β1	transforming growth factor β1

CHAPTER ONE

Introduction

1.1 The Biological Roles of Phosphate and Challenges of Vertebrate Phosphate Homeostasis

Phosphorus is considered one of the six chemical elements essential for the functions of all known organisms, along with hydrogen, carbon, nitrogen, oxygen and sulfur. Elemental phosphorus is highly reactive in an oxidizing environment, and consequently phosphorus is most commonly found in organisms in the form of the phosphate ion (PO_4^{3-}). In the pH range of the extracellular environment maintained by multicellular organisms, phosphate exists as a polyprotic acid ($H_2PO_4^{1-}$ and HPO_4^{2-}), a characteristic that enables phosphate to serve as a pH buffer in biological systems. Phosphate is a component of many essential and ubiquitous biological molecules such as individual nucleotides, DNA and RNA molecules, phospholipids and small organic metabolites containing phosphate esters. As a post-translational modification of proteins, phosphate can transmit or store information in cell signaling processes, or can affect protein structure (Nelson and Cox, 2008). In vertebrates, calcium and phosphate are principal ionic components of bone and polyphosphate molecules are mediators of inflammation and platelet aggregation (Müller et al., 2009). The essentiality of phosphate was recently challenged by a report presenting evidence that a bacterium

isolated from an arsenate-rich lake could survive and proliferate in the absence of phosphate by substituting arsenate for phosphate in biological molecules (Wolfe-Simon et al., 2011). This finding prompted a wave of critical examination, and two subsequent contrary reports appear to have restored, for now, phosphate's status as an essential chemical component of life (Erb et al., 2012; Reaves et al., 2012).

For unicellular organisms that cannot control the composition of their extracellular environment, a phosphate-sensing system enables them to mount responses to fluctuations in the availability of phosphate. In bacteria, a phosphate importing complex at the cell surface regulates a membrane-bound kinase, which in turn activates a transcription factor that controls the expression of phosphate-sensitive genes (nearly 400 genes in *E. coli*) to conserve phosphate when it is scarce. Extracellular phosphate is first recognized and bound by the PstS protein on the cell surface; then it is passed into the cell through the PstA and PstC proteins, which bear some similarity to mammalian ATP-binding cassette proteins. An open channel conformation, which indicates phosphate transport and therefore abundance, inhibits the nearby membrane-bound PhoR histidine kinase. When PhoR is active, it phosphorylates the PhoB transcription factor, activating it and initiating a program to conserve cellular phosphate (Hsieh and Wanner, 2010). In yeast, the unrelated Pho80-Pho85 cyclin/cyclin-dependent kinase (CDK) complex serves as a phosphate-sensitive regulator of genes involving phosphate utilization or transport. When phosphate is abundant, the kinase is active and phosphorylates the Pho4 transcription factor; phosphorylated Pho4 is retained in the cytosol and the phosphate conserving gene program is not activated. When phosphate is scarce, the concentration of the inositol pyrophosphate IP_7 rises due to increased activity of the IP_6 kinase Vip1.

IP_7 then forms an allosteric interaction with Pho80-Pho85 and Pho81, a CDK inhibitor that is constitutively bound to Pho80-Pho85, and inhibits kinase activity of the complex (Lee et al., 2007; Lee et al. 2008). Under these conditions, Pho4 is unphosphorylated and may enter the nucleus and activate the phosphate sensitive gene program. Of note, there is no ortholog of the bacterial phosphate-binding PstS protein in metazoans, and the phosphate sensing mechanism in yeast appears to be indirect, mediated by phosphate-sensitive production of IP_7. It remains unknown if there exists a direct phosphate sensing mechanism in mammals (Bergwitz and Jüppner, 2011).

In vertebrates, a complex hormonal system is responsible for maintaining appropriate mineral ion availability in the extracellular fluid and throughout the organism as a whole. This hormonal system coordinates the flux of phosphate through multiple organ systems and pools, enabling phosphate to be stored or released as needed when dietary phosphate intake varies. The vertebrate bones are the principal storage sites for calcium and phosphate, accounting for 99% and 85% of total body calcium and phosphate, respectively, in humans. These ions are stored in bone as solid-phase mineral, and as such only a small fraction of the total ions in bone can be released or deposited in bone by osteoblasts and osteoclasts (cells that carry out bone formation and resorption activities) over time, about 6 mg/kg total flux through bone per day for humans (Berndt and Kumar, 2007). The other major sites of phosphate flux are the intestine, extra-cellular fluid including blood serum, soft tissues and the kidneys. The intestine is the point of entry for dietary phosphate, but it remains unclear if this site plays a significant role in the *regulation* of phosphate homeostasis. This is because most (70%) of the dietary phosphate load, regardless of whether it is a small or large load, is absorbed in the

intestine via paracellular routes and through Na^+-dependent phosphate cotransporters (Sabbagh et al., 2009). Rather, day-to-day regulation of bodily phosphate flux is controlled by the balance of reabsorption and excretion in the kidney. Phosphate from blood is filtered into the kidney tubule lumen where it may be reabsorbed in a regulated fashion by type II Na^+-dependent phosphate cotransporters, particularly Npt2a (rodents) and Npt2c (humans) in the proximal tubules. The hormonal regulation of kidney phosphate reabsorption will be discussed below. Between these three entry and exit points (intestine, bone and kidney), phosphate is present in soft tissues in the form of biological molecules and in blood serum at a concentration of approximately 1 mM. In contrast to calcium, most of this blood phosphate exists as free ions; only about 12% is protein bound (Bringhurst et al., 2013).

The free ion concentrations of phosphate and calcium (approximately 1.2 mM) in serum pose a potential inorganic chemical problem to vertebrates because these two ions are present in quantities that approach their combined solubility limit in solution. Incompletely understood mechanisms, likely involving serum proteins and adequate control of serum ion concentrations, ensure that precipitation of calcium and phosphate occurs only appropriate sites and not indiscriminately in soft tissues (see Chapter 2). Nevertheless, in situations of impaired mineral ion homeostasis, such pathological mineral deposition can occur (Moe and Sprague, 2012). Failure to maintain phosphate homeostasis can lead to a number of other pathological consequences, particularly affect bone morphology and function. Hypophosphatemic disorders can cause rickets in children and osteomalacia in adults, characterized by structural changes to bones, hypomineralization and bone weakness. Hyperphosphatemic disorders can also lead to

changes in bone structure, as well as an increased risk of soft tissue calcification (Farrow and White, 2010). The hormonal system managing phosphate homeostasis is critical to preventing these potential problems. However, primary defects within this hormonal system itself can also cause pathological consequences even when there is no shortfall in the availability of dietary phosphate.

1.2 Hormonal Control of Phosphate: Parathyroid Hormone

Calcium and phosphate are stored jointly in the form of bone mineral, and bone resorption inevitably results in the release of both of these ions. It is not surprising, therefore, that the hormonal regulation of calcium and phosphate is coordinated, and in several instances both are affected by the same hormone. The peptide hormone parathyroid hormone (PTH) exemplifies this concept: it functions to maintain serum calcium ion concentration within a narrow range, but also promotes excretion of phosphate in the kidney. The secretion of synthesized PTH from parathyroid glands is acutely controlled by the calcium-sensing receptor (CaSR), a G protein-coupled receptor expressed in parathyroid chief cells. The extracellular domain of the CaSR directly binds serum calcium and initiates cellular signaling to inhibit PTH secretion when serum calcium is at normal or higher than normal concentrations (Hofer and Brown, 2003). When serum calcium is low, the CaSR is not activated, PTH secretion increases and circulating PTH acts on target organs to raise and restore the serum calcium concentration. The amount of active circulating PTH is additionally controlled by several other mechanisms, including transcription of the PTH gene, increases in parathyroid cell number, and cleavage (inactivation) of PTH both before and after secretion (Bringhurst et al., 2013).

In the kidney, PTH acts principally on the distal tubules, where the reabsorption of the final remaining amount of calcium in the filtrate is fine-tuned. At these sites, PTH enhances transcellular transport of calcium ions by increasing the expression of the luminal calcium uptake channels, the intracellular calcium binding protein calbindin and the basolateral sodium calcium exchanger NCX1, which completes the transcellular transport process. PTH also affects kidney reabsorption of phosphate, most of which occurs in proximal tubules. PTH rapidly causes the endocytosis of luminal Npt2a and Npt2c phosphate transporters, inhibiting the reabsorption of phosphate and increasing the excretion of any excess phosphate. Finally, PTH also increases the synthesis of active vitamin D (calcitriol) in the kidney by increasing the expression of the enzyme that synthesizes it and decreasing the expression of another enzyme that metabolizes calcitriol.

PTH has complex effects on bone, where it can both increase and decrease rates of bone formation and resorption. Traditionally, the action of PTH on bone has been viewed as primarily catabolic, serving to increase resorption and release calcium and phosphate from bone. Osteoclasts do not express the receptor for PTH; rather, PTH affects osteoclast activity indirectly by first binding to receptors expressed on osteoblasts. PTH binding to osteoblasts increases the expression of paracrine factors, such as MCSF1 and RANKL, which act on osteoclast precursors to promote their maturation and also increase the resorption activity of mature osteoclasts (Bringhurst et al., 2013). These effects complement the action of PTH on other organs to restore serum calcium concentration if it is low.

More recently, the anabolic effects of PTH on bone have become more greatly appreciated. PTH binding to osteoblasts increases their bone formation activity as well as their proliferation. Additionally, PTH binds to osteoblast precursors and enhances their maturation and recruitment to bone surfaces. These net effects of PTH on bone, either resorption or formation, appears to be determined by the duration of PTH exposure. PTH causes increases in both of these activities, but if PTH exposure is chronic, bone resorption will dominate over time. In contrast, intermittent PTH exposure has a net anabolic effect over time, and intermittent PTH treatment has been used to manage osteoporosis (Aslan et al., 2012). With regard to phosphate, PTH has opposing effects in different organs: PTH can increase serum phosphate if bone resorption activity is increased, but it also enhances renal excretion of phosphate. If these two activities are balanced, there may be little net effect on serum phosphate concentration.

1.3 Hormonal Control of Phosphate: Vitamin D

Vitamin D is a cholesterol-derived hormone that also has roles in both calcium and phosphate homeostasis. The vitamin D precursor (7-dehydrocholesterol) in skin is cleaved upon exposure to ultraviolet radiation, yielding vitamin D_3 (cholecalciferol) after chemical rearrangements. Vitamin D_3 is then subject to a hydroxylation reaction in the liver by the 25-hydroxylase enzyme to yield calcidiol (25-hydroxyvitamin D_3). Calcidiol is further hydroxylated in the kidneys to produce 1,25-dihydroxyvitamin D_3 (calcitriol), the form of vitamin D that most potently activates vitamin D nuclear hormone receptors. This second hydroxylation step is highly regulated by controlling the expression of 1α-hydroxylase, the enzyme that catalyzes the reaction. Calcitriol synthesis is positively regulated by PTH and hypophosphatemia, and negatively regulated by calcium, calcitriol

and FGF23 (discussed below). Additionally, calcitriol can undergo a further hydroxylation by a 24-hydroxylase enzyme to yield an inactivated vitamin D derivative.

Calcitriol enhances the absorption of calcium in the intestine by multiple mechanisms. Expression of the calcium channels TRPV5 and TRPV6 on apical membranes is enhanced by calcitriol, as well as other proteins involved in transcellular calcium transport such as calbindin-D9K and the ATP-dependent calcium pump which completes the process. Calcitriol also enhances intestinal phosphate absorption, perhaps through increased expression of intestinal Npt2b (Sabbagh et al., 2009). In the kidney, calcitriol increases calcium reabsorption via transcellular transport, similar to PTH. In bone, calcitriol promotes both bone formation and remodeling, and deficiency in calcitriol results in bone morphological defects. Calcitriol stimulates osteoblasts to produce the extracellular molecules that are essential for subsequent formation of mineralized tissue as well as RANKL, the osteoclast differentiation factor. Calcitriol also enhances osteoclast differentiation and resorption activity directly. However, studies of mice lacking the ability to produce calcitriol (e.g. 1α-hydroxylase deficient mice) have demonstrated that bone defects caused by lack of calcitriol can be largely rescued by correcting abnormalities in serum calcium or phosphate concentration. Therefore, the ability of calcitriol to contribute to ion homeostasis is at least as important as its direct effects on cellular activity for ensuring proper bone mineralization (Bringhurst et al., 2013; Moe and Sprague, 2012).

1.4 Hormonal Control of Phosphate: FGF23, a Novel Phosphaturic Hormone

The distinctive features of the paraneoplastic disease known as tumor-induced osteomalacia, first described in 1947, suggested that there might exist an additional

hormone with a major role in phosphate homeostasis. Patients with this disorder present with hypophosphatemia, abnormally low calcitriol and osteomalacia. Two case studies from Japan and the United States provided evidence that these tumors produced a phosphaturic factor that is distinct from PTH or other known hormones (Miyauchi et al., 1988; Cai et al., 1994). In both cases, the patients presented with symptoms typical of tumor-induced osteomalacia (TIO), including hypophosphatemia and low calcitriol, and bone biopsies revealed osteomalacia. The Japanese patient had mildly elevated PTH, while the American patient had PTH concentration in the normal range. Tubular reabsorption of phosphate in the Japanese patient was low (52% vs. 80-98% for normal subjects). Both patients possessed a sclerosing hemangioma in the thigh, which was surgically removed. After tumor removal, both patients experienced normalization of serum concentrations of calcitriol and phosphate. Samples from each tumor were preserved for subsequent experimental analysis.

Tumor samples from the Japanese patient were implanted in immunodeficient mice and effects on bone and mineral metabolism were observed. After tumor implantation, serum phosphate concentration fell and urinary phosphate excretion rose while serum calcium and urinary calcium excretion were unaffected. Implantation of an unrelated control tumor (hepatoma) did not cause these changes. Primary renal cell cultures treated with an extract from the hemangioma produced significantly less calcitriol than untreated controls. This inhibitory activity could be eliminated by boiling the extract, suggesting the unknown factor is a protein. Treatment with the extract did not increase intracellular cyclic-AMP levels, suggesting the factor is not PTH, which is know to increase intracellular cyclic-AMP in target cells (Miyauchi et al., 1988).

Tumor samples from the American patient were cultured and conditioned media obtained from these cultures were used to evaluate the effects of factors secreted by the cells. Conditioned media was added to cultures of opossum kidney (OK) cells to assay the effects of tumor secretions on phosphate transport. The conditioned media significantly reduced phosphate uptake by the OK cells, and boiling or dialyzing the media with a 25 kD filter abolished this inhibitory activity, again suggesting the phosphaturic factor is a small protein. Treatment with the conditioned media did not increase cyclic-AMP concentration in OK cells, unlike PTH (Cai et al., 1994). The evidence from these similar cases supports the existence of a small protein hormone that induces phosphaturia in the kidney and decreases the production of calcitriol.

The identity of the novel phosphaturic factor was determined by screening cDNA molecules synthesized from RNAs obtained from a TIO tumor and adjacent normal bone tissue (Shimada et al., 2001). The screening procedure was used to identify genes that were specifically expressed or overexpressed in the tumor tissue compared to the control tissue. Genes that were differentially overexpressed in the tumor tissue included dentin matrix protein-1 (DMP-1), heat shock protein-90, osteopontin and FGF23, a recently discovered member of the fibroblast growth factor protein family. FGF23 was of particular interest because the FGF23 genes resides at a chromosomal location that had been recently linked to autosomal dominant hypophosphatemic rickets (ADHR), a disease with biochemical findings similar to TIO (Econs et al., 1997). Recombinant FGF23 protein was produced by transfecting FGF23 cDNA into Chinese hamster ovary (CHO) cells and purifying the protein from conditioned media. Both full length FGF23 (~30 kD) and two cleavage products of 16 and 10 kD could be detected in the

conditioned media by immunoblotting. Injection of recombinant FGF23 into mice increased renal phosphate excretion and caused hypophosphatemia by 12 hours. Implantation of the CHO-FGF23 cells into immunocompromised mice reproduced these phosphaturic effects and caused a reduction of serum calcitriol concentration. Kidney expression of 1α-hydroxylase was substantially reduced in the mice bearing the CHO-FGF23 cells. Over time, bone mineral density was reduced and osteoid (unmineralized bone tissue) increased in these mice as well, similar to TIO (Shimada et al., 2001**)**. These *in vivo* findings constituted a strong case that FGF23 is the novel phosphaturic factor secreted by tumors in TIO. This hypothesis was strengthened by genetic linkage analyses of four families affected by ADHR that had more precisely located causative mutations of ADHR to the FGF23 gene (White et al., 2000). It would later be shown that these dominant mutations result in the production of cleavage-resistant FGF23, which in turn causes excessive renal phosphate excretion. A third hypophosphatemic disorder, X-linked hypophosphatemia, is caused by loss of function mutations in a protease that result in elevated FGF23 concentrations, though it is not yet clear if FGF23 is itself the direct substrate of this protease (Farrow and White, 2010; Kiela and Ghishan, 2009). Together, these studies strongly implied that FGF23 is a novel hormone regulator of phosphate homeostasis.

The importance of FGF23 for phosphate homeostasis was soon demonstrated in two studies of mice genetically engineered to lack expression of FGF23 (FGF23 KO mice) (Shimada et al., 2004; Sitara et al., 2004). These mice appeared normal at birth, but after 2 weeks of age began to exhibit impaired weight gain and growth, and surprisingly no FGF23 KO mice survived beyond 13 weeks of age (wild-type mice

typically have a lifespan of several years in laboratory conditions). The cause of death was not entirely clear, but may be attributable to a number of physiological abnormalities that were observed. FGF23 KO mice had atrophy of skeletal muscle, adipose tissue, and thymus and were hypoglycemic. Sexual organs in both males and females were atrophic, resulting in infertility. Vascular calcification, deposition of mineral in vascular tissues, was observed in the kidneys. Serum abnormalities included severe hyperphosphatemia (15 mg/dl vs. 9 mg/dl phosphate at 9 weeks of age), hypercalcemia, elevated calcitriol and a trend toward abnormally low PTH near the end of life in FGF23 KO mice. The expression of the enzyme responsible for calcitriol synthesis, 1α-hydroxylase, was elevated in kidneys of FGF23 KO mice, providing a possible explanation for the observed increase in serum calcitriol concentration. Expression of the Npt2a phosphate transporter was greater in the kidneys of FGF23 KO mice compared to wild-type littermates, and measurement of phosphate transport indicated that KO mice carried out significantly greater phosphate reabsorption in the kidney. Mice lacking FGF23 also possessed bone abnormalities. By 7 weeks of age, the long bones such as the femur were thicker and shorter than wild-type mice, with lower bone mineral density. There were fewer trabeculae present in the bones of FGF23 KO mice, and osteoid volume and thickness were increased. Various soft tissue calcifications in kidney, heart and vascular tissue were also observed, possibly due to the elevated serum concentrations of calcium and phosphate. These mouse studies indicate that FGF23 is required to maintain normal mineral ion homeostasis. FGF23, either directly or indirectly, suppressed kidney phosphate reabsorption and calcitriol synthesis. Many of the FGF23 KO phenotypes can be plausibly explained by primary changes to gene expression in the kidney (increased

1α-hydroxylase and Npt2a expression), raising the possibility that the kidney is a target organ of FGF23 action.

1.5 Klotho, a Co-Receptor for FGF23 Signaling

Shortly before the identification of FGF23 as the causative factor of TIO, a new gene had been identified by experimental manipulation in mice that would also in time be recognized as an important component of phosphate homeostasis. In an effort to create mice overexpressing a sodium-proton exchanger, Kuro-o et al. generated a mouse homozygous for a transgene insertion at an unknown genomic locus that displayed a wide variety of phenotypes resembling human aging (Kuro-o et al., 1997). These mice develop normally until 3 or 4 weeks of age then begin to develop growth retardation, fail to gain weight normally and ultimately die prematurely at 8 or 9 weeks of age. Homozygous mutant mice were smaller than their wild-type or heterozygous littermates by 8 weeks of age and developed kyphosis (excessive spinal curvature). They exhibited abnormalities in the concentrations of blood and serum constituents, including mild hypercalcemia, hyperphosphatemia (15 mg/dl vs. 8.5 mg/dl in normal mice) and hypoglycemia, while some other parameters such as cholesterol, triglyceride and albumin concentrations were not significantly different from normal mice. There were ectopic calcifications in soft tissues such as stomach, lung, skin, cardiac muscle and vascular tissues including the thoracic section of the aorta. A number of organs and tissues were atrophic in adult mutant mice, including skin, adipose tissue, sexual organs in males and females (causing infertility) and thymus. There were also bone abnormalities such as reduced bone mineral density and low bone turnover. The cause of early death in these mice was not clear, and may result from the combination of many abnormalities.

However, mice lacking matrix GLA protein (MGP), a protein expressed in vascular tissue and believed to play a role in protecting against ectopic mineral deposition, also develop calcifications in the aorta and die prematurely by 8 weeks (Luo et al., 1997) due to rupture of the blood vessel and hemorrhage. Therefore, severe calcification in major blood vessels may be sufficient to cause early death in the mice with the novel mutation as well.

The genomic location of the transgene insertion was determined by sequencing the mouse genomic DNA that was flanking the transgene introduced by the experimenters. A novel protein-encoding gene was found at this location that possessed a single transmembrane domain and an extracellular domain that consists of two tandem repeats with homology to bacterial β-glucosidase enzymes. A homologue of the mouse protein was also found in the human genome with 86% identity to the mouse protein. Insertion of the transgene greatly reduced the expression of the endogenous gene at the insertion locus. This novel gene was termed *Klotho*, after one of the three mythological Greek goddesses that spin the thread of life, in reference to the aging-like phenotypes of the mutant mouse. In wild-type mice, *Klotho* is expressed most abundantly in the kidney, choroid plexus of the brain, and pituitary, with lesser expression in the testis and ovary (Kuro-o et al., 1997). The extracellular domain of the Klotho protein is also secreted into the blood, either by cleavage of the membrane-bound protein or by alternative splicing of the *Klotho* gene transcript (Matsumura et al., 1998; Imura et al., 2004).

Because of the wide array of pathologies resulting from lack of *Klotho* expression, the normal biological function of Klotho protein was not immediately clear. However, the dramatic similarities of the FGF23 KO mouse and the *klotho* mutant mouse

suggested that these two genes interacted genetically and possibly even physically. Though FGF23 belongs to the FGF family, FGF23 binding to known FGF receptors is relatively low affinity and requires supply of glycosaminoglycans to support activation of cellular FGF signaling (Yu et al., 2005). FGF23 also lacks the heparin-binding domains present on other FGF proteins, which are believed to limit diffusion of these growth factors from their site of secretion (Goetz et al., 2007). This difference could enable FGF23 to travel from its site of production in bone and act as a true endocrine hormone, affecting distant organs such as the kidney. The interaction between Klotho and FGF23 was revealed by *in vitro* cell culture studies (Kurosu et al., 2006; Urakawa et al., 2006). Klotho from kidney homogenate was found to bind FGF23 in vitro, and CHO cells transfected with *Klotho* expression vector bound FGF23 avidly while little binding was observed in control CHO cells (Urakawa et al., 2006). Klotho protein also bound and immunoprecipitated with multiple FGF receptor isoforms (FGFRs); this interaction was strongest with the c isoform of FGFR1, the c isoform of FGFR3 and FGFR4 (Kurosu et al., 2006). FGF23 could be immunoprecipitated with these FGF receptors when Klotho was co-expressed, but FGF23 failed to bind strongly enough for immunoprecipitation if Klotho was absent. Klotho expression also supported cellular signaling initiated by FGF23 treatment. Cells expressing appropriate FGFRs and Klotho displayed activation of FGF receptor substrate 2α and the MAP kinases ERK1 and ERK2 (Kurosu et al., 2006). Klotho therefore acts as a co-receptor with certain FGFRs to support signaling by FGF23 and restrict responsiveness to FGF23 to those tissues that contain Klotho, whose expression is more limited than the widely expressed FGF receptors.

Through the course of subsequent studies performed in several laboratories, a new hormonal axis for the regulation of phosphate homeostasis has emerged that complements and integrates with the calcitriol and PTH systems (Martin et al., 2012). FGF23 binding to Klotho-FGFR complexes in the kidney leads to downregulation of 1α-hydroxylase and calcitriol synthesis, upregulation of 24-hydroxylase and calcitriol metabolism, and downregulation of Npt2a and Npt2c, leading to increased renal phosphate excretion. Notably, Klotho is expressed most abundantly in kidney distal tubules while its phosphaturic effect is carried out in proximal tubules. It remains unclear how FGF23 signaling in distal tubules ultimately leads to changes in phosphate reabsorption in proximal tubules (Liu et al., 2008; Martin et al., 2012). Calcitriol is a potent inducer of FGF23 expression in bone cells, and therefore FGF23 participates in a negative feedback loop with calcitriol (Liu et al., 2006). Outside of the kidney, FGF23 may suppress PTH secretion by parathyroid glands, but interactions of FGF23 with the PTH hormonal system remain controversial (Martin et al., 2012). The soluble Klotho protein also appears to have functions in addition to FGF23 signaling. Soluble Klotho protein may itself be a phosphaturic factor in the kidney (Hu et al., 2010), and Klotho enzymatically removes sialic acid residues from side chains on the TRPV5 calcium channel found in kidney tubules, causing the channel to be retained on the cell surface (Cha et al., 2008).

1.6 Pathological Consequences of Excessive Phosphate Retention

Using the knowledge gained about the physiological roles of FGF23 and Klotho, the phenotypes of the *klotho* mutant mice and FGF23 KO mice can be reevaluated in the context of mineral ion homeostasis. Even though these mice display a wide range of

pathological abnormalities, suggesting a complex etiology, studies of dietary interventions performed on mice of each genotype have demonstrated that excessive phosphate retention plays a major causative role in most of the observed pathologies. When *klotho* mutant mice were fed a diet low in inorganic phosphate, body weight gain and survival were significantly improved compared to mice fed typical laboratory diet. Several males fed the low phosphate diet survived until the end of the experimental period at 29 weeks of age, compared to an average lifespan of 9.6 weeks for mice fed control diet (female mice did not respond as well in this experiment for unknown reasons) (Morishita et al., 2001). The low-phosphate diet also restored serum glucose levels, reduced atrophy of skin and sexual organs and reduced calcification in the kidney (Morishita et al., 2001). Of note, the low-phosphate diet partially restored expression of the endogenous *klotho* gene through unknown reasons in *kl/kl* mice, which made it difficult to unequivocally conclude that lack of Klotho protein *per se* was not the main cause of lethality in *klotho* mutant mice but rather the disturbances in phosphate homeostasis are largely responsible. However, similar dietary experiments were carried out with FGF23 KO mice, and similar results were obtained (Stubbs et al., 2007). When FGF23 KO mice were fed a low-phosphate diet, survival rate at 14 weeks of age was 90% versus 0% for FGF23 KO mice fed a standard control diet. Calcifications in the kidneys and the aorta were largely absent in mice fed low-phosphate diet, but were abundant in mice fed the control diet. Hyperphosphatemia of FGF23 KO mice was reversed to hypophosphatemia in mice fed the low-phosphate diet (serum phosphate was also low in wild-type mice fed a low phosphate diet). Notably, calcitriol levels remained elevated in FGF23 KO mice on low-phosphate diet, suggesting that elevated calcitriol

levels were not the principal cause of mortality in FGF23 KO mice (Stubbs et al., 2007). The results of these dietary studies suggest that adequate control of phosphate homeostasis is critical to a normal life span to an extent not appreciated before.

Disturbances in phosphate homeostasis have also been documented in human patients, both in the cases of elevated blood levels of FGF23 mentioned above and in the case of a patient with a *de novo* chromosomal translocation resulting in elevated expression of Klotho protein. This patient presented persistent hypophosphatemia due to excessive renal phosphate excretion, with consequent bone abnormalities (Brownstein et al., 2008). Conversely, inactivating mutations in FGF23 in human patients result in tumoral calcinosis, characterized by hyperphosphatemia and ectopic calcifications (Chafetz et al., 2005; Larsson et al., 2005).

The human disease condition that perhaps could be most impacted by greater understanding of phosphate homeostasis is chronic kidney disease (CKD). This disease is characterized by the progressive loss of renal function over time, and its most common causes are hypertension, glomerulonephritis and diabetes mellitus. The disease is categorized by stages of declining renal function as measured by glomerular filtration rate, with stage 5 representing the most severe disease category. CKD-mineral and bone disorder (CKD-MBD) is a term that has been recently developed to describe three abnormalities that commonly arise together in later stages of CKD: disorders of biochemical measures of mineral ion homeostasis, skeletal abnormalities and ectopic mineral deposition (KDIGO Working Group, 2009). The serum abnormalities most evident in CKD-MBD are increases in PTH with disease progression, eventually reaching very high levels, decreases is calcitriol production with disease progression and increases

in phosphate concentration at late stages of the disease. The development of secondary hyperparathyroidism is of particular concern because the catabolic actions of chronic PTH exposure lead to dangerous bone abnormalities and weakness (Goodman and Quarles, 2008; Moe and Sprague, 2012). A bone biopsy may be performed to allow detailed examination of bone microstructure and assess the severity of bone disease (KDIGO Working Group, 2009). The third component, ectopic calcification, is also of particular concern when vascular tissue becomes the target of mineral deposition. Vascular calcification increases blood vessel stiffness and impairs normal function, likely contributing to the increased cardiovascular disease risk seen in CKD patients. Complications from cardiovascular disease represent the single largest cause of death in CKD patients (Mizobuchi et al., 2009). Each of these three components of CKD-MBD is a target for therapeutic intervention. Hyperphosphatemia can be addressed by adjusting dietary phosphate intake (compliance with this therapy is difficult), dialysis (in patients with advanced CKD), or oral phosphate binders (Hutchison, 2009). Elevated PTH concentrations can be treated with calcitriol or the calcimimetic cinacalcet, or parathyroidectomy in severe cases. Resolving these biochemical abnormalities will hopefully slow the progression of bone disorders, though drugs such as bisphosphonates may also be used specifically to treat bone weakness (KDIGO Working Group, 2009).

There exist several lines of evidence to support the notion that disturbances of phosphate homeostasis are responsible for much of the disease burden of CKD-MBD, particularly vascular calcification (Hruska et al., 2008). The concentration of serum phosphate was positively correlated with vascular and valvular calcification in CKD patients (Adeney et al., 2008). In a meta-analysis of many clinical trials, serum

phosphate was also positively correlated with increased risk of death and cardiovascular disease (Palmer et al., 2011). One straightforward mechanistic explanation for these associations is that elevated serum phosphate will exceed its solubility in serum and deposit in vulnerable tissues (Hruska et al., 2011), though more complex changes may also be occurring (see Chapter 2). In the experiments presented here, our aim was to explore in a more detailed way the pathological consequences that are a result of impaired phosphate homeostasis. The FGF23 KO and *klotho* mutant mice demonstrate in a dramatic way the effects of excess phosphate retention, and the dietary rescue experiments demonstrate in an equally dramatic way the possible benefits of correcting this abnormality. By examining how high extracellular phosphate perturbs cells and tissues, we hope to better understand development and progression of diseases that involve this loss of homeostasis.

CHAPTER TWO

Studies of the Effects of Elevated Extracellular Phosphate Concentrations on Cultured Cells

2.1 Introduction

The experimental *klotho* mouse and human patients with naturally arising conditions such as chronic kidney disease (CKD) both exhibit pathological changes that may in part be due to increased retention of phosphate. The centrality of excessive phosphate retention to the establishment of *klotho* phenotypes is demonstrated by dietary experiments: *klotho* mice fed a diet low in inorganic phosphate to compensate for their excessive phosphate retention experience full or partial rescue of characteristic *klotho* phenotypes such as impaired body weight gain, soft tissue calcifications and premature death (see above). In the setting of CKD, elevated serum phosphate has been associated with an increased risk of mortality, and accumulating evidence supports the argument that serum phosphate should be evaluated as an independent risk factor for CKD-related morbidity and mortality (Palmer et al., 2011). Therefore, an important goal for both the study of the *klotho* mouse and CKD is to gain an understanding of the mechanism by which excessive phosphate retention leads to adverse pathological changes in cells and tissues and increased risk of mortality in the organism as a whole.

As a foundation for investigations into the effect of elevated extracellular phosphate on cells, useful insights can be drawn from previous research in the field of osteoblast biology. In vertebrates, the skeleton becomes mineralized as a result of the cellular activities of chondrocytes and osteoblasts. The mineralization process requires both an adequate supply of inorganic components (calcium, phosphate and other ions) as well as the production of an extracellular environment that is favorable for mineralization. This latter requirement plays a key role in limiting the formation of mineralized tissue to appropriate locations in the organism: the expression of cellular products that facilitate mineralization is normally restricted to tissue sites that will ultimately become mineralized (Murshed et al., 2005). As a consequence of these multiple requirements for mineralization, local environments that possess sufficient or excess inorganic components (calcium and phosphate) may not necessarily mineralize if essential extracellular protein components are missing or molecules that inhibit mineralization are present. Genetic mouse models, cell culture studies and human diseases have each contributed to our understanding of the mineralization process, and the results of these studies support a model in which mineralization at local tissue sites is the result of a *balance* between active cellular processes, the availability of inorganic components, and the presence of inhibitory molecules (van de Lest and Vaandrager, 2007). It is these multiple regulatory factors that determine the ultimate result when an organism is confronted with an excess of one of the inorganic components of mineralization, such as phosphate in the case in *klotho* mice. Several of these factors will be considered here because they likely play a role in pathological calcification, which can be observed in situations of excessive phosphate retention.

The Mineralization Process In Vivo

Cells that carry out the mineralization process, such as osteoblasts, can release extracellular products termed matrix vesicles that are believed function in the initialization of mineral formation. These specialized vesicles accumulate high concentrations of calcium and phosphate by using ion transporters and Ca^{2+} binding phospholipids, creating an intra-vesicular environment that favors the formation of calcium and phosphate-containing hydroxyapatite mineral. The growing mineral destroys the matrix vesicle and becomes a nidus for further extracellular mineral formation (Anderson, 2007). Apoptotic bodies released by dying cells may serve a similar seeding function, though the mechanism by which they promote mineral formation may be different (van de Lest and Vaandrager, 2007). Extracellular collagen molecules serve as a scaffold for the larger-scale structural organization of bone and become embedded with mineral over time, giving bone its composite-material properties. Various non-collagenous proteins such as proteoglycans and a group of proteins called SIBLINGs (small integrin-binding ligand, N-linked glycoprotein) regulate the growth of extracellular mineral, either nucleating or inhibiting further growth. Finally, a balance between local concentrations of phosphate and pyrophosphate appears to play a crucial role in controlling mineralization, a notion supported by evidence from several genetically modified mouse models. Alkaline phosphatase proteins expressed by osteoblasts and chondrocytes generate locally elevated concentrations of phosphate by liberating phosphate from various substrates, a process that favors mineral formation (Golub and Boesze-Battaglia, 2007). At the same time, extracellular pyrophosphate binds to growing hydroxyapatite mineral and interferes with further mineral growth.

Extracellular pyrophosphate may be generated from extracellular nucleoside triphosphates by NPP1 (nucleotide pyrophosphatase/phosphodiesterase) or exported from the cell by the pyrophosphate transporter ANK (ankylosis protein). Mice lacking ANK develop ectopic calcifications, demonstrating the importance of pyrophosphate for control of appropriate mineralization (Ho et al., 2000). Alkaline phosphatase also degrades pyrophosphate into two phosphate ions, further supporting mineral formation. Thus, the relative abundance of these two small inorganic molecules, and the expression of the proteins that generate them, in part determines whether mineral will form in a tissue, as summarized in Figure 2-1.

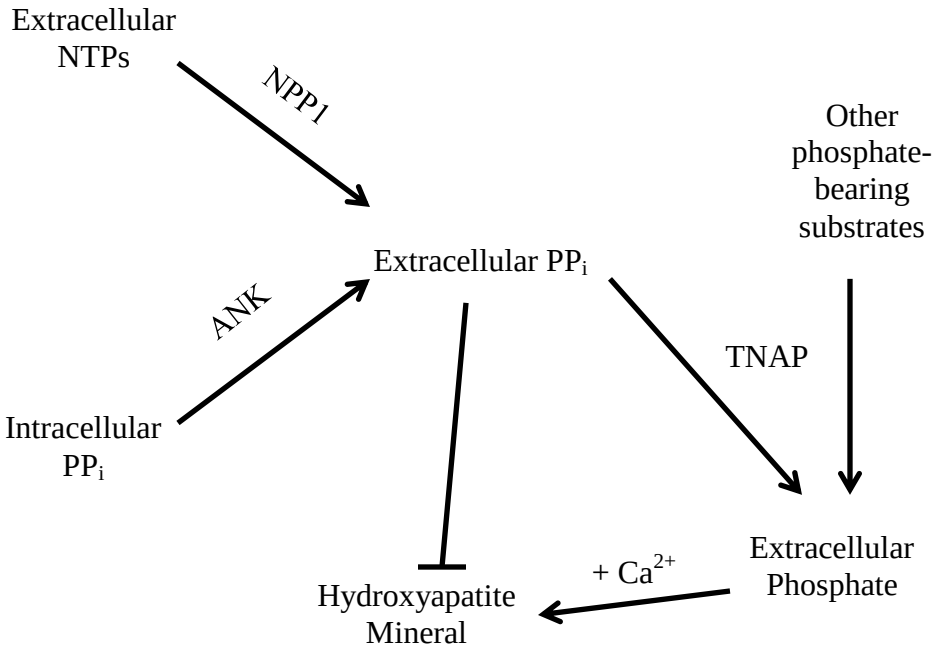

Figure 2-1: Roles of phosphate and pyrophosphate in mineral formation. Pyrophosphate (PP_i) is generated outside the cell either by exporting it from the cell via the ANK PP_i transporter or by cleaving PP_i from nucleotides (NTPs) outside the cell. Extracellular PPi inhibits mineral formation but may be broken down into two phosphate molecules by tissue-nonspecific alkaline phosphatase (TNAP). TNAP generates phosphate from PP_i or other extracellular phosphate-bearing molecules. This newly available phosphate may then be used in mineral formation. Figure adapted from Golub and Boesze-Battaglia, 2007.

Cell Culture Studies

The ability of cells to generate and regulate these various mineralization factors during the process of bone formation has been studied *in vitro* using primary cultures of osteoblast precursors and osteoblast cell lines. Primary cells for mineralization studies are most commonly isolated from fetal calvaria (developing skullcap). These structures are not yet fully mineralized and cultures of calvarial osteoblasts do not contain mineral initially. A commonly used mouse cell line, MC3T3-E1, is also derived from calvaria and has been used extensively to study changes in gene expression during the course of mineralization and the effects of extracellular proteins or small molecules on the extent of mineralization. Previous studies indicate that several factors must be produced or supplied to consistently achieve mineralization *in vitro*: sufficient phosphate and calcium ions must be present to saturate the culture media with respect to hydroxyapatite; an extracellular matrix must be produced to receive deposited mineral; and appropriate growth factors are required to ensure the expression of early osteoblastic genes that initiate the process (Boskey and Roy, 2008). Ideally, these osteoblast cultures would contain all of the factors that regulate physiological bone mineralization so as to accurately model the *in vivo* mineralization process.

Cell media formulations that support mineralization in culture have been developed and termed 'osteogenic media'. These formulations typically include minimal essential media (α-MEM), 10% FCS, 50 μg/ml ascorbic acid and up to 10 mM of β-glycerophosphate. The original purpose of ascorbic acid supplementation was to ensure adequate collagen synthesis in the cultures (ascorbic acid is used to produce hydroxyproline residues which are critical for collagen protein structure). However, it

was later found that ascorbic acid supplementation increased the activity of alkaline phosphatase and promoted the expression of characteristic osteoblast genes independent of its role in collagen synthesis. Subsequently, it has been retained in the osteogenic media formulation as a differentiation factor. β-glycerophosphate serves as an organic phosphate donor molecule. Once cells begin expressing alkaline phosphatase, the enzyme cleaves extracellular β-glycerophosphate to generate the free phosphate ions required for mineralization.

Phosphate as an Inducer of Gene Expression

The cell culture systems outlined above can be used to assay candidate genes or activities that contribute to mineralization. Cells are incubated in osteogenic medium for 2 or 3 weeks and then stained with alizarin red or silver nitrate (von Kossa staining) to evaluate the extent of mineral formation. Over the course of this incubation period, there is a sequential induction of characteristic osteoblast genes beginning with alkaline phosphatase and collagen-1α, followed later by SPARC (secreted protein acidic and rich in cysteine), osteocalcin and the SIBLING protein osteopontin. Beck et al. used this cell culture system to identify transcription factors that may be necessary to carry out the gene expression program that is initiated by incubation with osteogenic medium (Beck et al., 1998; Beck et al., 2000). Beck et al. introduced the adenovirus protein E1A, which blocks the activity of the transcription factors p300, pRB and CREB binding protein (CBP), into MC3T3-E1 cells and observed that the formation of mineral after incubation in osteogenic medium was blocked. The activity of these transcription factors had previously been shown to be required for differentiation in a number of other cell types, and the experimental goal was to determine whether that might be the case for osteoblasts

as well. Closer analysis of the expression of genes in the osteoblast developmental program revealed that introduction of the E1A protein suppressed the induction of alkaline phosphatase and osteopontin but not collagen, SPARC or osteocalcin. Interestingly, when exogenous alkaline phosphatase was supplied to cells expressing the E1A protein, both osteopontin expression and the mineralization phenotype were rescued (Beck et al., 1998). These results suggested that alkaline phosphatase activity was required to cleave β-glycerophosphate in the osteogenic medium and supply phosphate needed for mineralization, and that induction of osteopontin also required alkaline phosphatase activity. This led to the hypothesis that elevated phosphate in the cell culture medium is a specific inducer of osteopontin expression. Beck et al. tested this hypothesis in a subsequent study by again introducing the E1A protein into MC3T3-E1 cells (Beck et al., 2000). These cells did not induce alkaline phosphatase or osteopontin during incubation with osteogenic medium and osteopontin expression could again be rescued by supplying exogenous alkaline phosphatase, but when β-glycerophosphate was left out of the osteogenic medium under these conditions the rescue of osteopontin expression was lost. This suggested that indeed the elevation of extracellular phosphate was required for osteopontin induction rather than some other function of alkaline phosphatase. This idea was tested directly by incubating E1A-expressing MC3T3-E1 cells with media containing 4-10 mM phosphate but without supplying alkaline phosphatase and β-glycerophosphate. The added phosphate was sufficient to induce osteopontin expression, indicating that this gene is responsive to elevations in extracellular phosphate. Ascorbic acid was not required for osteopontin induction by phosphate, suggesting that this process occurred independently of other developmental

steps in this cell culture system. In fact, direct addition of phosphate could induce osteopontin expression in these cells within 48 hours, whereas during the conventional incubation process with osteogenic medium osteopontin expression does not increase until after at least a week of incubation, suggesting earlier developmental steps can be bypassed and osteopontin is directly responsive to phosphate. Beck et al. also tested whether phosphate ions must be able to enter the cell for the MC3T3-E1 cells to sense and respond to elevated phosphate concentrations. Cells were treated with phosphonoformic acid (PFA), a phosphonic acid containing a carbon-phosphorus bond that impairs phosphate uptake into cells via Na^+-dependent phosphate transporters (Szczepanska-Konkel et al., 1986). Incubation with PFA prevented the induction of osteopontin caused by treatment with elevated phosphate, suggesting that phosphate entry into cells was required. Finally, Beck et al. showed that osteopontin could be induced by phosphate in NIH/3T3 fibroblasts as well, demonstrating that this phenomenon was not restricted to osteoblast-like cells (Beck et al., 2000).

Together, these data provide initial support for an expanded role for phosphate ions in the development of bone cells and the mineralization process. Phosphate ions are required as an inorganic component of mineral, but may also have a signaling function at a certain point in the bone development process. When alkaline phosphatase expression rises early in the process of mineralization, extracellular phosphate rises and induces osteopontin expression. Osteopontin in turn can bind to newly formed mineral and modulate its growth and become incorporated into mature bone (see Chapter 3). In this way, phosphate acts as a feedback signal to ensure appropriate expression timing of this noncollagenous bone protein.

Pathological Calcification

The novel concept that extracellular phosphate can cause changes in gene expression and cell behavior has implications not only for the study of normal bone formation but pathological mineralization processes as well. It may be the case that in situations where local phosphate concentrations are elevated, such as hyperphosphatemia, phosphate could be affecting cell behavior adversely. Indeed, as Beck et al. demonstrated, non-osteoblast cells (fibroblasts) responded to treatment with elevated phosphate and began producing a protein characteristic of osteoblasts (osteopontin) that is not normally produced by fibroblasts. A series of experiments by Giachelli et al. suggest that phosphate may be having this negative effect in the development of pathological calcifications of vascular tissue (Giachelli et al., 2009).

Calcification of blood vessels is a prominent phenotype in *klotho* mice, which likely contributes to the premature death of these mice. Vascular calcification is also observed in CKD and confers additional morbidity and mortality risk (see Chapter 1). It is reasonable to suspect that a major cause of these pathological calcifications is excessive phosphate retention, which can lead to persistent hyperphosphatemia. If phosphate concentrations rise above their solubility limit with respect to calcium in a local tissue environment, ectopic mineral deposition could occur. As mentioned above, when *klotho* mice are fed a low phosphate diet, these pathological soft tissue calcifications are prevented, supporting a key role for excessive phosphate retention in the development of these disorders (Stubbs et al., 2007). However, studies during the last 15 years have revealed that the pathological mineralization process likely involves cell-mediated events and is not solely the result of an inorganic ion imbalance, though that

may be the initiating event. Rather, a mineral deposit can affect the behavior of nearby cells, perhaps in a manner analogous to an atherosclerotic plaque.

Giachelli et al. incubated primary cultures of human and bovine vascular smooth muscle cells with excess phosphate in the form of β-glycerophosphate at a concentration of 10 mM (Jono et al., 2000; Steitz et al., 2001). Smooth muscle cells were used because calcification is frequently observed in the smooth muscle layer of blood vessels (Lau et al., 2011). Interestingly, phosphate treatment resulted in the progressive deposition of mineral over the course of several days, an unexpected result since these cells were not osteoblasts or osteoblast precursors. Phosphate treatment was also accompanied by upregulation of the Runx2 transcription factor, a key differentiation factor for osteoblasts, as well as other osteoblast lineage genes such as alkaline phosphatase and osteopontin. These cultures also lost expression of genes characteristic of smooth muscle cells such as smooth muscle α actin and SM22α. Extracellular collagen deposition and matrix vesicles were also observed on the surface of smooth muscle cells following phosphate treatment (Wada et al., 1999). Thus, treatment with elevated phosphate appears to cause vascular smooth muscle cells to lose their smooth muscle identity and adopt features of osteoblasts. Several studies document such changes in vascular smooth muscle cells *in vivo* using samples from hyperphosphatemic mouse models as well as dialysis patients (Shanahan et al., 2011). Lineage tracing studies confirm that vascular smooth muscle cells are the source of mineralization-related proteins such as osteopontin, rather than new cell types that may appear at sites of mineralization (Speer et al., 2009). Elevated phosphate retention therefore appears to cause changes in gene expression in vascular cells that lead to an osteoblast-like character, which could potentially exacerbate the

mineralization problem because these cells typically facilitate mineral formation. This concern is highlighted by evidence suggesting that the changes in gene expression *precede* mineral formation (Speer et al., 2009). Therefore, a critical ongoing research goal is to understand the precise causes and consequences of these changes in cell behavior and determine if they are indeed maladaptive.

Research Aim of the Present Studies

The primary aim of the following studies presented here is to understand the mechanisms by which excessive phosphate retention in mammals leads to the pathologies outlined above. In particular, we are interested in determining how elevated extracellular phosphate modifies cellular behavior, and how these changes subsequently contribute to disease processes such as tissue calcification. Such knowledge could provide new approaches to intervene against the development of pathological calcifications in settings of disturbed mineral ion balance such as CKD. We began our investigation by using an established model for studying the effects elevated phosphate on cell behavior, the osteoblast cell line MC3T3-E1. Our initial focus was on cell signaling events caused by elevation of extracellular phosphate. We used this cellular response to assay factors that could mediate the effects of extracellular phosphate on cells.

2.2 Methods

Cell Culture

MC3T3-E1 osteoblast precursor cells and 3T3-L1 fibroblasts were obtained from American Type Culture Collection (ATCC). Cells were cultured in 10 cm dishes and experiments were performed in 12 well plates purchased from Corning-Costar. Cells were maintained using Dulbecco's Modified Eagle Medium (DMEM) supplemented with 10% fetal bovine serum (FBS) and antibiotics (penciling and streptomycin, 100 U/ml and 100 µg/ml respectively), all obtained from Life Technologies, Gibco Brand. Prepared buffers lacking phosphate used in signaling experiments had the following compositions: 137 mM NaCl, 5.4 mM KCl, 2.8 mM $CaCl_2$, 1.2 mM $MgSO_4$, and 10 mM HEPES pH 7.5 (salt buffer); 137 mM choline chloride, 5.4 mM KCl, 2.8 mM $CaCl_2$, 1.2 mM $MgSO_4$, and 10 mM HEPES pH 7.5 (Na^+-free buffer), 137 mM NaCl, 5.4 mM KCl, 1.2 mM $MgSO_4$, and 10 mM HEPES pH 7.5 (Ca^{2+}-free buffer). 100 mM stock buffers of sodium phosphate (pH 7.5), potassium phosphate (pH7.5) and sodium pyrophosphate (pH 7.0) were used for experimental treatments. Insulin, citric acid, phosphonoformic acid (PFA) and anisomycin were obtained from Sigma-Aldrich and basic FGF was obtained from Santa Cruz Biotechnology.

Immunoblot Analysis

Cells were collected in cell lysis buffer (20 mM HEPES, 100 mM NaCl, 1.5% Triton-X100, 15 mM NaF, 20 mM phosphatase inhibitor cocktail (Sigma), protease inhibitor mix (Roche), 1 mM EDTA and 20 mM sodium pyrophosphate) and centrifuged for 10 minutes at 13,000 rpm. Supernatants were collected and SDS sample buffer was added before boiling samples for 5 minutes. Protein samples were subjected to SDS-

polyacrylamide gel electrophoresis (SDS-PAGE) and proteins were then transferred to nitrocellulose membranes. Membranes were incubated in blocking buffer (2% milk, 0.05% v/v Tween 20 in TBS) then incubated with primary antibodies. The phospho-Akt Thr308, phospho-Akt Ser473, phospho-p38, phospho-JNK, phospho-CREB, total CREB, phospho-ERK1/2, and total ERK1/2 antibodies were obtained from Cell Signaling Technologies, while the β-tubulin antibody was obtained from Santa Cruz Biotechnologies. All antibodies were diluted at a ratio of 1:1000 except β-tubulin, which was diluted 1:2000. Membranes were washed in a TBS-Tween solution and then incubated with appropriate secondary antibodies conjugated with horseradish peroxidase (GE Healthcare). Blots were developed using SuperSignal West Dura Extended Duration Substrate from Thermo Scientific.

In-Vitro *Precipitate Formation Assay*

Phosphate and pyrophosphate buffers were added to the prepared buffers (see 'Cell Culture' section above) and formation of precipitates over time was monitored using a Beckman DU530 UV/Vis spectrophotometer. Buffers were combined in cuvettes to yield the indicated final salt concentrations and blank readings were obtained in the spectro-photometer immediately prior.

Light Microscopy and Microphotography

Microscopy images were obtained using a Leica Microsystems DM IL inverted microscope. A SPOT-idea™ digital camera was used to capture images in conjunction with SPOT Advanced Plus software.

2.3 Results

To identify cell signaling pathways that may be activated by treatment with extracellular phosphate, Beck et al. evaluated several major growth factor pathways and observed that phosphate treatment acutely activated the extracellular signal-regulated kinase (ERK 1/2) pathway in MC3T3-E1 cells (Beck and Knecht, 2003). Other arms of the mitogen-activated kinase pathway, c-Jun N-terminal kinase (JNK) and p-38, were not activated by phosphate treatment, implying a degree of signaling specificity caused by this stimulation (Beck and Knecht, 2003). To further investigate signaling pathways activated by phosphate treatment, we stimulated MC3T3-E1 cells with 1-8 mM extracellular phosphate for 20 minutes and prepared cell lysates for immunoblot analysis. Phosphate treatment was carried out by replacing the culture medium (normally containing 1 mM phosphate) with equivalent medium inherently lacking phosphate but supplemented with 1-8 mM sodium phosphate buffer to create increasing treatment doses. Cells were starved of serum for the previous 24 hours and during the treatment period to lower the cell signaling tone and make signal activation events clearly discernable. Activating phosphorylations on the Akt protein, a major growth and metabolic control kinase, ERK1/2, JNK, p38, and CREB (cyclic-AMP response element binding protein) were evaluated using phospho-specific antibodies. Insulin, basic FGF and anisomycin were used as positive controls for the ERK1/2, Akt and p-38/JNK pathways, respectively. As shown in Figure 2-2, none of the tested signaling pathways was activated within 20 minutes by phosphate (P_i) treatments below 6 mM. However, P_i treatment at concentrations of 7 mM and above caused activating phosphorylations of ERK1/2 and CREB proteins while Akt, p38 and JNK remained inactivated. The

activation of ERK1/2 appeared to exhibit a graded dose-response over 6-8 mM, though some variability occurred over repeated experiments. A possible explanation for this phenomenon will be offered below. Thus, treatment with P_i over a 20-minute period activated ERK1/2 and the transcription factor CREB, suggesting one possible cell signaling pathway that could facilitate the transcriptional changes that occur following P_i treatment.

We next examined changes in ERK1/2 activation over time following P_i treatment. MC3T3-E1 cells were treated with varying concentrations of P_i for 24 hours in medium containing a low concentration of fetal calf serum to sustain cell viability (Figure 2-3). We found that activation of ERK1/2 was sustained 24 hours following the addition of P_i, consistent with similar experiments reported previously (Beck and Knecht, 2003). We could not, however, observe biphasic activation of ERK1/2 reported by Beck et al., characterized by decreased ERK1/2 phosphorylation beginning 2 hours after P_i stimulation and reactivation beginning at 16 hours (data not shown) (Beck and Knecht, 2003). These results demonstrate that P_i treatment causes a sustained activation of ERK1/2, which may therefore play a direct role in activating transcription factors responsible for changes in gene expression following P_i treatment, since these occur within 24 hours (Beck and Knecht, 2003).

A potentially important property of P_i-induced cell signaling is its cell-type specificity. If phosphate can affect the behavior of cells other than bone cells, it is possible that elevated extracellular phosphate could be directly, rather than indirectly, contributing to pathological processes in non-bone tissues. We treated 3T3-L1 fibroblasts, which is a cell line commonly used to study adipocyte development, with 7

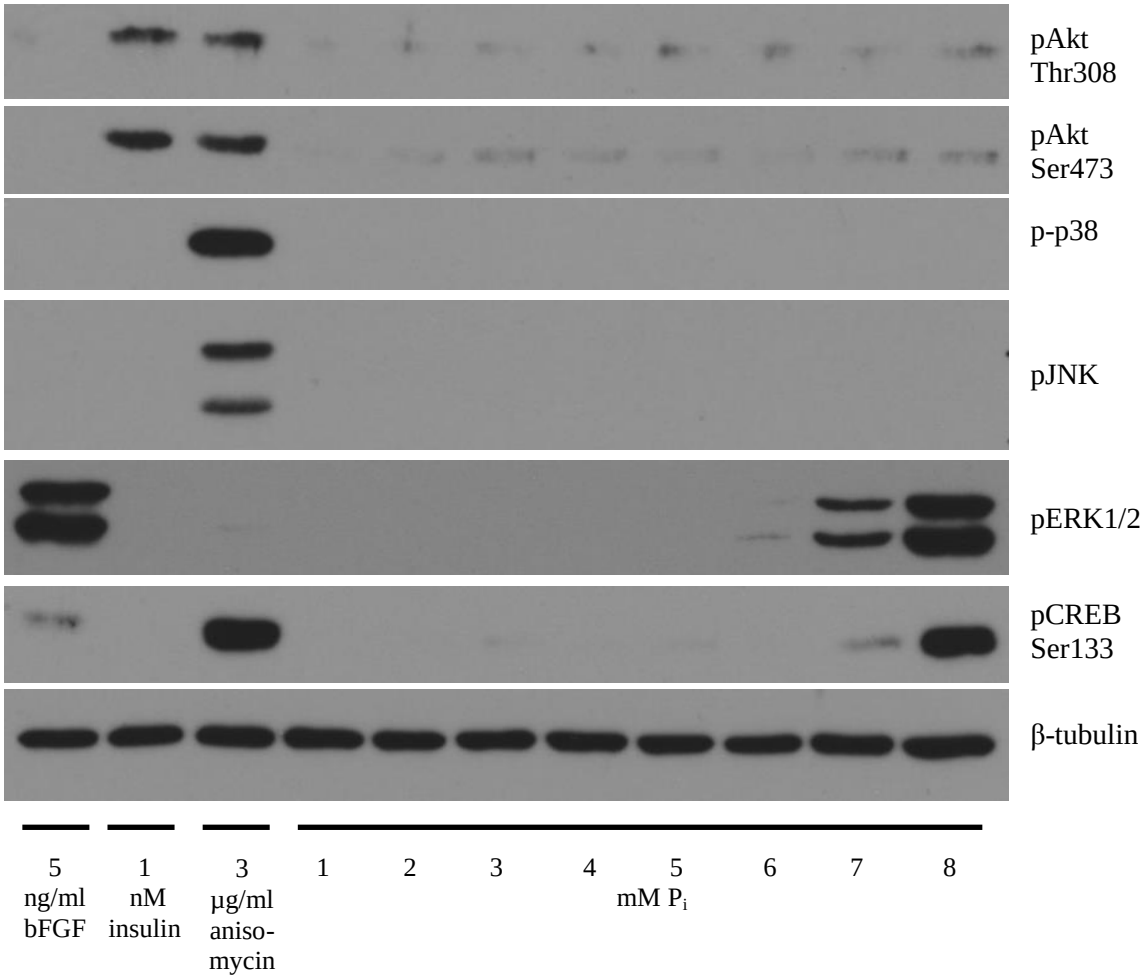

Figure 2-2: Activation of cell signaling pathways following exposure to elevated extracellular phosphate.
MC3T3-E1 cells were starved of serum for 1 hour prior to addition of sodium phosphate buffer resulting in final phosphate concentrations in the culture medium as indicated. Cells were also treated with basic FGF, insulin or anisomycin as positive controls. After 20 minutes of treatment, cells were harvested and proteins subjected to SDS-PAGE. Immunoblotting was performed using phospho-specific antibodies to detect activation of the indicated proteins as well as β-tubulin, used as a loading control.

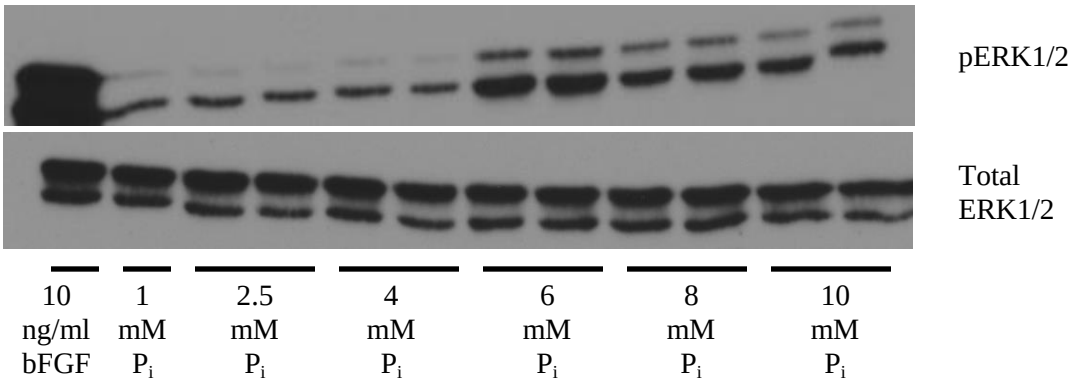

Figure 2-3: 24-hour stimulation of MC3T3-E1 cells with extracellular phosphate. MC3T3-E1 cells were incubated in media containing 0.5% fetal calf serum to preserve cell viability while lowering background ERK1/2 activation. Cells were then treated for 24 hours with phosphate (P_i) buffer to raise final extracellular P_i concentrations to the indicated amounts. Cells were lysed and proteins were subjected to SDS-PAGE, then immunoblotted for activated ERK1/2 (p-ERK1/2) as well as total ERK1/2 protein. The two lanes for elevated P_i treatments represent two different cell culture wells and treatments.

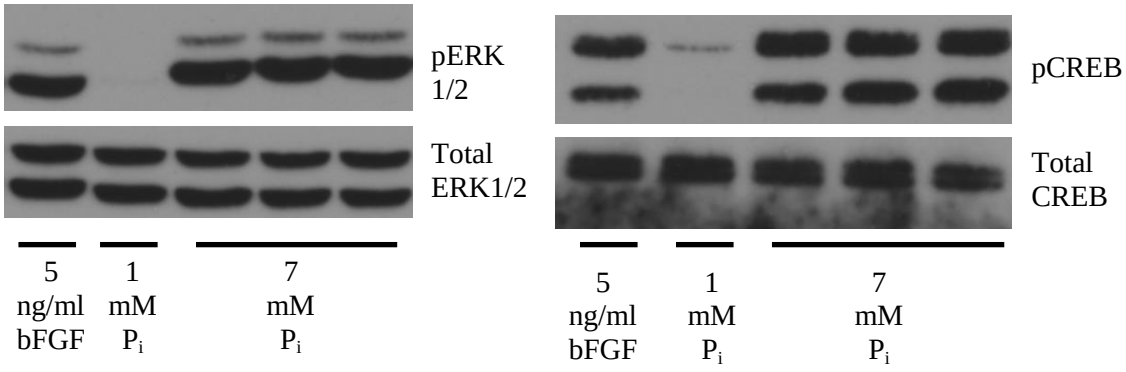

Figure 2-4: Treatment of non-osteoblast cells with elevated extracellular P_i. 3T3-L1 fibroblasts were starved of serum for 1 hour prior to addition of P_i buffer resulting in the final P_i concentrations indicated, or treatment with 5 ng/ml bFGF. Cells were treated for 15 minutes, lysed and proteins were subjected to SDS-PAGE. Proteins were immunoblotted using antibodies against activated ERK1/2 and CREB as well as total ERK1/2 and CREB. The three lanes for 7 mM P_i treatment represent three different cell culture wells and treatments.

mM P_i for 15 minutes. We evaluated cell signaling pathways by immunoblot and found that ERK1/2 and CREB were activated while Akt, p38 and JNK were not, similar to the results seen when MC3T3-E1 cells were treated with P_i (Figure 2-4). We therefore found that osteoblasts were not the only cell type responsive to elevated extracellular P_i, in agreement with the observation by Beck et al. that NIH3T3 fibroblasts were also responsive. We also observed activation of ERK1/2 after short-term incubation with P_i in liver (H4IIE), kidney (HEK293) and muscle (C2C12) cell lines (data not shown). These results suggest both that a wide variety of cells are responsive to phosphate and that the mechanism for sensing elevated extracellular P_i is not restricted to bone cells.

Several possible mechanisms exist by which elevated extracellular P_i could be sensed by cells. A threshold concentration of P_i could be detected by a cell surface receptor as is the case for calcium, which is sensed in certain tissues by a cell surface G-protein coupled receptor (Pin et al., 2003). Alternatively, P_i could affect cells from within by being transported into the cell and activating a specific sensory system there, or could affect P_i-dependent processes generally in such a way as to activate cell signaling pathways such as ERK1/2. Another possibility is that elevated P_i could affect the extracellular environment in some way that is in turn sensed by cells, constituting an indirect P_i-sensing mechanism. To begin to distinguish among these possibilities, we performed experiments to determine whether P_i must be actively transported into cells to initiate cell signaling. PiT-1 and PiT-2 are cell surface Na^+-dependent P_i co-transporters which are widely expressed in most mammalian tissues and are believed to play a 'housekeeping role' in supplying cells with P_i, though some P_i can enter the cell by unfacilitated diffusion (Virkki et al., 2007). We hypothesized that if the high

concentration of sodium outside the cell were removed, the sodium gradient necessary for PiT-1 function would be lost and P_i would no longer be transported into the cells by this protein. If P_i-initiated cell signaling events require P_i entry into the cell, they would presumably be affected by such a treatment. We prepared saline solutions for cell culture lacking phosphate and also replaced sodium chloride in one buffer with an equivalent concentration of choline chloride as a placeholder salt. MC3T3-E1 cells were incubated in saline solutions either containing or lacking sodium chloride, then treated with varying concentrations of potassium phosphate buffer for 20 minutes. As shown in Figure 2-5, ERK1/2 activation by P_i treatment was not reduced by lack of extracellular sodium, and may have been slightly enhanced. While some of the added extracellular P_i may have entered the cell by diffusion over the course of the treatment period, these results indicate that Na^+-dependent P_i entry was not necessary to initiate cell signaling. If P_i sensing occurs within the cell, one could reasonably expect inhibition of this major route of P_i entry to have at least some effect on the ERK1/2 signaling response, but dose-responses under both conditions were matched (Figure 2-5). Therefore we conclude that initial P_i sensing occurs outside the cell or at the cell surface.

We next addressed other ionic requirements by determining whether or not calcium played an essential role in the P_i sensing process. We prepared two saline solutions (both containing NaCl), one of which contained 2.5 mM $CaCl_2$ and one that omitted this salt. MC3T3-E1 cells were washed several times with these buffers and then incubated in them and treated with P_i for 20 minutes. As shown in Figure 2-6a, omitting calcium from the extracellular solution completely prevented the activation of ERK1/2 caused by incubation with 8 mM P_i. We also tested the requirement of extracellular

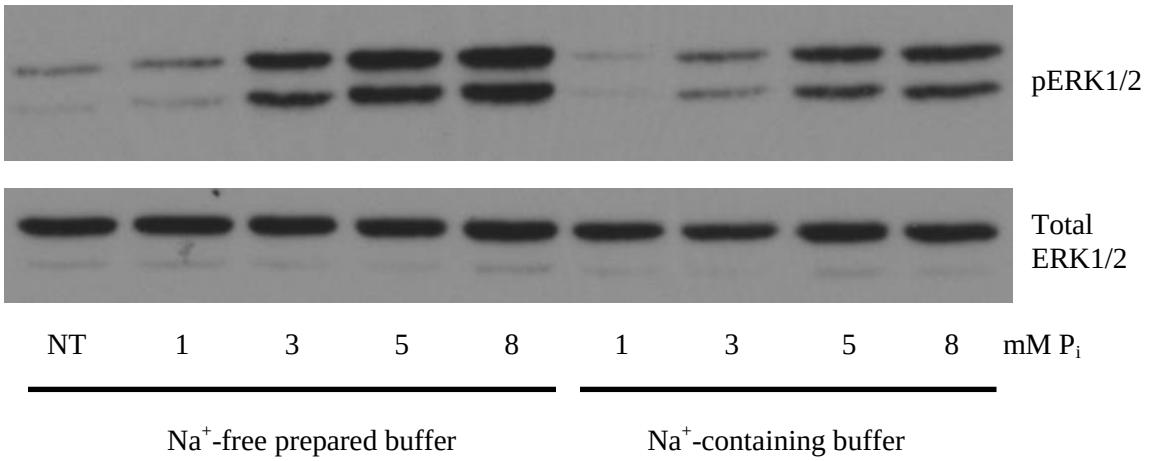

Figure 2-5: Requirement of extracellular sodium for cell signaling initiated by P_i treatment.
MC3T3-E1 cells were incubated for 1 hour in prepared salt buffers prior to treatment with potassium phosphate buffer resulting in the final P_i concentrations indicated. 'NT' indicates no treatment. The composition of the two buffers was as follows:
Na^+-free buffer: 137 mM choline chloride, 5.4 mM KCl, 2.8 mM $CaCl_2$, 1.2 mM $MgSO_4$, and 14 mM HEPES pH 7.5.
Na^+-containing buffer: 137 mM NaCl, 5.4 mM KCl, 2.8 mM $CaCl_2$, 1.2 mM $MgSO_4$, and 14 mM HEPES pH 7.5.
Note that both buffers lacked P_i. Cells were treated for 20 minutes, lysed and proteins were subjected to SDS-PAGE. Proteins were immunoblotted using antibodies against activated ERK1/2 and total ERK1/2.

calcium by adding 1 mM citric acid to the calcium-containing solution, which partially depleted the pool of extracellular free calcium ions. We found that this co-treatment also prevented activation of ERK1/2 following addition of 8 mM P_i (Figure 2-6a). Lack of extracellular calcium did not non-specifically inhibit all ERK1/2 activation, as treatment of MC3T3-E1 cells with basic FGF elicited the appropriate ERK1/2 response in the absence of supplied extracellular calcium (Figure 2-6a). To test whether calcium was required for P_i induced ERK1/2 activation within or outside the cell, we used two different calcium-binding compounds. EDTA, which does not enter the cell, was used to deplete free extracellular calcium ions but leave intracellular calcium intact. Lower concentrations of BAPTA-AM, which can enter the cell and must be cleaved by intracellular enzymes to become activated, were used to deplete intracellular calcium stores. MC3T3-E1 cells were incubated with these compounds in phosphate-free DMEM and treated with 8 mM P_i. The P_i treatment activated ERK1/2 within 20 minutes, but this activation was prevented by co-incubation with either 0.5 mM or 1 mM EDTA (Figure 2-6b). However, incubation with 1 μM or 10 μM BAPTA-AM, concentrations that have been shown to inhibit Ca^{2+}-dependent cell signaling processes, did not prevent P_i-induced ERK1/2 activation (Figure 2-6b). These results suggest that free calcium ions are required outside, but not inside, the cell for elevated P_i to cause activation of cell signaling.

A recent study examined the effect of pyrophosphate (PP_i) on MC3T3-E1 cells and found that, in addition to its known properties in inhibiting mineralization, PP_i also activated ERK1/2 signaling and induced osteopontin expression in a manner similar to P_i treatment (Addison et al., 2007). The authors concluded that the effects of PP_i were not

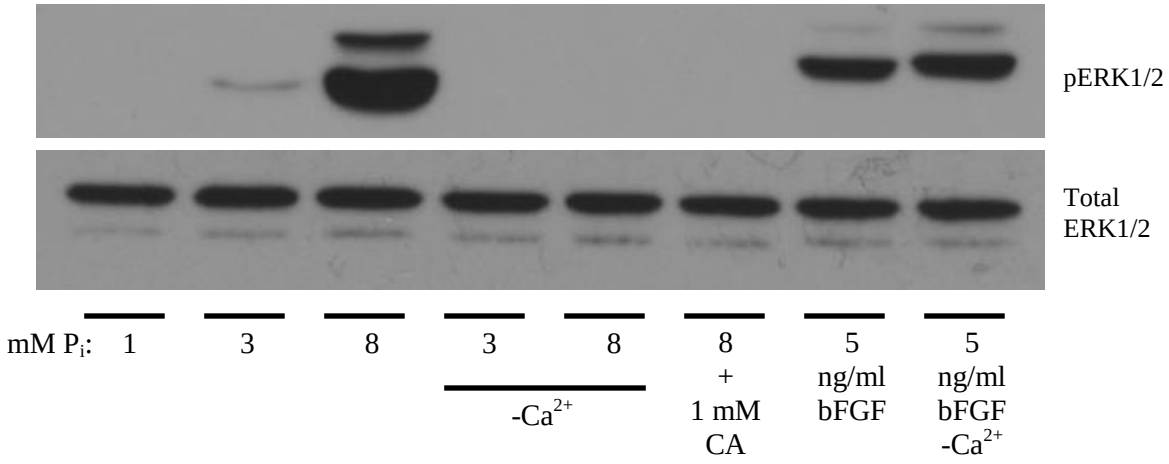

Figure 2-6a: Requirement of calcium for cell signaling initiated by P_i treatment MC3T3-E1 cells were incubated for 1 hour in prepared salt buffers prior to treatment with sodium phosphate buffer resulting in the final P_i concentrations indicated, or with bFGF. The buffer had the following composition: 137 mM NaCl, 5.4 mM KCl, 2.8 mM $CaCl_2$, 1.2 mM $MgSO_4$, and 14 mM HEPES pH 7.5. The center two lanes and rightmost lane were incubated in buffer with identical composition except $CaCl_2$ was omitted. 'CA' refers to co-incubation with citric acid. Cells were treated for 20 minutes, lysed and proteins were subjected to SDS-PAGE. Proteins were immunoblotted using antibodies against activated ERK1/2 and total ERK1/2.

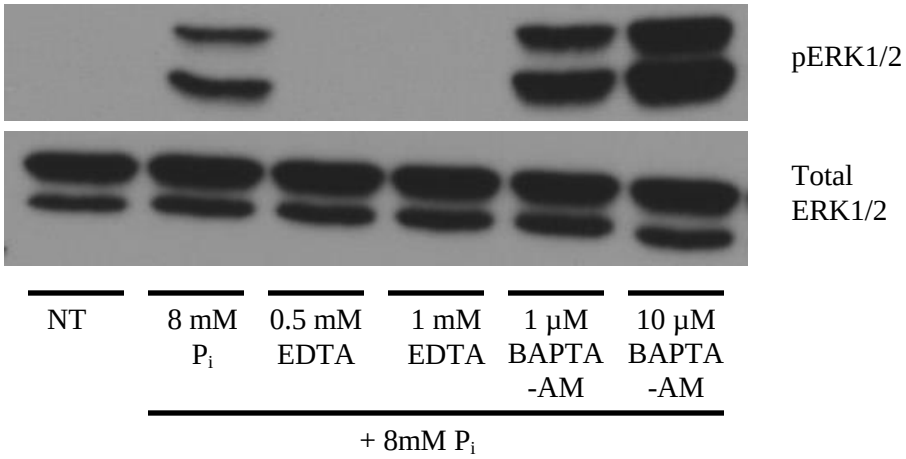

Figure 2-6b: Discriminating between an intracellular and extracellular Ca^{2+} requirement. MC3T3-E1 cells were incubated in serum-free DMEM lacking P_i for 1 hour prior to treatment and co-incubated with the indicated concentrations of EDTA or BAPTA-AM. 'NT' indicates no treatment. After pre-treatment, cells were incubated with the indicated concentrations of sodium phosphate buffer for 20 minutes. Cells were then lysed and proteins were subjected to SDS-PAGE. Proteins were immunoblotted using antibodies against activated ERK1/2 and total ERK1/2.

simply the result of PP_i cleavage into two P_i molecules because: 1) PP_i had its effects at lower concentrations (500 μM) than could be achieved by the equivalent amount of P_i after cleavage (1 mM, which has no effect) and 2) inhibition of alkaline phosphatase activity by levamisole did not prevent PP_i from having its effects. PP_i, therefore, appears to have an effect related to but distinct from elevated extracellular phosphate. Nevertheless, we thought it was intriguing that these two closely related substances, P_i and PP_i, shared some but not all cell signaling properties, implying that the cell is able to sense each independently. To further explore the cell signaling properties of PP_i, we subjected MC3T3-E1 cells to similar experiments using P_i described above. First, we performed a dose-response experiment using both P_i and PP_i. MC3T3-E1 cells were treated for 15 minutes with P_i in concentrations ranging from 1 mM to 10 mM or PP_i in concentrations ranging from 100 μM to 1 mM. P_i treatments up to 6 mM did not activate ERK1/2 in the time frame of this experiment while 8 and 10 mM P_i caused ERK1/2 activation (Figure 2-7a). In contrast, PP_i treatment at 100 μM caused slight activation of ERK1/2 while 500 μM and 1 mM treatments caused robust activation of ERK1/2, consistent with the finding by Addison et al. that a lower concentration of PP_i is needed to achieve equivalent effects (Figure 2-7a). We next determined if extracellular Na^+ and Ca^{2+} were required to be present for PP_i to activate cell signaling. MC3T3-E1 cells were incubated in prepared saline solutions lacking Na^+ or Ca^{2+} and treated with 500 μM PP_i. Interestingly, PP_i had similar ionic requirements as P_i; Ca^{2+} was required in the extracellular solution while Na^+ was dispensable for ERK1/2 activation (Figure 2-7b). Reducing free extracellular calcium with citric acid also inhibited ERK1/2 activation by PP_i, though a higher concentration of citric acid was required for this effect than for the

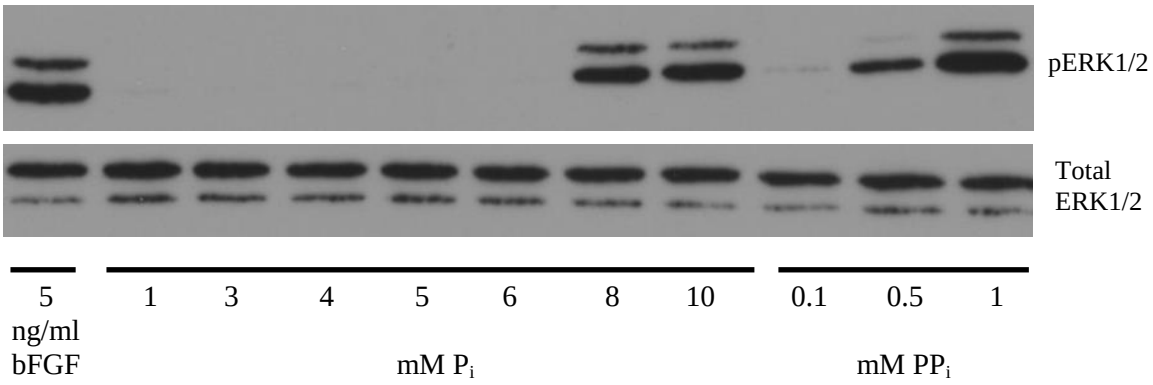

Figure 2-7a: Comparison of ERK1/2 activation following P_i and PP_i treatment. MC3T3-E1 cells were incubated in serum-free DMEM lacking P_i for 1 hour prior to treatment with P_i or PP_i at the final concentrations indicated. Cells were treated for 15 minutes then lysed and proteins were subjected to SDS-PAGE. Proteins were immunoblotted using antibodies against activated ERK1/2 and total ERK1/2.

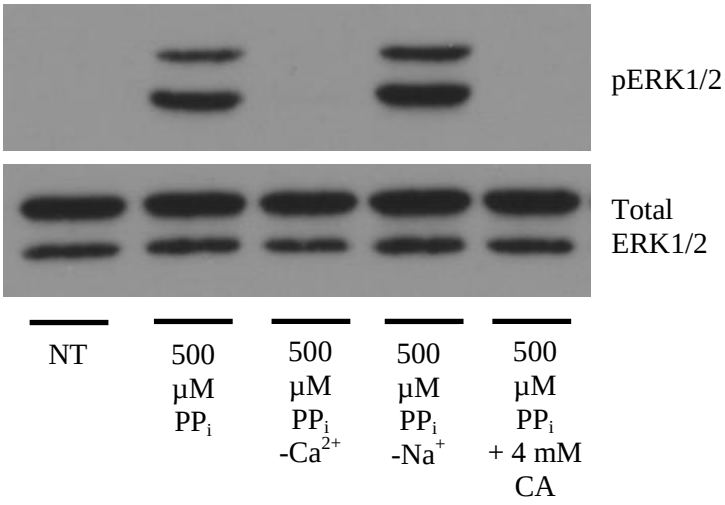

Figure 2-7b: Ionic requirements for ERK1/2 activation by pyrophosphate. MC3T3-E1 cells were incubated in prepared salt buffers for 1 hour prior to treatment. The buffers contained the following: 137 mM NaCl, 5.4 mM KCl, 2.8 mM $CaCl_2$, 1.2 mM $MgSO_4$, and 14 mM HEPES pH 7.5. The '-Na^+' buffer substituted choline chloride for NaCl, while the '-Ca^{2+}' buffer omitted $CaCl_2$. 'NT' refers to no treatment, and CA refers to citric acid co-incubation. Cells were treated for 20 minutes with 500 µM PP_i. Cells were then lysed and proteins were subjected to SDS-PAGE. Proteins were immunoblotted using antibodies against activated ERK1/2 and total ERK1/2.

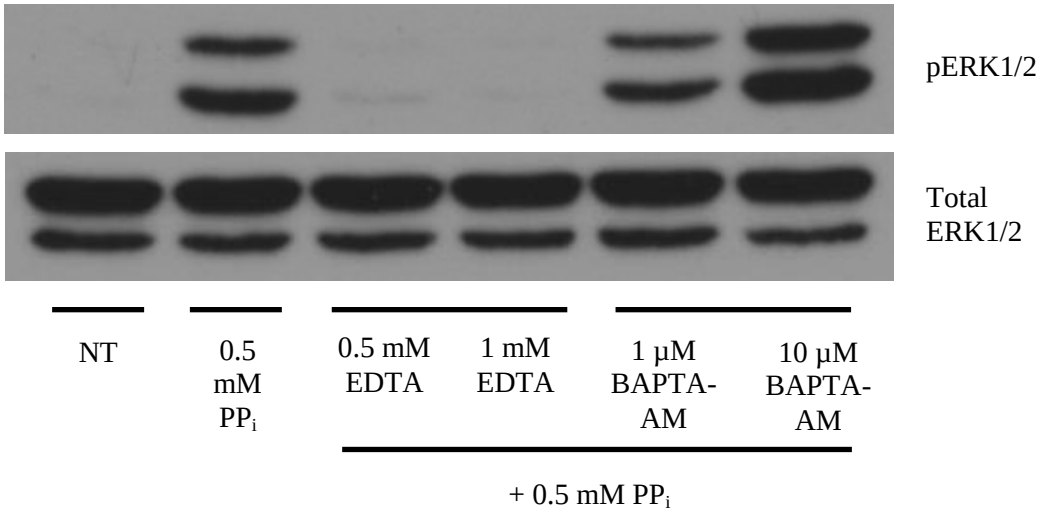

Figure 2-7c: Discriminating between an intracellular and extracellular Ca^{2+} requirement for PP_i signaling. MC3T3-E1 cells were incubated in serum-free DMEM for 1 hour prior to treatment and co-incubated with the indicated concentrations of EDTA or BAPTA-AM. 'NT' indicates no treatment. After pre-treatment, cells were incubated with the indicated concentrations of PP_i for 20 minutes. Cells were then lysed and proteins were subjected to SDS-PAGE. Proteins were immunoblotted using antibodies against activated ERK1/2 and total ERK1/2.

inhibition of P_i-induced signaling (Figure 2-7b). Incubation with EDTA also prevented ERK1/2 activation by 500 µM PP_i while 1 or 10 µM BAPTA-AM had no effect (Figure 2-7c), indicating that PP_i also requires extracellular, but not intracellular, calcium to initiate cell signaling.

An important piece of evidence in support of the hypothesis that the effects of elevated P_i require its entry into the cell is that co-treatment with PFA, which inhibits PiT-1 and PiT-2 transport activity, eliminates these effects. To investigate this interaction further, we incubated MC3T3-E1 cells in a prepared saline buffer in which NaCl was substituted with choline chloride. We then treated these cells for 20 minutes with 8 mM potassium phosphate (KP_i) buffer and co-treated with 0-2 mM PFA. Since the Na^+ gradient is compromised by lack of extracellular Na^+ under these conditions, we would not expect PFA to further impair Na^+-dependent P_i transport in these cells. However, we observed that co-incubation with PFA did in fact inhibit activation of ERK1/2 by addition of the KP_i buffer in a dose-dependent manner (Figure 2-8a). We performed a similar experiment with PP_i by incubating MC3T3-E1 cells in the same prepared buffers and co-incubating PP_i and PFA. The PP_i solution contains Na^+ as a counter-ion, however the concentration used (500 µM) is very low compared to usual extracellular concentrations (130-150 mM), and therefore a functional sodium gradient is still absent under these conditions. Surprisingly, we found that PFA also inhibited activation of ERK1/2 caused by PP_i treatment (Figure 2-8b). There is no known PP_i importing system, Na^+-dependent or otherwise, that would support the notion of PP_i entry as a requirement for activation of cell signaling. Yet since the signal-initiating properties of both P_i and PP_i are inhibited by PFA, these results suggest that some property of PFA

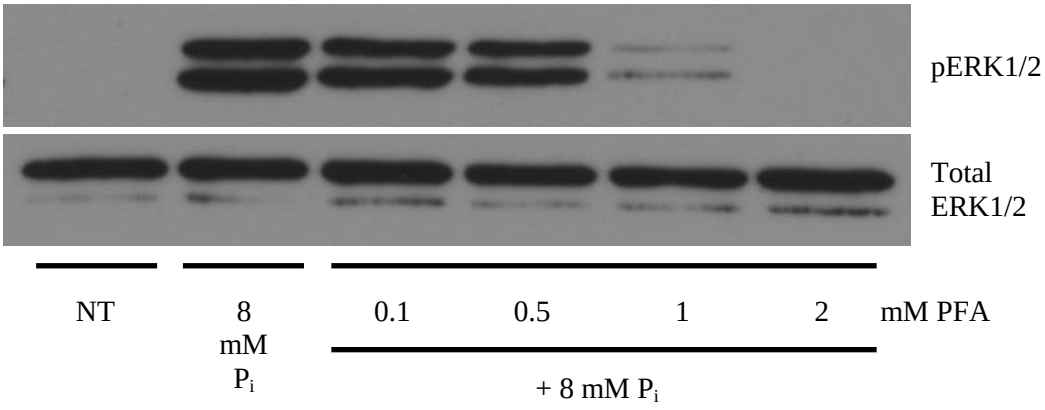

Figure 2-8a: Effect of PFA co-incubation on P_i-induced cell signaling.
MC3T3-E1 cells were incubated in Na^+-free prepared buffer for 1 hour prior to treatment. 'NT' refers to no treatment. Cells were treated for 20 minutes with potassium phosphate buffer to yield a final concentration of 8 mM P_i. Cells were also co-treated with increasing concentrations of phosphonoformic acid (PFA) as indicated. Cells were then lysed and proteins were subjected to SDS-PAGE. Proteins were immunoblotted using antibodies against activated ERK1/2 and total ERK1/2.

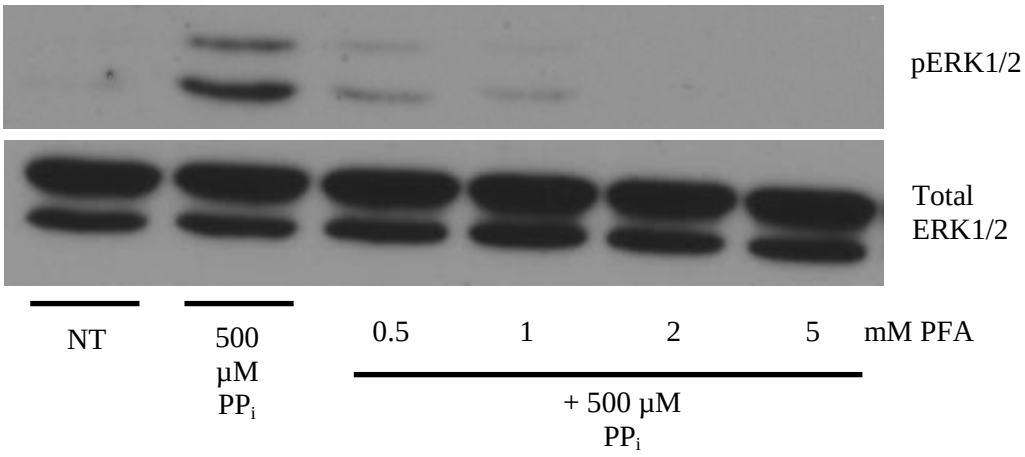

Figure 2-8b: Effect of PFA co-incubation on PP_i-induced cell signaling.
MC3T3-E1 cell were incubate in serum-free DMEM for 1 hour prior to treatment. 'NT' refers to no treatment. Cells were treated for 20 minutes with 500 µM PP_i and co-incubated with increasing concentrations of phosphonoformic acid (PFA) as indicated. Cells were then lysed and proteins were subjected to SDS-PAGE. Proteins were immunoblotted using antibodies against activated ERK1/2 and total ERK1/2.

other than its ability to impede Na^+-dependent P_i uptake is responsible for inhibiting cell signaling induced by these molecules.

The results presented thus far indicate that initial sensing of P_i occurs outside the cell or at the cell surface, and that extracellular calcium is required for this process. One possible explanation that could account for these observations is that P_i itself is not the molecule that is sensed by cells but rather a complex of calcium and P_i that is formed outside the cells. It has been previously noted that addition of P_i in calcium-containing culture medium can potentially result in the formation of such complexes when these two ions are present in concentrations that exceed their solubility limit (see Discussion below). To determine if such complexes form under the conditions used in our cell culture experiments, we performed a series of *in-vitro* assays using the chemically defined buffers we had prepared previously for those studies. When the Pi concentration was raised to 10 mM in a cuvette containing 2.5 mM $CaCl_2$ and other salts, a white precipitate formed over the course of several minutes. To monitor the formation of this precipitate in a quantitative manner, we measured the absorption spectra of the salt buffer lacking P_i, the P_i solution, and the precipitate that is formed after the P_i solution is added to the salt buffer to raise the concentration of P_i in the combined solution to 10 mM (see Figure 2-9a and Methods). Both the salt buffer and the P_i buffer individually had little light absorbance at wavelengths between 250 and 600 nm. However, when P_i was added to the salt solution to a final concentration of 10 mM and incubated for several minutes, a broad absorbance peak covering much of this range (250-600 nm) appeared (Figure 2-9a), co-incident with precipitate formation. We chose to monitor precipitate formation at 300 nm because this wavelength fell within the broad absorbance peak caused by

precipitate formation but there is little absorbance at this wavelength in either solution before they are combined. We next monitored the formation of precipitates after addition of various concentrations of P_i buffer over time to determine if these precipitates could form within the time frame of the cell signaling experiments (less than 15 minutes). As shown in Figure 2-9b, raising the P_i concentration to 2.5 mM, 5 mM or 10 mM resulted in the formation of precipitates within 4 minutes as measured by absorbance at 300 nm. The highest dose of P_i (10 mM) resulted in the most precipitate formation, though the 2.5 mM dose also resulted in some detectable precipitate formation, but additional precipitate formation had ceased by 4 minutes at this dose. These *in vitro* assays demonstrate that precipitates can indeed form using the same buffers and within the time frame of the previous cell signaling experiments. We next established that calcium is a necessary component of these precipitates by using the salt buffers including or lacking 2.5 mM $CaCl_2$. When 10 mM P_i was added to the buffer lacking $CaCl_2$, no precipitate formed over the course of 4 minutes as was the case for the buffer including calcium (Figure 2-9c). If citric acid is added to the buffer including calcium, there again is a lack of precipitate formation following P_i addition, suggesting free calcium and phosphate ions are necessary components of the precipitates.

We next used this *in vitro* assay to evaluate the effect that addition of PFA has on mineral precipitate formation. We added 5 mM P_i buffer to the salt buffer containing no added PFA or PFA at concentrations of 1 mM, 3 mM or 5 mM. The presence of PFA impeded the formation of precipitates as measured by absorbance at 300 nm in a dose dependent manner, with precipitation almost completely inhibited by co-incubation with 3 mM PFA (Figure 2-9d). Similar results were obtained by incubation of PFA with 10

mM P_i in the salt buffer, though the inhibition of mineral precipitation was less complete (data not shown). Thus, PFA has an inherent ability to inhibit mineral formation in a cell-free system, which could account for the ability of this compound to inhibit the effects P_i treatment on cells independent of the effects it may have on cellular P_i uptake. We then hypothesized that similar chemical characteristics might account for the effects of PP_i treatment on cells. When 500 μM or 1 mM PP_i was added to the salt buffer solution, a large amount of white precipitate was quickly formed. This precipitate had similar spectroscopic properties as the precipitate formed by P_i addition, and we used absorbance at 300 nm to monitor the formation of the PP_i precipitate over time. Precipitate formation began quickly after addition of PP_i to the salt buffer solution, and after 4 minutes the precipitate formed by a concentration of 1 mM PP_i had an absorbance reading over twice that of the precipitate formed after raising the P_i concentration to 10 mM (compare Figures 2-9b and 2-9e). Addition of PP_i to salt buffer lacking calcium produced no precipitate, and addition of citric acid also slowed the formation of precipitates following PP_i addition (Figure 2-9e), suggesting that Ca^{2+} and PP_i are necessary components for precipitate formation. Co-incubation of 3 mM PFA with 500 μM PP_i also impeded precipitate formation, suggesting that the effect of PFA on cell signaling induced by PP_i might also be accounted for by its ability to inhibit mineral formation (Figure 2-9e). Lastly, we determined if precipitates might be formed in the DMEM cell culture solutions used for some of our previous experiments as they had in our chemically defined salt buffers. We added either KP_i buffer or NaP_i buffer to cell culture dishes containing serum-free DMEM to a final concentration of 10 mM P_i, recapitulating the conditions our cell culture experiments, but in the absence of cells, to

facilitate visualization of any precipitates that might form. We found that addition of the excess phosphate resulted in the formation of precipitates near the bottom of the cell culture dish that could be visualized within 15-30 minutes (Figure 2-10). Interestingly, the two different P_i buffers produced structurally distinct precipitates. Addition of the KP_i buffer resulted in the formation of larger, more diffuse precipitates while addition of the NaP_i buffer produced smaller precipitates that seeded on the bottom of the cell culture dish and slowly grew in size over time, eventually forming a coating that covered the bottom surface of the dish (Figure 2-10). Notably, the appearance of these precipitates was much more difficult to discern by light microscopy when cells were present in the dish, though the precipitates caused by KP_i addition could still be seen with careful observation.

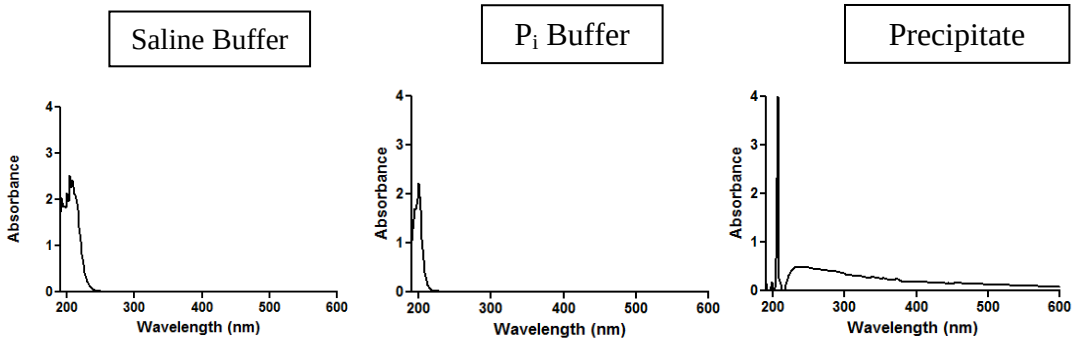

Figure 2-9a: UV-Visual light spectrum of saline buffer, P_i buffer, and precipitate formed after buffers are combined. Absorption spectra over the 200-600 nm range were obtained of the prepared saline buffer (137 mM NaCl, 5.4 mM KCl, 2.8 mM $CaCl_2$, 1.2 mM $MgSO_4$, and 10 mM HEPES pH 7.5), and the P_i buffer (sodium phosphate pH 7.1). The absorption spectrum was also obtained of the precipitate formed after addition of P_i buffer to the saline buffer to yield a final concentration of 10 mM P_i in the combined solution. The spectrum was obtained 10 minutes after the two buffers were combined.

b.

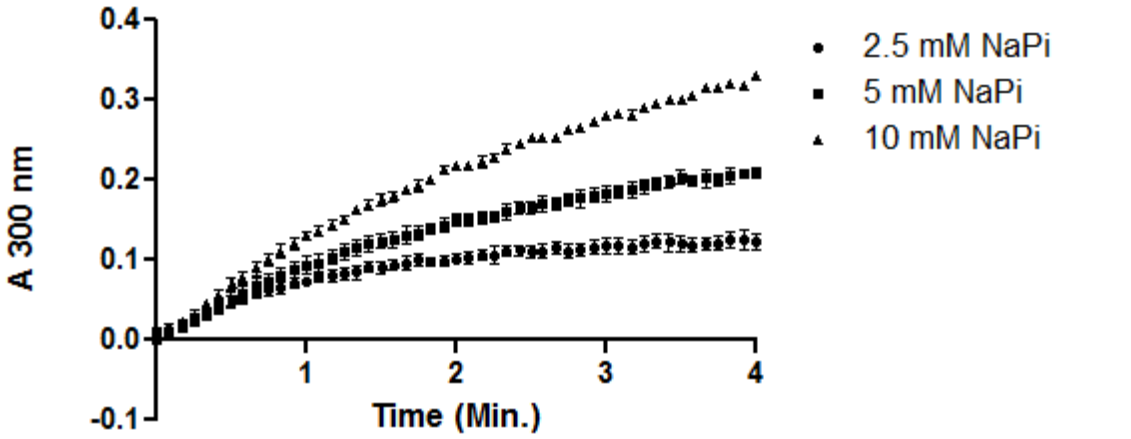

c.

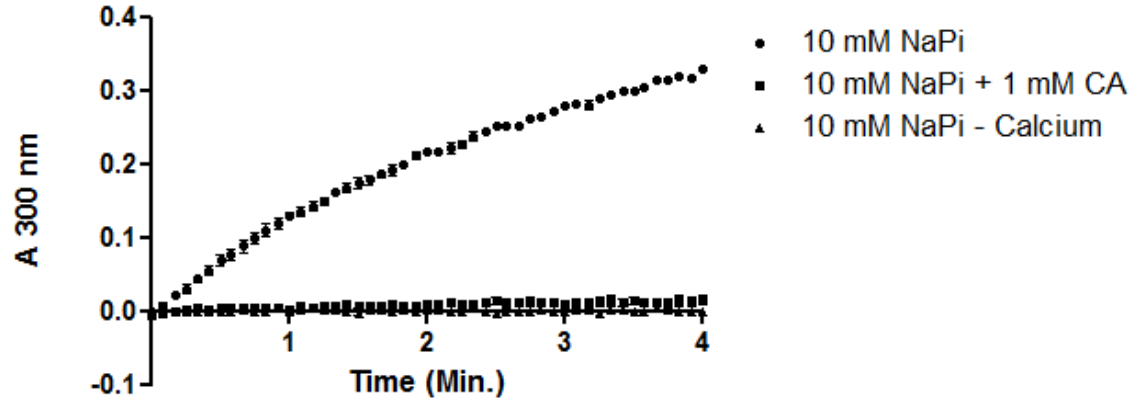

Figure 2-9b: Formation of precipitates following addition of P_i to saline buffer.
Sodium phosphate buffer (NaP_i) was added to saline buffer at time = 0 to yield the final concentrations indicated and absorbance at 300 nm was recorded. Measurements are averages of 3 independent trials and bars represent standard error about the mean.

Figure 2-9c: Requirement of calcium for formation of precipitates.
Sodium phosphate buffer (NaP_i) was added to saline buffer at time = 0 to yield a final concentration of 10 mM and absorbance at 300 nm was recorded. The requirement of calcium was tested by omitting Ca^{2+} (- Ca^{2+}) from the buffer or by adding 1 mM citric acid (CA). Measurements are averages of 3 independent trials and bars represent standard error about the mean.

d.

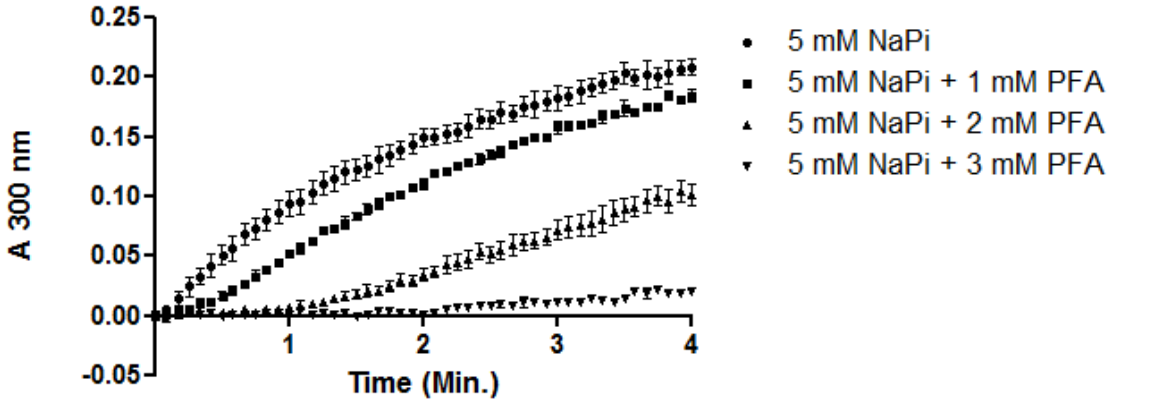

e.

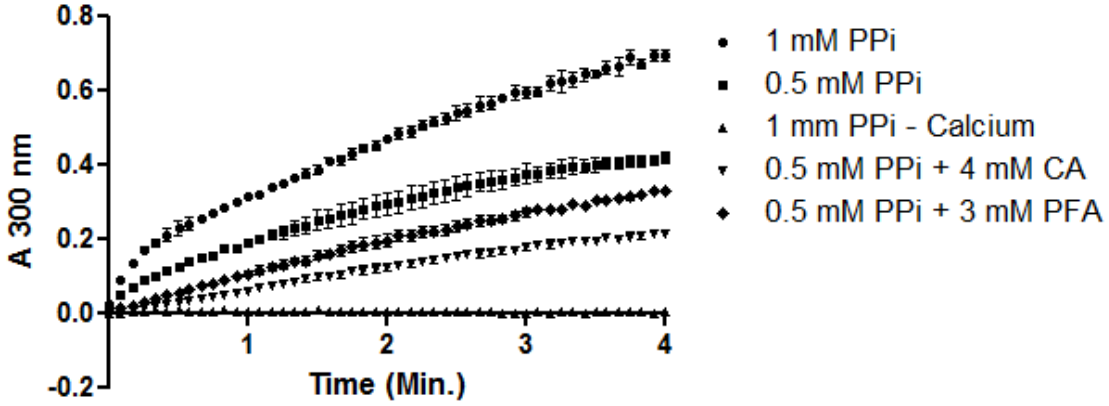

Figure 2-9d: Effect of PFA co-incubation on precipitate formation over time. Sodium phosphate buffer (NaP_i) was added to saline buffer at time = 0 to yield a final concentration of 5 mM P_i and absorbance at 300 nm was recorded. Phosphonoformic acid (PFA) was co-incubated at the indicated concentrations. Measurements are averages of 3 independent trials and bars represent standard error about the mean.

Figure 2-9e: PPi precipitation and effect of calcium and PFA on precipitation. Sodium pyrophosphate (PP_i) buffer was added to saline buffer at time = 0 to yield a final concentration of 0.5 mM or 1 mM as indicated and absorbance at 300 nm was recorded. The requirement of calcium was tested by omitting Ca^{2+} (- Ca^{2+}) or by adding citric acid (CA). PFA was co-incubated at the indicated concentration. Measurements are averages of 3 independent trials and bars represent standard error about the mean.

a.

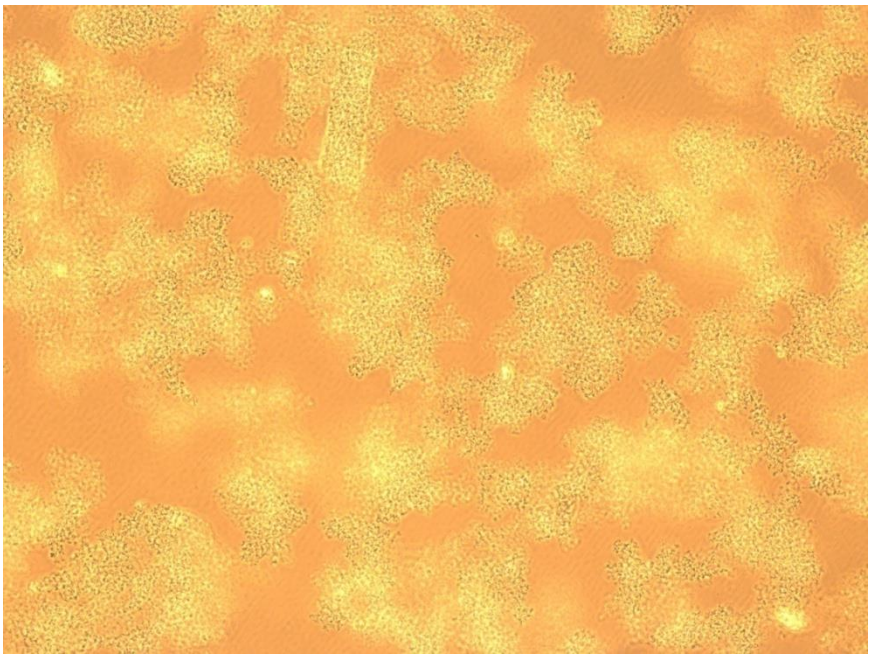

b.

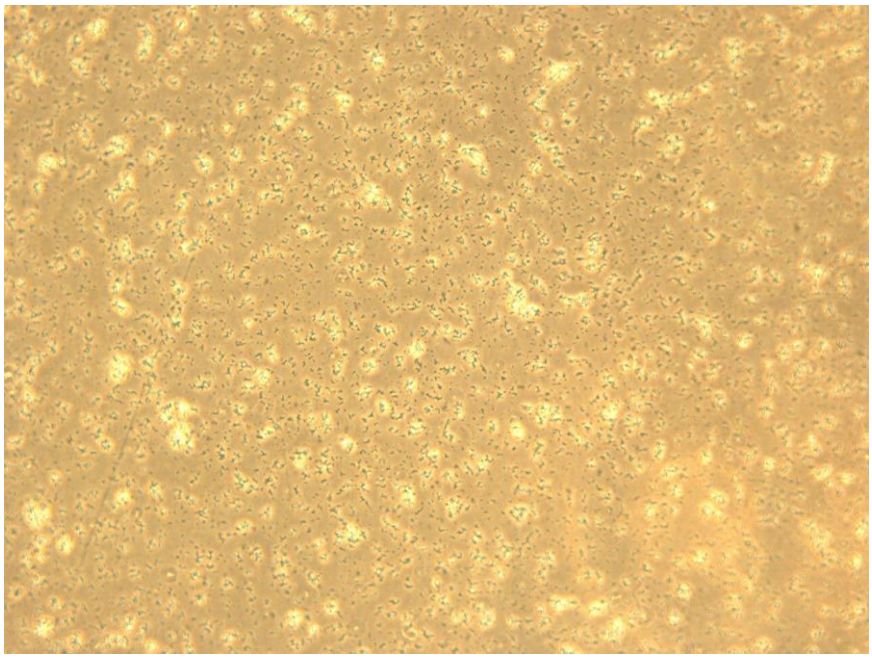

Figure 2-10: Precipitation of mineral in serum-free DMEM.
Potassium phosphate (a.) or sodium phosphate (b.) buffer was added to serum-free DMEM to a final concentration of 10 mM and incubated for 30 minutes. Light microscopy images (100X total magnification) were taken of precipitates near the bottom surface of the cell culture dishes.

2.4 Discussion

Recent research in the fields of bone biology and the pathology of abnormal mineral metabolism has revealed a potential new biological role of inorganic phosphate in the extracellular environment. In the process of bone development and mineralization, high local concentrations of P_i is are produced by cellular activity and combine with calcium to form mineral at appropriate extracellular locations. Using cell culture studies, Beck et al. found that incubation with high concentrations of P_i could activate certain cell signaling pathways and induce the expression of osteopontin, a protein expressed in bone cells and secreted into the extracellular space where it regulates mineral formation (Beck et al., 2000). Extracellular P_i may therefore serve a feedback mechanism to cells in a mineralizing environment: after sufficient P_i has been generated outside the cell, it signals that conditions are appropriate for subsequent developmental steps, such as osteopontin production. In cells other than osteoblasts that are exposed to a local environment of elevated P_i, some of these osteoblast developmental processes may be induced inappropriately (Lau et al., 2011). Such phenotypic transformations have indeed been observed in mouse models of vascular calcification. However, the extent to which these transformations cause or exacerbate vascular pathology, or are instead the secondary effects of prior vascular calcification, is a subject of ongoing research.

We performed a series of cell-culture experiments in an effort to gain an understanding of how cells sense an elevation in the extracellular concentration of P_i. Previous studies had suggested that P_i must enter the cell via Na^+-dependent co-transporters where an unidentified P_i-responsive mechanism begins a cell signaling response that includes activation of ERK1/2. However, we found that P_i-induced

signaling was unaffected after modifying extracellular ion concentrations to eliminate the Na^+ gradient across the cell plasma membrane. In contrast, sufficient extracellular calcium ions were essential for P_i-induced signaling. We found similar extracellular requirements for signaling induced by PP_i. While co-treatment with PFA, a compound known to inhibit Na^+-dependent P_i co-transporters, did indeed block activation of ERK1/2 caused by treatment with elevated P_i, it also blocked signaling induced by PP_i, which does not use an equivalent importing system. This result prompted the hypothesis that PFA has its inhibitory effects for reasons other than its ability to inhibit ion transport. Indeed, several recent studies by Sorribas et al. suggest that PFA has inhibitory effects in studies of this type because of its ability to inhibit mineral formation, not because it blocks ion transport (Villa-Bellosta and Sorribas, 2009).

The requirement of extracellular, rather than intracellular, calcium raised the possibility that P_i and calcium ions could be forming precipitates during the course of our cell culture experiments. We performed a series of *in vitro* studies and determined that precipitates do form under the conditions used in the previous experiments, both in the prepared salt buffers and in serum-free DMEM. Therefore, treatment with P_i may affect cells first by forming mineral precipitates that in turn interact with cells and elicit a response from them. This concept has some precedents in the research literature. Beck et al. refer to two earlier studies that had previously noted that PFA has the capacity to inhibit mineral formation (Fleisch et al., 1970; Williams and Sallis, 1979), though they concluded that this property was not responsible for its inhibition of P_i-induced signaling (Beck et al., 2000). In the field of arthritis research, Cheung et al. have treated cells with basic calcium phosphate crystals (BCPs) and observed activation of the ERK1/2 pathway

(Nair et al., 1997). Finally, Chung et al. noted the formation of calcium phosphate precipitates in cell culture using the osteogenic media, and such precipitation could also occur in cell-free systems (Chung et al., 1992). The authors therefore suggested avoiding incubating cells in concentrations of P_i over 2 mM to avoid mineral formation that is not the result of cellular activity. Sorribas et al. documented "progressive mineralization" on cells that had been killed, emphasizing the need to carefully distinguish between cell culture mineralization that is due to cellular activity or merely the result of precipitation of inorganic ions (Villa-Bellosta and Sorribas, 2009). Nevertheless, many researchers continue to use the established cell culture mineralization assay with P_i or β-glycerophosphate concentrations of 10 mM and attribute all subsequent mineralization to cellular activity.

We confirmed that cell signaling is activated in cultured osteoblasts and fibroblasts following incubation with elevated concentrations of P_i. This process was dependent on extracellular calcium and not extracellular sodium. These properties were shared by PP_i-induced signaling, suggesting that these stimuli may share a common mechanism of action. We found that precipitates quickly formed under the conditions used in the cell culture experiments and at concentrations that correlated with activation of cell signaling. These data support an alternative hypothesis in which calcium-containing precipitates, rather than P_i or PP_i ions, elicit the observed cellular responses.

CHAPTER THREE

Studies of Osteopontin Gene Induction in Response to Phosphate Treatment

3.1 Introduction

During the mineralization process of normal bone development, calcium and phosphate ions are released by cells into the extracellular space. These ions will precipitate in specialized extracellular tissue environments and eventually form the major inorganic components of bone. Recent studies and experiments presented here suggest that high concentrations of phosphate, such as those present during bone development, can in turn affect cellular behavior, possibly representing a novel feedback mechanism that regulates bone cell development (Beck et al., 2000). We have further investigated the mechanism by which elevated extracellular phosphate causes these cellular responses, and have presented evidence that calcium phosphate precipitates, rather than the phosphate ion alone, cause activation of cell signaling following phosphate treatment. These calcium phosphate complexes could also be considered physiologically relevant developmental signals since they also appear during bone development. As mineralization proceeds, osteoblasts come into contact with newly created mineral and this interaction may indicate to cells how far bone development has progressed. This signaling mechanism may also be operating in situations of abnormal mineral ion

concentrations or locations where mineral has formed ectopically. In these cases, there is concern that elevated extracellular phosphate or mineral could be causing changes in cell behavior that favor further mineral deposition. This concern is substantiated by evidence that cells at sites of ectopic mineralization produce proteins that are not typically expressed at those sites but rather in bone cells.

Osteopontin Structure and Mineralization Function

One representative of such proteins is osteopontin (OPN), a multifunctional and structurally complex secreted protein. OPN is expressed in cartilaginous regions prior to bone mineralization as well as mature bones in the adult, the kidneys, and epithelial linings. OPN also acts as a cytokine and is highly expressed in tissue macrophages and some T cells (Scatena et al., 2007). The OPN protein contains an arginine-glycine-aspartate (RGD) containing domain, which is known to facilitate cell-surface integrin binding. OPN also contains a collagen-binding domain, prompting the hypothesis that one of the functions of OPN is to act as a link between cells and collagen rich extracellular matrix. OPN also contains several putative mineral-binding regions, such as a stretch of nine consecutive aspartic acid residues near the N-terminus of the protein. Many post-translational modifications of OPN have also been documented, including 28 N- and O-linked glycosylation sites and 19 phosphorylation sites (George and Veis, 2008). These many charged residues and post-translational modifications provide the chemical characteristics that may confer to OPN proteins the ability to bind extracellular mineral.

Studies of OPN knockout mice have revealed roles for this protein in modifying the mineral structure of bone. While mice lacking OPN did not exhibit any obvious

histological differences in gross bone structure, detailed analysis of the mineral content of bone showed that OPN knockout mice have greater mineral density in cortical bone and that the bone mineral is more mature (greater mineral crystal size and perfection) than in wild-type controls (Boskey et al., 2002). These results led the authors to conclude that OPN functions to inhibit mineral deposition and maturation, either directly or indirectly. These results are also consistent with *in-vitro* studies showing that OPN directly binds and inhibits the growth of hydroxyapatite mineral (Boskey et al., 1993; Hunter et al., 1994). In the bone, therefore, OPN appears to play a role in controlling and limiting mineralization during development.

Osteopontin and Inflammation

OPN is expressed abundantly in tissue macrophages and has macrophage-chemotactic activity (Scatena et al., 2007**).** OPN may play a key role in situations where organic or inorganic extracellular debris must be cleared by macrophages. One study found that calcified cellular debris became coated with OPN molecules that were then taken up and cleared by macrophages (McKee and Nanci, 1995). OPN also appears to support chronic inflammatory processes. Mice deficient in OPN exhibited less macrophage infiltration and a milder inflammatory response in a variety of models of chronic inflammation (Scatena et al., 2007). OPN is also a subject of research in cancer biology because OPN is overexpressed in a variety of cancers. In these cases, OPN may contribute to cancer progression by modulating the inflammatory response in a way that favors tumor growth (Fedarko et al., 2001).

Osteopontin and Vascular Damage

The mineral binding and inflammatory functions of OPN may both be activated in locations when the protein is expressed in locations of vascular damage. In mice lacking matrix Gla protein (MGP), another secreted mineral binding protein, blood vessels spontaneously calcify leading to premature death by 3 months of age (El-Maadawy et al., 2003). OPN expression was greatly increased near the sites of these ectopic calcifications, and lacking both MGP and OPN further increased the extent of vascular calcification (Speer et al., 2009). In this setting, OPN appears to be induced by mineral formation and to defend against further mineral deposition. OPN is also induced in vascular cells (endothelial cells and smooth muscle cells) near sites of atherosclerotic plaques and in plaque-associated macrophages, though whether OPN is harmful or beneficial for controlling the growth and stability of plaques remains under investigation (Scatena et al., 2007).

Osteopontin in the Kidney

OPN can also be induced in renal tubule cells in response to renal injury in several disease models. Cell culture and *in vitro* studies demonstrated that OPN can bind and interfere with the growth of calcium oxalate crystals, a mineral commonly found to nucleate kidney stones (Wesson et al., 1998). In the ethylene glycol feeding model of calcium oxalate nephrolithiasis, mice lacking OPN developed intra-tubular deposits of calcium oxalate crystals while wild-type mice developed no such deposits at equivalent doses of ethylene glycol (Wesson et al., 2003). Cell culture studies also indicated that oxalate crystals directly induce OPN expression (Umekawa et al., 2006). Therefore,

OPN may serve a similar protective role against ectopic mineral formation in the kidney as it does in vascular tissue.

As mentioned above, Beck et al. observed OPN induction in MC3T3-E1 cells following treatment with high concentrations of phosphate (Beck et al., 2000). To determine if the requirements for cell signaling induced by phosphate also apply to gene induction, we performed cell culture experiments using OPN as a model gene. We were particularly curious to know if precipitate formation was required for OPN induction since this protein has a known ability to bind mineral.

3.2 Methods

Cell Culture

MC3T3-E1 osteoblast precursor cells and 3T3-L1 fibroblasts were obtained from American Type Culture Collection (ATCC). Cells were cultured in 10 cm dishes and experiments were performed in 12 well plates purchased from Corning-Costar. Cells were maintained using Dulbecco's Modified Eagle Medium (DMEM) supplemented with 10% fetal bovine serum (FBS) and antibiotics (penciling and streptomycin, 100 U/ml and 100 µg/ml respectively), all obtained from Life Technologies, Gibco Brand. 100 mM stock buffers of sodium phosphate (pH 7.5) and calcium chloride (pH 7.0) were used for experimental treatments. Citric acid was obtained from Sigma-Aldrich and basic FGF was obtained from Santa Cruz Biotechnology.

Immunoblot Analysis

Cells were collected in cell lysis buffer (20 mM HEPES, 100 mM NaCl, 1.5% Triton-X100, 15 mM NaF, 20 mM phosphatase inhibitor cocktail (Sigma), protease inhibitor mix (Roche), 1 mM EDTA and 20 mM sodium pyrophosphate) and centrifuged for 10 minutes at 13,000 rpm. Supernatants were collected and SDS sample buffer was added before boiling samples for 5 minutes. Protein samples were subjected to SDS-polyacrylamide gel electrophoresis (SDS-PAGE) and proteins were then transferred to nitrocellulose membranes. Membranes were incubated in blocking buffer (2% milk, 0.05% v/v Tween 20 in TBS) then incubated with primary antibodies. The phospho-ERK1/2, and total ERK1/2 antibodies were obtained from Cell Signaling Technologies, while the β-tubulin, osteopontin and IRS-1 antibodies were obtained from Santa Cruz Biotechnologies. All antibodies were diluted at a ratio of 1:1000 except β-tubulin, which

was diluted 1:2000. Membranes were washed in a TBS-Tween solution and then incubated with appropriate secondary antibodies conjugated with horseradish peroxidase (GE Healthcare). Blots were developed using SuperSignal West Dura Extended Duration Substrate from Thermo Scientific.

3.3 Results

Our previous experiments demonstrated that treatment with elevated extracellular P_i caused activation of the kinases ERK1/2 and that this response required extracellular calcium as a co-factor (Figure 2-2 and Figure 2-6). The OPN gene is induced in cultured osteoblasts following incubation with elevated concentrations of extracellular P_i (Beck et al., 2000), while mineral formation appears to induce OPN expression in nearby tissues *in vivo* (Speer et al., 2009). Since mineral formation occurs in cell culture conditions quickly after the addition of P_i and these precipitates are likely the true stimulus for ERK1/2 activation, we hypothesized that OPN induction following incubation with P_i also requires the formation of calcium phosphate precipitates. To test this hypothesis, we treated MC3T3-E1 cells incubated in DMEM containing 10% FBS with a 6 mM or 8 mM final concentration of P_i for 48 hours. As shown in Figure 3-1, osteopontin protein could be detected by immunoblotting in MC3T3-E1 cells treated with either 6 or 8 mM P_i for 48 hours, but not in untreated cells. To determine if sufficient free extracellular calcium ions are an essential co-requirement for the induction of OPN by P_i treatment, we supplemented the culture medium with 2 mM citric acid. This concentration of citric acid was adequate to prevent precipitation when 10 mM P_i was added to prepared salt buffer (Figure 2-9c). When MC3T3-E1 cells were incubated with 6 or 8 mM P_i for 48 hours in DMEM supplemented with citric acid, no production of OPN protein was observed (Figure 3-1). These results suggest that, like activation of ERK1/2 by P_i treatment, production of OPN protein following P_i treatment requires sufficient free extracellular calcium ions to facilitate precipitate formation.

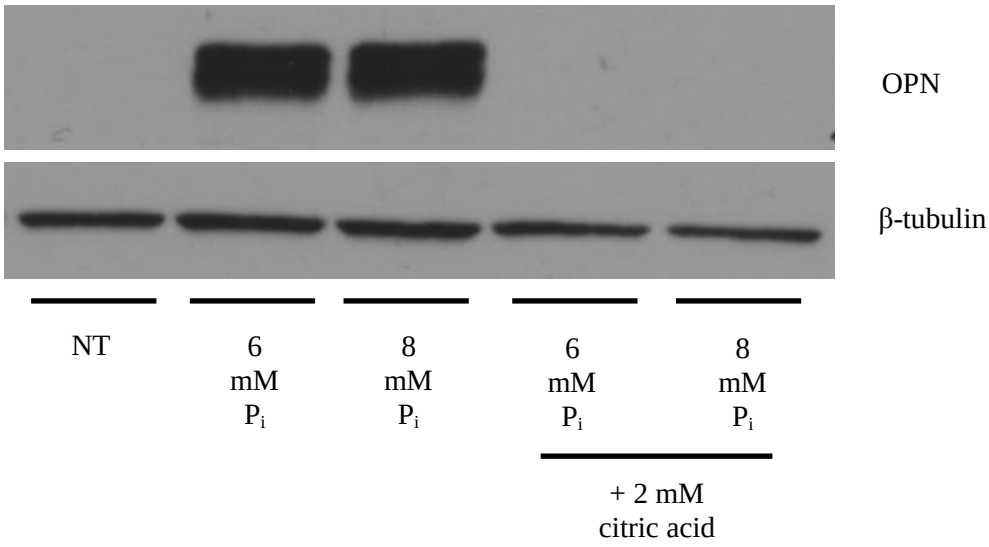

Figure 3-1: Induction of osteopontin by treatment with P_i and requirement of extracellular calcium.
MC3T3-E1 cells were incubated in DMEM containing 10% FBS and treated with the indicated concentrations of phosphate (P_i) for 48 hours. Some cells were co-treated with 2 mM citric acid in combination with P_i. 'NT' denotes no treatment. After the treatment period, cells were lysed and proteins were subjected to SDS-PAGE, then immunoblotted for osteopontin (OPN) and β-tubulin.

OPN can be induced in osteoblast cells in culture following exposure to elevated extracellular P_i, which may represent a feedback mechanism that induces a mineral-binding protein when such minerals are being formed during normal bone development. Additionally, OPN appears to be induced *in vivo* in non-osteoblastic cells at sites of ectopic mineral formation (Speer et al., 2009). Whether OPN is induced at these sites as a defensive response to ectopic calcification or represents a maladaptive response to an extracellular environment containing excessive P_i remains unclear at this point. We were curious to know if P_i treatment of cells other than osteoblasts in culture could result in the induction of OPN, as documented in non-osteoblast cells *in vivo*, and whether this induction also requires adequate free extracellular calcium. To determine if this is the case, we treated 3T3-L1 fibroblasts with 8 mM P_i for 48 hours. At the end of the treatment period, OPN protein could be detected in three biological replicates treated with P_i (Figure 3-2). This result demonstrates that these fibroblasts are capable of both sensing elevated P_i (Figure 2-4) and responding with a change in gene expression. We next co-incubated cells with 2 mM citric acid to determine if free extracellular calcium ions were a co-requirement for OPN induction. As shown in Figure 3-2, cells treated with the combination of 8 mM P_i and 2 mM citric acid produced no OPN protein detectable by immunoblot, indicating that sufficient extracellular calcium is required for OPN induction by both osteoblastic and non-osteoblastic cells.

Treatment with extracellular pyrophosphate (PP_i) can also initiate the production of OPN in MC3T3-E1 cells. The purpose of this response may be to augment the other anti-mineralizing properties of PP_i by inducing a protein with mineral-binding properties (Addison et al., 2007). As shown above, addition of PP_i causes ERK1/2 activation

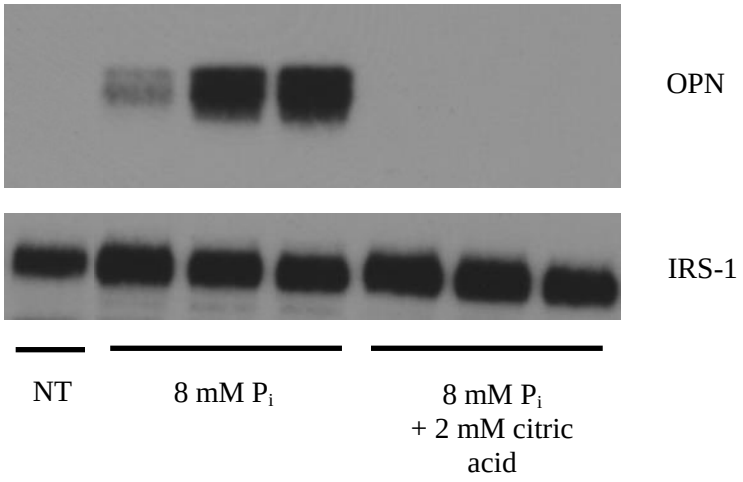

Figure 3-2: Induction of OPN by P_i treatment in non-osteoblast cells and requirement of extracellular calcium.
3T3-L1 cells were incubated in DMEM containing 10% FBS and treated with the indicated concentrations of phosphate (P_i) for 48 hours. Some cells were co-treated with 2 mM citric acid in combination with P_i. 'NT' denotes no treatment. The three lanes for P_i treatment and combination treatment represent independent biological replicates; the extent of OPN induction may vary. After the treatment period, cells were lysed and proteins were subjected to SDS-PAGE, then immunoblotted for osteopontin (OPN) and insulin receptor substrate 1 (IRS-1), expressed by 3T3-L1 cells and used as a loading control.

(Figure 2-7) and precipitate formation (Figure 2-9d) at lower concentrations (500 μM) than are required for P_i to have those effects (typically 6 mM and above). Precipitate formation after PP_i addition in the *in vitro* assay could be prevented by removing calcium from the solution (Figure 2-9d). To test if extracellular calcium is a co-requirement for OPN induction by PP_i, we incubated MC3T3-E1 cells in DMEM containing 10% FBS and treated cells for 48 hours with 500 μM PP_i. At the end of the incubation period, OPN protein could be detected in the cells treated with PP_i but not in untreated cells (Figure 3-3). We also co-incubated cells with either 2 or 4 mM citric acid to partially chelate calcium in the culture medium. Complete removal of calcium from the culture medium was not feasible because cell viability would be very adversely affected. In cells co-incubated with the higher dose of citric acid, 4 mM, treatment with 500 μM PP_i failed to induce osteopontin (Figure 3-3). At the lower dose of citric acid co-treatment, 2 mM, PP_i treatment still induced OPN, but this may reflect the fact more citric acid was required to prevent precipitation *in vitro* following PP_i addition (Figure 2-9d). Thus, like P_i treatment, incubation with PP_i also appears to achieve its cell signaling and gene induction effects by first forming calcium-containing precipitates.

It is possible that extracellular calcium is a co-requirement for P_i and PP_i to have their effects for a reason other than the formation of mineral precipitates. For example, it is conceivable that a cell surface receptor could sense P_i ions and require calcium ions as a co-factor, and accordingly calcium phosphate precipitation would not play a role in this hypothetical sensing mechanism but yet both of these ions would be required. To discriminate amongst these possibilities, we created calcium phosphate precipitates using

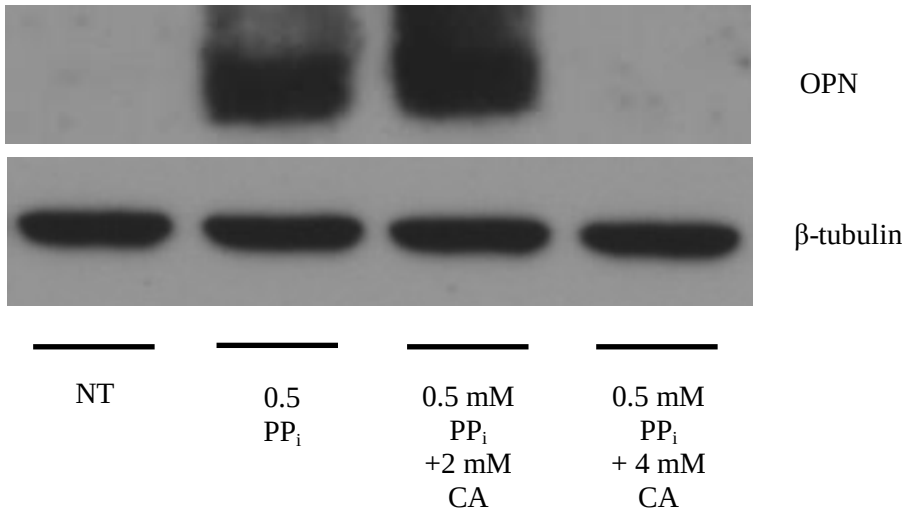

Figure 3-3: Induction of OPN by PP_i and requirement of extracellular calcium. MC3T3-E1 cells were incubated in DMEM containing 10% FBS and treated with the indicated concentrations of pyrophosphate (PP_i) for 48 hours. Some cells were co-treated with 2 or 4 mM citric acid in combination with PP_i. 'NT' denotes no treatment. After the treatment period, cells were lysed and proteins were subjected to SDS-PAGE, then immunoblotted for osteopontin (OPN) and β-tubulin.

a different combination of calcium and phosphate ion concentrations. Previously, we had formed precipitates by increasing the concentration of phosphate in solution while the calcium concentration remained constant. Precipitates also form *in vitro* when calcium is added in excess to solutions containing 1 mM P_i (data not shown). To provide further evidence that precipitates, rather than the free ions, are responsible for ERK1/2 activation and OPN induction, we incubated MC3T3-E1 cells in serum-free DMEM containing 1 mM P_i and 1.8 mM $CaCl_2$ and further raised the calcium ion concentration by 1, 3 or 5 mM. After 15 minutes of incubation, ERK1/2 was activated in cells treated with excess calcium (Figure 3-4a). Interestingly, when these treatments were repeated in media that lacked P_i, addition of excess calcium failed to activate ERK1/2 (Figure 3-4a). These results again suggest that the precipitates formed by these two ions, rather than the individual ions, are the true stimulus because excess calcium alone was not sufficient to initiate signaling in these cells. We also tested if adding excess calcium could induce OPN expression by forming precipitates. Using *in vitro* studies, we found that if 10% serum is present in the culture medium, addition of excess calcium will not result in precipitate formation because serum proteins will buffer the added calcium ions (data not shown). However, serum growth factors are required to maintain the cells over the course of the 48-hour incubation period required to test the induction of OPN. To overcome this problem, we supplemented serum-free DMEM with 20 ng/ml bFGF to maintain cell viability during the incubation period while allowing precipitate formation to occur. We treated MC3T3-E1 for 48 hours cells with 5 or 7 mM $CaCl_2$ in addition to the calcium already contained in the DMEM, which was supplemented either with 10% FBS or 20 ng/ml bFGF. In the cells supplemented with bFGF alone, which allowed

precipitate formation, OPN was induced (Figure 3-4b; P_i remains 1 mM under these conditions). However, in the cells supplemented with serum, which prevented precipitate formation, addition of excess calcium did not result in OPN production (Figure 3-4b). These results suggest that precipitate formation, regardless of the particular concentrations of P_i or calcium used to achieve that precipitation, is responsible for ERK1/2 activation and OPN induction.

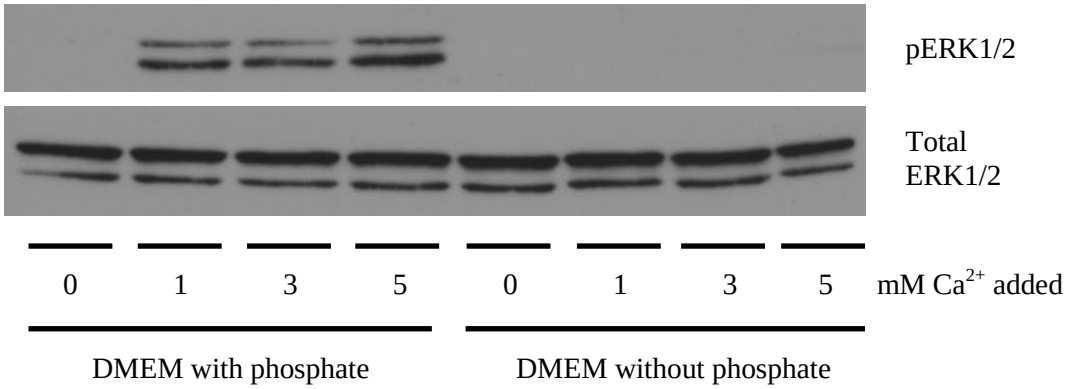

Figure 3-4a: Activation of cell signaling following addition of excess calcium.
MC3T3-E1 cells were incubated in serum-free DMEM lacking or containing P_i as indicated for 1 hour prior to treatment with 0-5 mM $CaCl_2$. Cells were treated for 20 minutes then lysed and proteins were subjected to SDS-PAGE. Proteins were immunoblotted using antibodies against activated ERK1/2 and total ERK1/2.

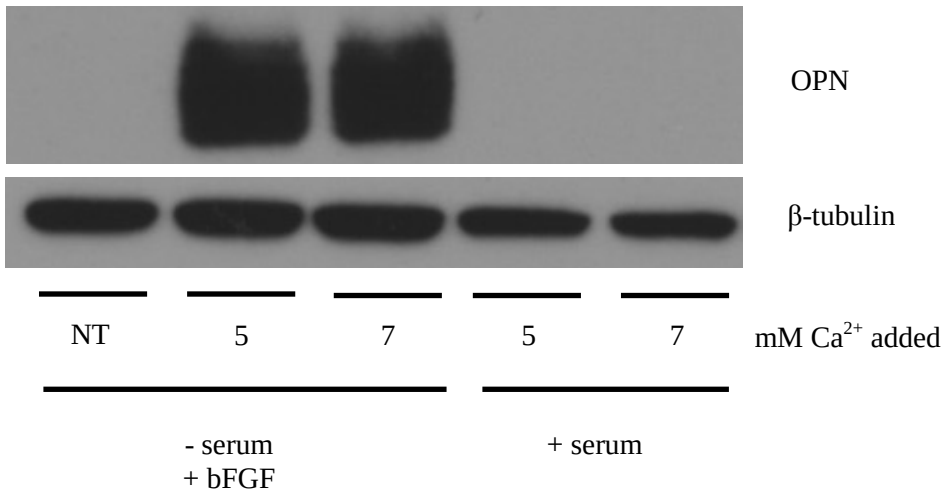

Figure 3-4b: Induction of OPN by elevated extracellular calcium.
MC3T3-E1 cells were incubated in DMEM containing 10% FBS or DMEM lacking serum but supplemented with 20 ng/ml basic FGF. Cells were treated for 48 hours with 5 or 7 mM additional $CaCl_2$ as indicates. 'NT' denotes no treatment. After treatment, cells were lysed and proteins were subjected to SDS-PAGE, then immunoblotted for osteopontin (OPN) and β-tubulin.

3.4 Discussion

We have demonstrated that P_i treatment initiates cell signaling in various cultured cell lines and have provided evidence that calcium phosphate precipitates form during the course of P_i treatment. The results of additional experiments suggest that these precipitates, rather than the phosphate ion *per se*, cause the observed cellular responses. Beck et al. proposed a biological rationale for these effects of P_i treatment in the context of bone development. The secreted protein OPN is produced by osteoblasts during the course of bone development, and it can bind and become incorporated into newly formed mineral (Boskey et al, 2002). P_i treatment induces OPN; cellular responses to elevated extracellular P_i may therefore represent a feedback mechanism in which extracellular P_i generated during an early stage of bone development stimulates OPN production in a subsequent stage of bone development (Beck et al., 2000).

We extended our hypothesis that calcium phosphate precipitates produce the observed responses in osteoblasts and other cells by studying the induction of OPN gene expression following P_i treatment. OPN protein was detectable 48 hours after treating osteoblasts or fibroblasts with elevated P_i, but this induction was prevented if extracellular calcium was lowered by co-treatment with citric acid (Figure 3-1 and 3-2). Similar results were obtained in when OPN induction by PP_i was examined (Figure 3-3). We reasoned that if calcium phosphate precipitates were responsible for OPN induction, the response should occur whenever these precipitates are formed in our cell culture studies regardless of the precise combination of calcium or P_i concentrations that are used to produce them. Consistent with this hypothesis, addition of excess calcium to media containing normal concentrations of P_i (1mM) produced the same results as high P_i

treatment, but these responses were abolished when P_i was removed from the system or precipitates could not form (Figure 3-4).

These results prompt an extension and refinement of the recently proposed models describing how extracellular P_i affects cells and tissues during bone development and pathological mineralization. We suggest that solid-phase mineral precipitates, rather than individual calcium or phosphate ions, interact with cells and initiate a cell signaling response and changes in gene expression, including the mineral-binding protein osteopontin. We believe this refinement is still consistent with the previously proposed functions of such a cellular response: the formation of inorganic mineral in the extracellular environment is detected by cells that in turn mount a response during pathological or developmental processes. This response may be appropriate during bone development or potentially maladaptive during pathological processes such as ectopic calcification. During chronic kidney disease, P_i retention in the body increases and ectopic tissue deposition may occur, affecting the behavior of nearby cells (Giachelli, 2009). Understanding how cells respond to the formation of nearby mineral could aid efforts to reverse the adverse effects that ectopic calcification has on tissues such as blood vessels and on overall physiological function.

CHAPTER FOUR

Investigation of the Mechanism by which Mineral Precipitates Affect Cell Behavior

4.1 Introduction

We began our cell culture studies with the goal of understanding how elevated extracellular P_i may be affecting cell behavior. We found that P_i treatment acutely activated cellular signaling, specifically components of the MAP kinase pathway such as ERK1/2 and CREB, and that with longer-term treatment cells began producing the mineral-binding protein OPN. Both of these effects exhibited a co-requirement of extracellular calcium, and we propose that mineral precipitates formed during P_i treatment are the stimulus for the observed cellular responses. We therefore turned the focus of our investigations toward understanding how these solid particles and precipitates are sensed by cells.

The interaction of foreign material with cells has been studied previously in several different contexts. Immune cells such as macrophages recognize large particles and micro-organisms using various classes of scavenger receptors (Martínez et al., 2011). In the kidney, dietary oxalic acid or ethylene glycol poisoning can lead to the formation of calcium oxalate crystals that damage tubular epithelial cells. Contact of these crystals with the epithelial cells provokes responses by the cells that may be similar to reactions

of other cells to extracellular minerals (Koul et al., 2002; Kleinman et al., 2004**)**. In addition, calcium phosphate crystals are found in vertebrate bone joints affected by osteoarthritis. Exposure of cells to these crystals, in cell culture studies meant to model osteoarthritis, resulted in activation of the MAP kinase pathway and the NF-κB pathway (Nair et al., 1997; McCarthy et al., 1998). Knowledge gained from these other fields can potentially be applied toward understanding how cells are affected by a high-phosphate environment.

Oxalate Crystals Adhere to Kidney Cells

Ingestion of oxalic acid found in various plants or of ethylene glycol, which forms oxalic acid after metabolic breakdown, results in the accumulation of oxalate ions in the urine. This small organic ion can complex with calcium ions to form crystal precipitates which adhere to kidney epithelial surfaces and grow over time, creating macroscopic pathological kidney stones. Cell culture studies used to model this process showed that these crystals can bind to kidney cells and become internalized, eventually leading to toxic effects and cell apoptosis (Lieske et al., 1994; Khan, 2004; Schepers et al., 2005). If developing crystals fail to attach to tubule cells or other kidney tissue they will be eliminated in the urine, so much effort has been given to understanding the factors that contribute to crystal-cell interactions. One hypothesis is that urine macromolecules and locally produced proteins alter the growth and surfaces of growing oxalate crystals, making them less likely to adhere to cells (Sheng et al., 2005). OPN may be one of these factors: multiple studies have observed that oxalate crystals can induce the expression of OPN in cell lines and using *in vivo* models (Lieske et al., 1997; Umekawa et al., 2006; Kleinman et al., 2004). In mice lacking OPN, ethylene glycol feeding exhibited

significantly greater deposition of calcium oxalate crystals than wild-type controls, which increased their expression of OPN several-fold after ethylene glycol feeding (Wesson et al., 2003). In the kidney, therefore, OPN may have a protective role by virtue of its mineral-binding properties: OPN may bind to oxalate crystals and render them less harmful by decreasing their ability to adhere to cells. Kidney epithelial cells treated with oxalate caused activation of the p38 and JNK MAP kinase pathways (though not the ERK1/2 kinases), indicating that these crystals are also capable of initiating cell signaling (Chaturvedi et al., 2002; Koul et al., 2002). Oxalate crystals, and possibly other types of crystals, may also affect cells by causing reactive oxygen species (ROS) to be generated. It is unclear how these ROS are generated, but one possibility is that crystals somehow activate cellular NADPH oxidase, which can generate ROS. Inhibition of NADPH oxidase prevented the induction of a crystal-responsive gene (MCP-1) (Umekawa et al., 2005). It remains to be determined how these cells initially sense and respond to oxalate crystals, but these studies suggest that inorganic crystals may generally perturb cells via common mechanisms, and produce a similar response (OPN production) despite the fact that the stimuli are chemically distinct.

Basic Calcium Phosphate Crystals Cause Pathological Changes in Cell Behavior

Another example of mineral-cell interactions comes from studies of osteoarthritis. In this disease of joint degeneration, crystals of basic calcium phosphate (BCP) and calcium pyrophosphate (CPPD) can be found in patients with advanced disease using radiological methods or by sampling synovial fluid. It is controversial whether these crystals initiate and contribute to progression of osteoarthritis, or rather if they appear only late in the course of osteoarthritis and are merely disease-associated, not a cause of

disease (Pritzker, 2009). Nevertheless, a number of cell culture studies using synovial fibroblasts have clearly established that treatment with these crystals causes inflammatory responses in the cells that would be detrimental to joint function if they were to occur *in vivo* (McCarthy and Cheung, 2009). It remains unclear how exactly these crystal deposits form in joint tissue, but two hypotheses have been proposed: 1) degradation of the extracellular matrix early in the course of osteoarthritis makes the tissue more prone to mineral formation and deposition 2) aging or damage in the joint changes the behavior of chondrocytes, which begin to inappropriately produce additional mineral in the joint. Once formed, these crystals have pathologically relevant biological activities, as observed using cell culture studies and in patients. Fibroblasts treated with BCP or CPPD begin producing matrix metalloproteinase enzymes (MMPs), which are secreted from cells and degrade extracellular matrix molecules (Cheung et al., 1996). If such enzymes are produced excessively in joint tissue, there will be further degradation of the tissue and progression of osteoarthritis. To understand how these crystals cause an increase in MMP production, Cheung et al. performed experiments on synovial fibroblasts using synthetically prepared BCP crystals. These crystals were sterile and were delivered as aggregates 10-20 μm in diameter. Fibroblasts were treated with 50 μg/ml of these crystal aggregates and activation of the MAP kinase cell signaling pathway was evaluated by immunoblotting. The authors found that, like treatment with P_i, the ERK1/2 kinases were activated by treatment of cells with BCP crystals within 10 minutes, while the p38 MAP kinase was not activated (Nair et al., 1997). Treatment with BCP or CPPD crystals also activated the CREB transcription factor within 30 minutes, also similar to P_i treatment. In a subsequent study, BCP and CPPD crystals were also found to activate protein kinase

C and the NF-κB pathways in fibroblasts (McCarthy et al., 1998). Interestingly, co-treatment with phosphocitrate, closely chemically related to citrate, at a concentration of 1 mM prevented activation of ERK1/2 and CREB following treatment with BCP or CPPD (Nair et al., 1997). Phosphocitrate interferes with the nucleation, growth and aggregation of calcium-containing crystals (Nair et al., 1997), and the authors suggest that phosphocitrate may bind the crystals used in the treatments and interfere with its interaction with cells. Another possibility is that phoshocitrate may be partially or completely dissolving the treatment crystals into their constituent ions, which fail to activate cell signaling in the same manner. Such a hypothesis would be consistent with the model we have proposed, wherein excessive P_i has its effects by first forming insoluble precipitates.

Initial Consequences of Mineral-Cell Interactions Remain Unclear

Studies of a diverse array of disease states including oxalate stone formation, osteoarthritis and diseases caused by asbestos (silicon-containing crystals) inhalation reveal common reactions following cell-crystal interaction (Liu et al., 2013; Buder-Hoffman et al., 2009). These common reactions include activation of MAP kinases, particularly ERK1/2 but also in some cases p38 and JNK, and production of various inflammatory mediators and proteins. However, the identity of the cell's initial sensory mechanism for extracellular mineral particles remains unclear in all these cases. What is clear is that a variety of chemically distinct particles seem to have common effects, and generation of ROS may be a key early step preceding later cell-signaling events (Aihara et al., 2003; Liu et al., 2013).

4.2 Methods

Cell Culture

NIH/3T3 fibroblasts were obtained from American Type Culture Collection (ATCC). Cells were cultured in 10 cm dishes and experiments were performed in 12 well plates purchased from Corning-Costar. Cells were maintained using Dulbecco's Modified Eagle Medium (DMEM) supplemented with 10% fetal bovine serum (FBS) and antibiotics (penciling and streptomycin, 100 U/ml and 100 μg/ml respectively), all obtained from Life Technologies, Gibco Brand. 100 mM stock buffers of sodium phosphate (pH 7.5) and potassium phosphate (pH 7.5) were used for experimental treatments. Oxalic acid, gadolinium chloride, phorbol 12-myristate 13-acetate, hydrogen peroxide solution, dihydroethidium, and N-acetylcysteine were obtained from Sigma-Aldrich. The receptor tyrosine kinase inhibitor PD089828 was obtained from Millipore. Basic FGF was obtained from Santa Cruz Biotechnology.

Immunoblot Analysis

Cells were collected in cell lysis buffer (20 mM HEPES, 100 mM NaCl, 1.5% Triton-X100, 15 mM NaF, 20 mM phosphatase inhibitor cocktail (Sigma), protease inhibitor mix (Roche), 1 mM EDTA and 20 mM sodium pyrophosphate) and centrifuged for 10 minutes at 13,000 rpm. Supernatants were collected and SDS sample buffer was added before boiling samples for 5 minutes. Protein samples were subjected to SDS-polyacrylamide gel electrophoresis (SDS-PAGE) and proteins were then transferred to nitrocellulose membranes. Membranes were incubated in blocking buffer (2% milk, 0.05% v/v Tween 20 in TBS) then incubated with primary antibodies. The phospho-ERK1/2, total ERK1/2, phospho-FRS2α Y196, phospho-FRS2α Y436, phospho-PLCγ

and total PLCγ antibodies were obtained from Cell Signaling Technologies. The α-actin and osteopontin antibodies were obtained from Santa Cruz Biotechnologies. All antibodies were diluted at a ratio of 1:1000 except phospho-FRS2α antibodies, which were diluted 1:500. Membranes were washed in a TBS-Tween solution and then incubated with appropriate secondary antibodies conjugated with horseradish peroxidase (GE Healthcare). Blots were developed using SuperSignal West Dura Extended Duration Substrate from Thermo Scientific.

Flow Cytometry

Cells were labeled for 30 minutes with dihydroethidium at a concentration of 2 μM in DMSO, then rinsed and resuspended in PBS solution. Cells were then analyzed using a BD LSR II flow cytometer using an excitation wavelength of 488 nm and absorption measured at 610 nm. Data were analyzed using FlowJo software (Tree Star).

Light Microscopy and Microphotography

Microscopy images were obtained using a Leica Microsystems DM IL inverted microscope. A SPOT-idea™ digital camera was used to capture images in conjunction with SPOT Advanced Plus software.

4.3 Results

Because cells seem to exhibit common responses when exposed to crystals of various different chemical compositions, we hypothesized that the calcium phosphate precipitates that form in settings of high P_i concentration may share a common mechanism of action with these other crystals. We can begin to investigate whether or not this is the case by determining if P_i treatment causes responses already observed by crystals in other diseases, such as ROS generation and inflammatory responses. First, however, we wanted to determine if other types of crystals indeed have similar effects as P_i treatment using our own cell culture experiment system. We chose to perform our experiments using NIH/3T3 fibroblasts rather than MC3T3-E1 osteoblasts because we wanted to demonstrate that the effects of crystal-cell interactions are not restricted to bone cells but also occur in a less specialized cell type. NIH/3T3 cells produce OPN when exposed to high P_i concentrations (Beck et al., 2000) and respond with activation of the ERK1/2 kinases after P_i treatment, as shown in Figure 4-2. Since calcium oxalate crystals induce OPN expression in kidney cells *in vivo* and *in vitro* (Kleinman et al., 2004), we tested if this response occurs in fibroblasts as well. After testing various concentrations of oxalic acid, we found that adding 5 mM or greater oxalic acid to cultures of NIH/3T3 cells incubated in DMEM containing 10% FBS resulted in crystal formation. These crystals formed within 10 minutes and were not amorphous but had regular cuboidal and star-shaped structures, and were 20-100 μm in length or diameter depending on their shape (Figure 4-1a,b). We treated NIH/3T3 cells in serum-free DMEM with bFGF, P_i or various concentrations of oxalate for 20 minutes and assessed

a.

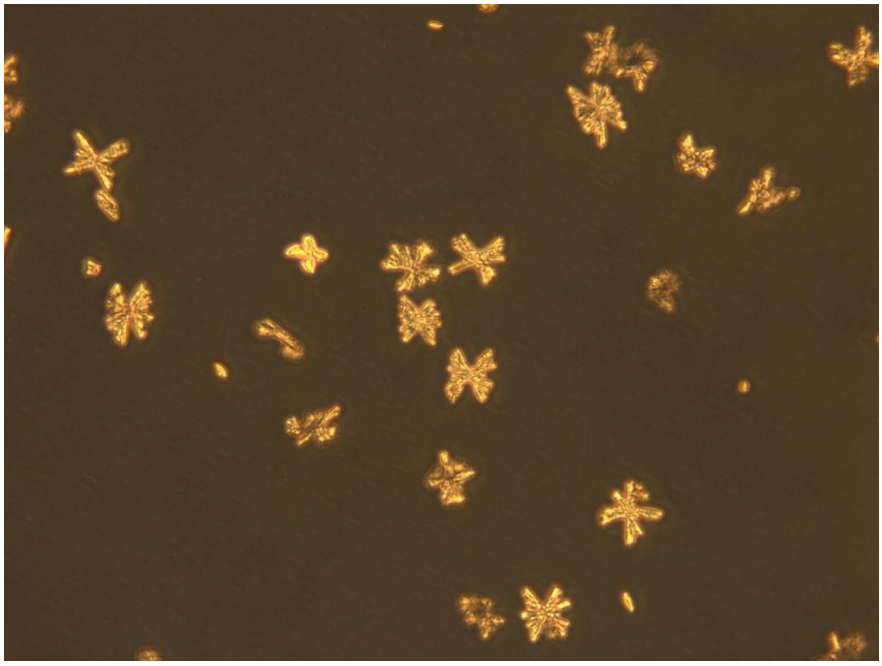

b.

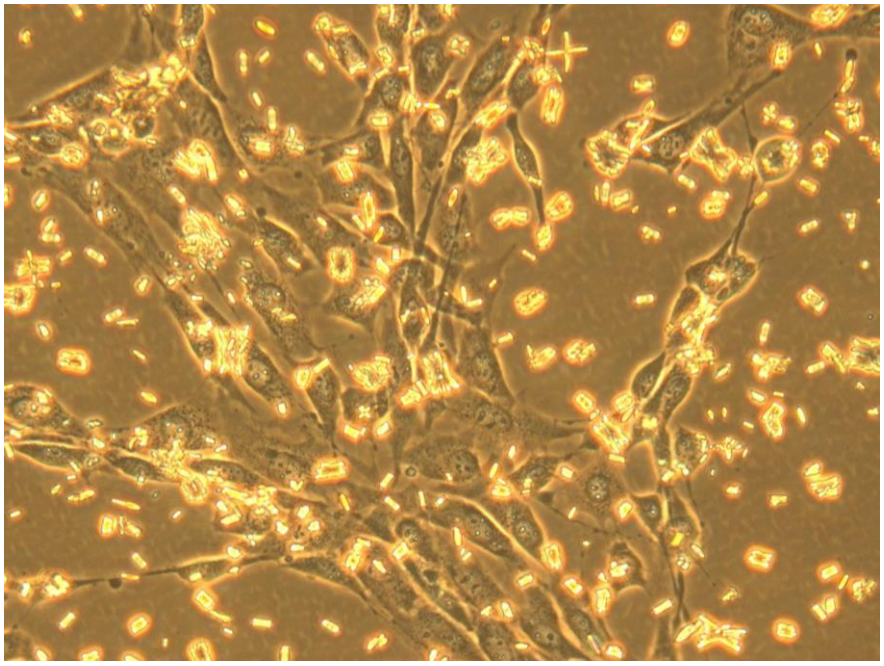

Figure 4-1: Formation of calcium oxalate crystals after addition of oxalic acid. Oxalic acid crystals formed within 10 minutes after addition of 5 mM oxalic acid to serum-free DMEM in the absence of cells (a), or in the presence of cells (b). Light microscopy images were taken at 100X total magnification.

activation of ERK1/2 by immunoblotting. As shown in Figure 4-2a, treatment with 3, 5 or 10 mM oxalate caused activation of ERK1/2, as did bFGF and P_i treatment. To determine if these oxalate crystals are capable of inducing OPN expression in fibroblasts, we treated NIH/3T3 cells incubated in DMEM containing 10% FBS with P_i or two concentrations of oxalate (0.1 mM and 0.5 mM) for 48 hours and detected OPN expression by immunoblotting. We found that the 0.5 mM dose, but not the 0.1 mM dose, which produced no visible oxalate crystals, induced expression of OPN after the 48-hour incubation period (Figure 4-2b). These results demonstrate that crystals of significantly different chemical composition (oxalic acid is a small organic molecule) have effects similar to P_i treatment in fibroblasts, suggesting that cells sense some general feature of these particles rather than a specific surface or chemical signature.

Since cells appear to be responding to the presence of extracellular crystals generally, we hypothesized that physical stimulation of cells by these particles may be the mechanism by which they have their effects. A primary way by which physical stimulation is sensed by cells is through the use of stretch receptors, which are non-specific cation channels that open when the membranes surrounding them are deformed (Orr et al., 2006). Gadolinium ions (Gd^{3+}) are a reagent commonly used to inhibit stretch-activated ion channels (Yang and Sachs, 1989). We performed co-treatment experiments with P_i buffers and Gd^{3+} to determine if blocking putative stretch-activated ion channel activity would prevent the ERK1/2 activation response following P_i treatment. NIH/3T3 cells were pre-incubated with GdCl for 30 minutes, then treated with 10 mM P_i buffer for 20 minutes. Other cells were treated with P_i buffer or GdCl alone. Unexpectedly, we found that treatment with Gd^{3+} alone at the concentrations it is

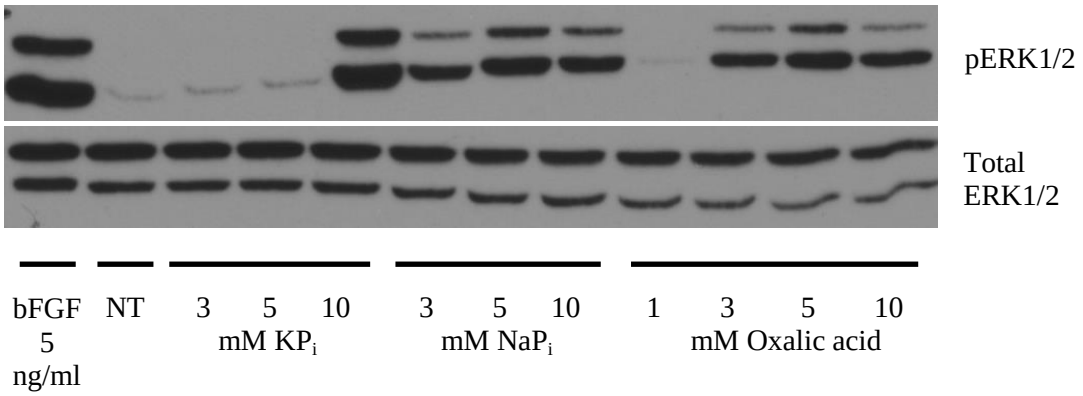

Figure 4-2a: Activation of ERK1/2 following oxalic acid treatment.
NIH/3T3 cells were incubated in serum-free DMEM for 1 hour prior to treatment with the indicated concentrations of basic FGF, phosphate buffers (potassium and sodium) and oxalic acid. 'NT' indicates no treatment. Cells were treated for 20 minutes then lysed and proteins were subjected to SDS-PAGE. Proteins were immunoblotted using antibodies against activated ERK1/2 and total ERK1/2.

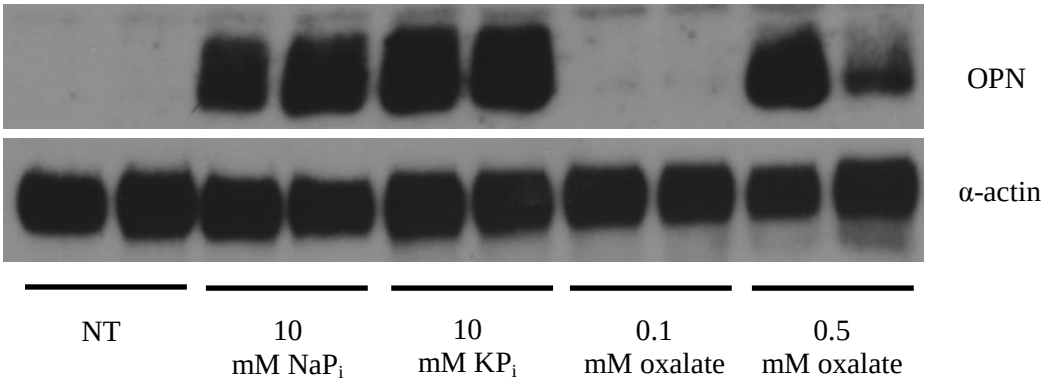

Figure 4-2b: Induction of OPN following oxalic acid treatment.
NIH/3T3 cells were incubated in DMEM containing 10% FBS and the indicated buffers for 48 hours. 'NT' indicates no treatment. Groups of two adjacent lanes represent independent duplicate experiments. After the incubation period, cells were lysed and subjected to SDS-PAGE. Proteins were immunoblotted using antibodies against osteopontin (OPN) and α-actin.

typically used as an inhibitor (1-10 μM) caused activation of ERK1/2 by itself, without P_i co-treatment (Figure 4-3a). When Gd^{3+} was added in combination with P_i buffer, there was no consistent inhibition of ERK1/2 activation in comparison with P_i treatment alone (Figure 4-3a). After observing this puzzling result, we inspected the cell culture dishes and noticed a possible explanation: addition of GdCl to culture medium produced insoluble precipitates at the 1-10 μM concentrations. We added GdCl to the prepared buffers lacking P_i (see Chapter 2), and noted that precipitates formed in these solutions as well. We were not able to determine the identity of other ion(s) that precipitate with the added Gd^{3+} because sequential removal of counter-ions from the prepared buffers led to incremental decreases of precipitate formation, suggesting that the precipitates are composed of a mixture of Gd^{3+} and various negative ions (data not shown). We wondered if these precipitates, like others we have used to treat cells, might cause OPN gene induction as well as the observed ERK1/2 response. We treated NIH/3T3 cells incubated in DMEM containing 10% FBS with 100 μM GdCl (a higher concentration was needed to produce precipitates in serum-containing medium) for 48 hours and measured OPN protein production by immunoblotting. Treatment with 10 mM P_i buffer and 100 μM GdCl both resulted in the production of OPN protein (Figure 4-3b). Oxalate treatment at a concentration of 0.4 mM was insufficient to produce observable crystals, and also failed to induce OPN protein (Figure 4-3b). Therefore, it appears that these precipitates are also capable of eliciting the cellular responses that calcium phosphate and oxalate crystals cause. Overall, these results do not provide support for the hypothesis that these various particles are sensed by cells as a result of mechanical stimulation and activation of stretch-activated ion channels.

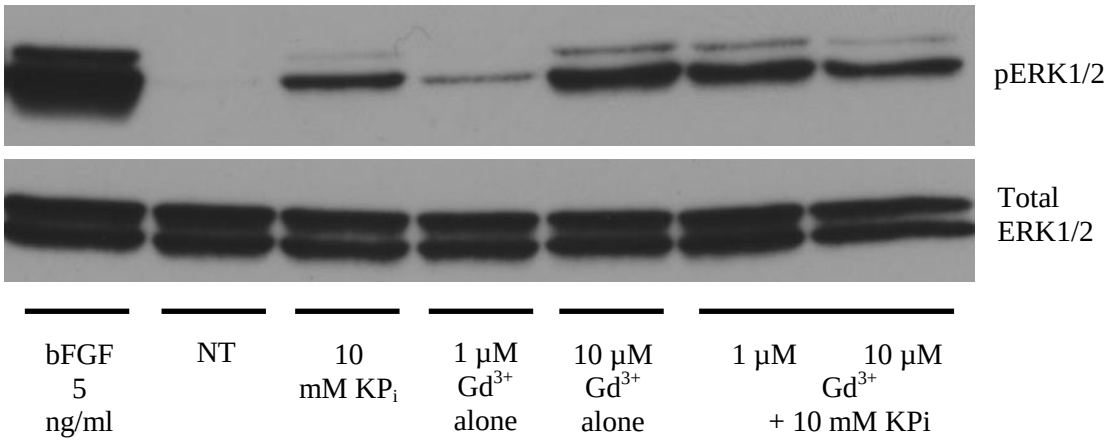

Figure 4-3a: Effect of gadolinium treatment on ERK1/2 activation by P_i.
NIH/3T3 cells were incubated in serum-free DMEM prior to treatment with the indicated concentrations of basic FGF, P_i buffer, GdCl or combination of P_i buffer and GdCl (rightmost two lanes). 'NT' indicates no treatment. Cells were treated for 20 minutes then lysed and proteins were subjected to SDS-PAGE. Proteins were immunoblotted using antibodies against activated ERK1/2 and total ERK1/2.

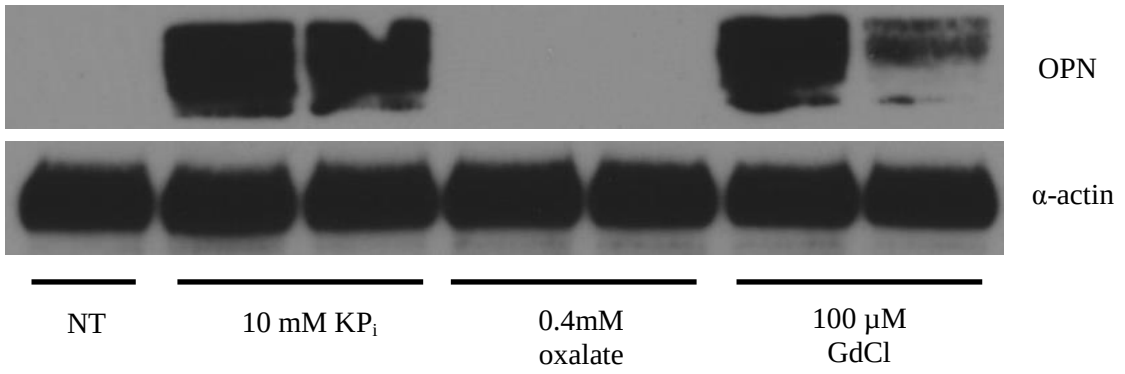

Figure 4-3b: Induction of OPN following GdCl treatment.
NIH/3T3 cells were incubated in DMEM containing 10% FBS and the indicated buffers or GdCl for 48 hours. 'NT' indicates no treatment. Groups of two adjacent lanes represent independent duplicate experiments. After the incubation period, cells were lysed and subjected to SDS-PAGE. Proteins were immunoblotted using antibodies against osteopontin (OPN) and α-actin.

An alternative approach to determining the mechanism by which insoluble precipitates and crystals affect cells is to examine the intracellular signaling pathways activated by treatment with these agents. By working from the 'inside-out', the proximal sensor of the extracellular material, or at least a class of candidate molecules, may be eventually identified. For example, stimulation by a wide variety of crystals results in activation of MAP kinases. Identifying the steps that lead to those activation events may uncover the earliest responses by cells following treatment. ERK1/2 and other kinases in the MAP kinase cascade are initially activated by the small G-protein Ras, which can in turn activated by a wide variety of cell-surface receptors. These include G-protein coupled receptors, integrins and receptor tyrosine kinases (RTKs) (Chen et al., 2001; Lemon and Schlessinger, 2010). Any of these cell-surface molecules could potentially serve as sensors of extracellular crystals.

In the course of studying FGF23 signaling in the laboratory, we often examine activation of FRS2α (FGF receptor substrate 2α), which is a docking molecule immediately downstream of FGF receptors. FRS2α is phosphorylated and activated directly by RTKs after the receptors bind their extracellular ligands, and as such serves as a specific indicator of RTK activation (Lemon and Schlessinger, 2010). Fortuitously, not deliberately, we found that P_i treatment can cause phosphorylation of FRS2α at two residues, indicating activation of this molecule upstream of the MAP kinase pathway. As shown in Figure 4-4a, incubation of NIH/3T3 cells in serum-free medium with 10 mM P_i buffer resulted in phosphorylation of FRS2α at Y196 and Y436 within 20 minutes. We also observed activation of another enzyme frequently found downstream of FGF receptor activation, PLC-γ (Figure 4-4b).

Concurrently with our experiments, Yamazaki et al. published the results of their studies of P_i-induced signaling in HEK293 cells. In serum-starved HEK293 cells treated with 10 mM P_i for 15 minutes, the ERK1/2 kinases were activated, as well as c-Raf (the initial kinase in the MAP kinase cascade), but the p38, JNK and AKT kinases were not activated (Yamazaki et al., 2010). P_i treatment also resulted in the of the early growth response 1 (EGR1) gene within 30 minutes after P_i addition (Yamazaki et al., 2010). Because FGF23 is a hormone that regulates P_i homeostasis, and because FGF23 uses FGF receptors and the membrane Klotho protein for signal transduction into the cell, Yamazaki et al. hypothesized that P_i treatment might also affect FGF signaling. They also observed that P_i treatment caused phosphorylation of FRS2α at Y196 within 15 minutes of P_i addition. To evaluate the requirement of FGF receptors for phosphorylation and activation of FRS2α, Yamazaki et al. performed siRNA knockdown experiments on HEK293 cells. They first determined by RT-PCR that FGFR1 and FGFR2 were the predominant FGF receptors expressed in these cells, and designed siRNA constructs to target these two genes. Knockdown of FGFR1 substantially reduced the extent of ERK1/2 activation following P_i treatment (approximately 90% reduction). Knockdown of FGFR2 had similar, though less substantial effects (40-50% reduction) (Yamazaki et al., 2010). Yamazaki et al. also observed direct phosphorylation and activation of the FGF receptor itself following P_i treatment when the FGF receptor was overexpressed. These results indicate that FGF receptors have a major role in contributing to the MAP kinase response in HEK293 cells following treatment with elevated P_i.

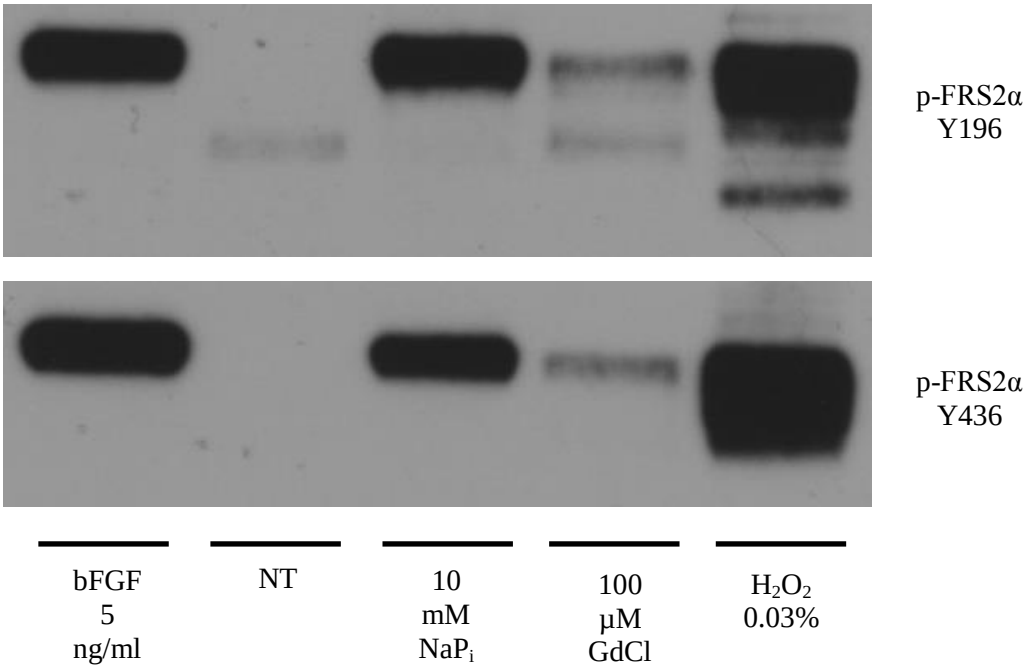

Figure 4-4a: Activation of FRS2α by various agents.
NIH/3T3 cells were incubated in serum-free DMEM for 1 hour prior to treatment with the indicated agents. 'NT' indicates no treatment. Cells were treated for 20 minutes then lysed and proteins were subjected to SDS-PAGE. Proteins were immunoblotted using antibodies against FRS2α phosphorylated at tyrosine 196 or tyrosine 436.

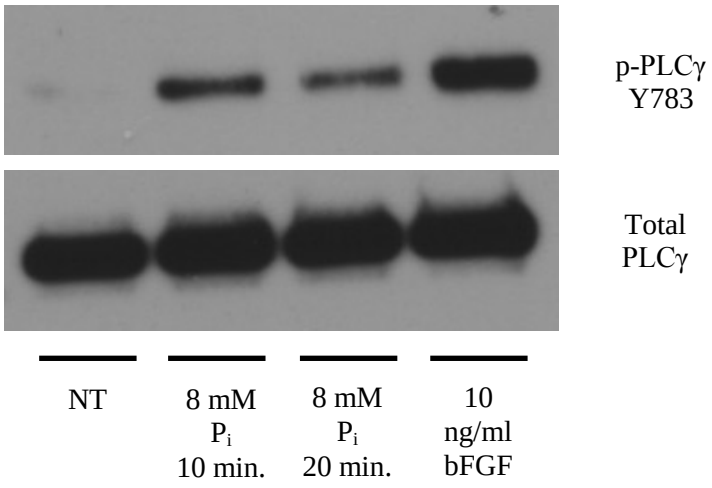

Figure 4-4b: Activation of PLCγ by P_i treatment and basic FGF.
NIH/3T3 cells were incubated in serum-free DMEM for 1 hour prior to treatment with P_i for 10 or 20 minutes, or treatment with basic FGF for 10 minutes. 'NT' indicates no treatment. Cells were then lysed and proteins were subjected to SDS-PAGE. Proteins were immunoblotted using antibodies against PLCγ phosphorylated at tyrosine 196 or total PLCγ.

The involvement of FGF receptors and their substrate protein FRS2α in mediating cell signaling caused by P_i treatment is seemingly unusual because FGF receptors are most often activated by extracellular FGF protein ligands (Lemon and Schlessinger, 2010). However there are documented examples of RTKs that can be activated by intracellular and extracellular stimuli besides their typical canonical ligand. For example, the epidermal growth factor (EGF) receptor can be activated by G-protein coupled receptors (GPCRs) residing in the same cell that have been activated by a GPCR agonist, in the absence of EGF. Extracellular UV radiation has also been shown to activate the EGF receptor in absence of the EGF ligand (Carpenter, 1999). Therefore, the finding that the FGF receptor can be activated in the absence of FGF ligands has some related precedents. More recently, a significant role for ROS, and H_2O_2 specifically, in cell signaling downstream of RTKs has been uncovered (Rhee, 2006; Woo et al., 2010), which may provide an explanation for how these growth factor receptors can be activated in the absence of their ligands. Early evidence of this phenomenon was noted in vascular smooth muscle cells treated with platelet-derived growth factor (PDGF). ROS increased in cells following PDGF treatment, as measured by 2',7'-dichlorofluorescin fluorescence, and co-treatment with the antioxidants catalase or N-actylcysteine blocked activation of the PDGF receptor by PDGF (Sundaresan et al., 1995). Later experiments demonstrated that H_2O_2 in the cell can inactivate protein tyrosine phosphatases (PTPs) by chemically modifying a critical catalytic cysteine residue in a reversible manner (Meng et al., 2002). These activity of these PTPs is critical for maintaining low activity of RTKs by de-phosphorylating activation sites on the RTKs in the absence of their ligands. In the current model, binding of a ligand to a growth factor receptor such as the PDGF receptor

or FGF receptor causes activating phosphorylations on the receptor itself as well as activation of nearby NADPH oxidase (Nox), which generates H_2O_2 locally. This H_2O_2 then inactivates the receptor-associated PTPs and allows signaling through the receptor to be sustained (Woo et al., 2010). Using this model, one can predict that treatment with ROS such as H_2O_2 could also result in activation of RTKs by *inactivating* the phosphatases that normally play an inhibitory role. Indeed, this is the case for the EGF receptor, which is activated by H_2O_2 treatment (Knebel et al., 1996).

We hypothesized that P_i treatment and other precipitates or crystals may cause ROS to be generated in our cell culture experiments, leading to activation of FGF signaling and MAP kinase activation in the absence of FGF ligands. Previous reports provide evidence that ROS may be generated following exposure of cells to oxalate crystals or calcium phosphate brushite crystals (Umekawa et al., 2005; Aihara et al., 2003). To explore this possible explanation, we determined if other crystals or H_2O_2 can also cause activation FRS2α, as would be predicted by the ROS activation model for growth factor receptors. Indeed, we found that treatment with 100 μM GdCl or 0.03% H_2O_2 (a concentration typically used to model chronic ROS stress) caused phosphorylation of FRS2α on Y196 and Y436 (Figure 4-4a). This result indicates that treatment with ROS can result in activation of molecules specific to the FGF signaling pathway (FRS2α). To measure directly ROS production caused by P_i treatment, we incubated NIH/3T3 cells for 18 hours in 1 mM P_i, 10 mM P_i, or 1 mM paraquat (a positive control for ROS generation). Cells were then labeled with dihydroethidium for 30 minutes (except for unlabeled control cells), which can be used to detect ROS production

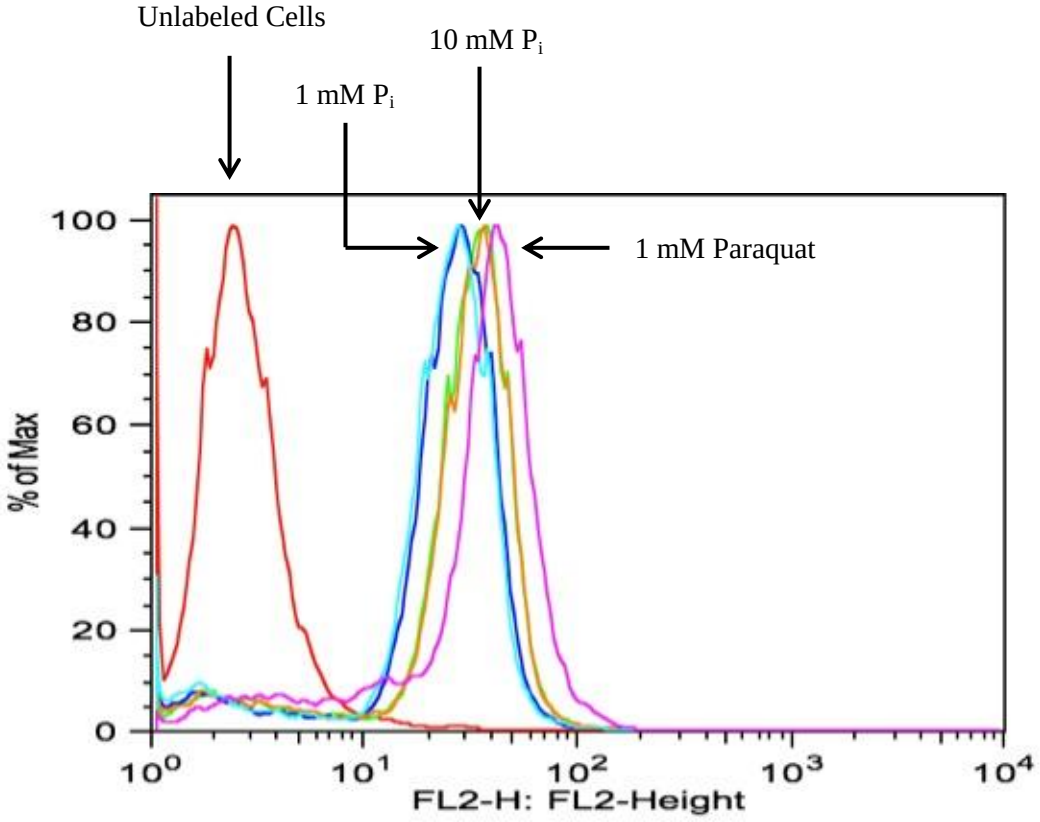

Figure 4-5: Measurement of reactive oxygen species following treatment with P_i or paraquat.
NIH/3T3 cells were incubated in DMEM containing 10% FBS for 18 hours with either 1 mM P_i, 10 mM P_i or 1 mM paraquat. After the incubation period, cells were collected and labeled with dihyrdoethidium for 30 minutes and fluorescence intensity was measured with a flow cytometer. The x-axis represents signal intensity while the y-axis represents cell counts. The different treatment groups are indicated by arrows. The 1 mM P_i and 10 mM P_i treatments were each performed in duplicate.

(Robinson et al., 2006). The fluorescence intensity of labeled cells was measured using a flow cytometer and the results are shown in Figure 4-5. Both the 10 mM P_i treatment and the paraquat positive control treatment caused a substantial increase in the overall signal intensity in the cells compared to the 1 mM P_i treatment control cells, indicated by the rightward shift in these population curves (Figure 4-5). This direct measurement method indicates that overnight P_i treatment results in an increase in cellular ROS.

If ROS are involved in initiating cell signaling caused by elevated phosphate, we predicted that antioxidant treatment would inhibit activation of ERK1/2 following P_i treatment. To test this hypothesis, we employed the antioxidant N-acetylcysteine (NAC). NIH/3T3 cells were treated for 20 minutes with basic FGF, 8 mM P_i or 8 mM P_i with NAC pre-treatment (10 or 25 mM, 1 hour). As shown in Figure 4-6a, co-treatment with NAC inhibited both ERK1/2 and FRS2α activation following P_i treatment in a dose-dependent manner. As a control, NAC co-treatment did not substantially reduce activation of ERK1/2 by a genuine FGF ligand, basic FGF (Figure 4-6b). These results provide further support that ROS play a role in initiating P_i-induced cell signaling.

Finally, we tested the requirement of RTK kinase activity by employing an inhibitor with specificity for the EGF, FGF and PDGF receptor kinases while not inhibiting other kinases. We treated NIH/3T3 cells with this inhibitor (abbreviated here as RTKi) in combination with basic FGF, 8 mM P_i or phorbol 12-myristate 13-acetate (PMA), which is a protein kinase C agonist and was used here as a positive control for ERK1/2 activation independent of RTK activity. After 15 minutes of treatment, FRS2α and ERK1/2 were activated by basic FGF, 8 mM P_i and PMA, while co-treatment with 1 μM RTKi prevented activation of these molecules by basic FGF and P_i while leaving

ERK activation by PMA unaffected (Figure 4-7). Thus, the kinase activity of RTKs seems to be required for subsequent MAP kinase activation caused by P_i treatment. Collectively, these data support a model wherein treatment with excess P_i causes the generation of ROS, which in turn activation of RTKs in the absence of their natural ligands and leads to downstream MAP kinase activation.

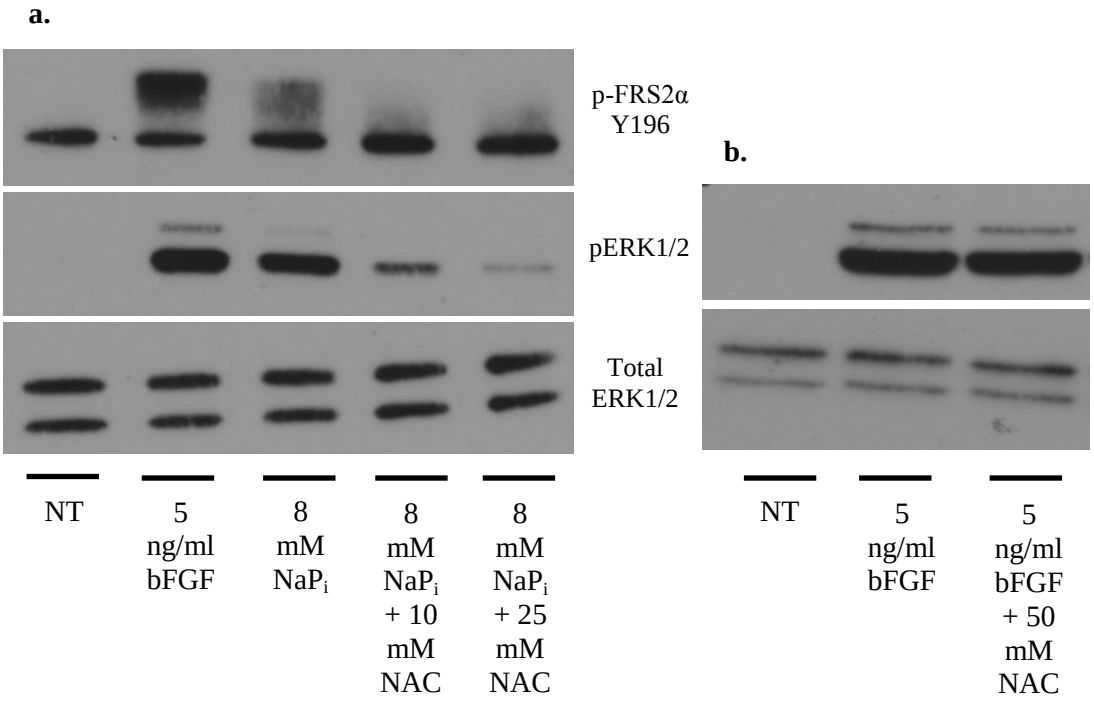

Figure 4-6a: Effect of antioxidant addition on signaling induced by P_i treatment. NIH/3T3 cells were incubated in serum-free DMEM for 1 hour prior to treatment with P_i with or without N-acetylcysteine (NAC) co-treatment, or treatment with basic FGF. 'NT' indicates no treatment. After 20 minutes of treatment, cells were then lysed and proteins were subjected to SDS-PAGE. Proteins were immunoblotted using antibodies against phospho-ERK1/2, total ERK1/2 or phospho-FRS2α Y196.

Figure 4-6b: Effect of antioxidant treatment on signaling induced by basic FGF. NIH/3T3 cells were incubated in serum-free DMEM for 1 hour prior to treatment basic FGF with or without N-acetylcysteine (NAC) co-treatment. 'NT' indicates no treatment. After 20 minutes of treatment, cells were then lysed and proteins were subjected to SDS-PAGE. Proteins were immunoblotted using antibodies against phospho-ERK1/2 and total ERK1/2.

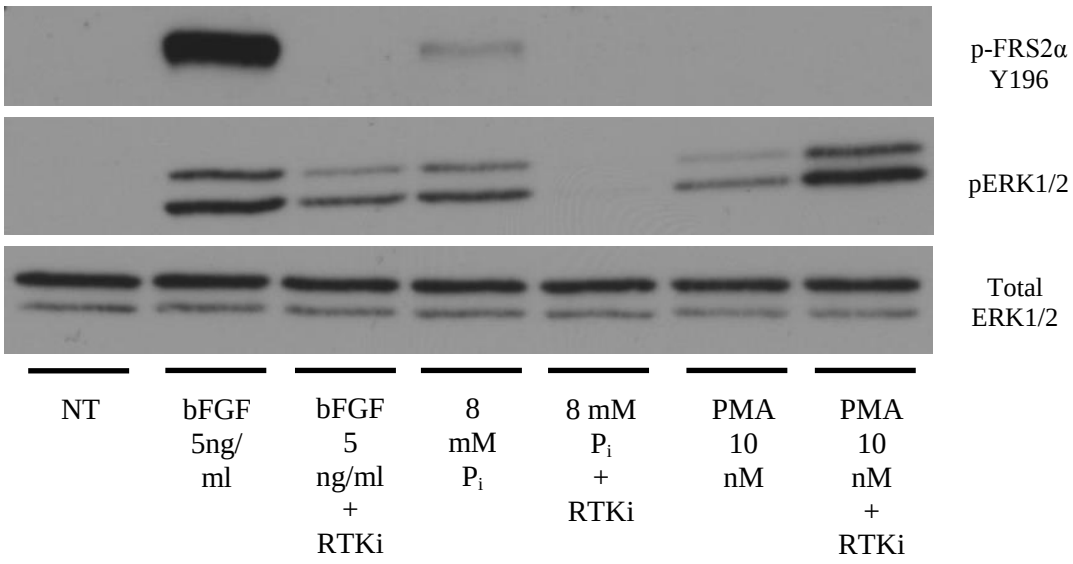

Figure 4-7: Effect of receptor tyrosine kinase inhibitor on cell signaling induced by P_i treatment.

NIH/3T3 cells were incubated in serum-free DMEM for 1 hour prior to treatments. Cells were treated with basic FGF, 8 mM P_i or phorbol 12-myristate 13-acetate (PMA) with or without co-treatment with 1 μM receptor tyrosine kinase inhibitor (RTKi) for 15 minutes. 'NT' indicates no treatment. Cells were then lysed and proteins were subjected to SDS-PAGE. Proteins were immunoblotted using antibodies against phospho-ERK1/2, total ERK1/2 or phospho-FRS2α Y196.

4.4 Discussion

In the previous chapters we established that elevated extracellular P_i affects cell behavior by first forming insoluble precipitates with calcium, which in turn are somehow sensed by cells. Through the experiments presented in this chapter, we attempted to discern the mechanism by which these precipitates are sensed by cells and activate signaling pathways within them. Established studies of several pathological conditions have yielded information which may be applicable to this question, including oxalate crystal toxicity, asbestos fiber inhalation, and crystal-cell interactions in osteoarthritis. Each of those phenomena caused some common reactions in cells, such as MAP kinase activation and ROS generation.

We first showed that oxalate crystals also activate MAP kinase signaling and induce OPN in fibroblasts, demonstrating that this type of crystal with a large organic acid component had properties similar to inorganic precipitates and crystals. Therefore, it seemed that cells respond to some general feature of crystals rather than a particular chemical composition or structure. Insoluble material may physically perturb cells. We tested this idea by using gadolinium, an inhibitor of stretch-activated ion channels, which are believed to operate in cells such as osteocytes that sense extracellular forces. However, addition of gadolinium caused precipitate formation and cell responses including OPN induction, suggesting that the sensing mechanism did not employ this type of ion channel. We did, however, find several lines of indicate that ROS are produced by P_i treatment, which provides a plausible explanation for our observation that FGF signaling is activated by P_i in the absence of FGF ligands. We directly measured an increase in ROS production following P_i treatment using a ROS-sensitive fluorescent

dye. We showed that co-treatment with an antioxidant largely abolished MAP kinase and FRS2α activation caused by P_i treatment, and we also showed that RTK kinase activity is probably necessary to initiate the observed MAP kinase activation by using an RTK inhibitor. These data together support the notion that generation of ROS following contact with insoluble precipitates is an early step in generating the observed cellular responses to high P_i treatment. It is unclear at this point how these ROS might be generated. The previously mentioned studies of RTK signaling propose that activation of membrane-adjacent Nox is responsible for generating ROS locally near RTKs. We tested this possibility using a Nox inhibitor, but found no effect on P_i-induced signaling (data not shown). Another possibility is that mitochondria are used as a source of ROS. However, it would seem that endocytosis of crystals or some other signaling response would need to communicate with mitochondria from the plasma membrane (where crystals initially interact with cells) to increase ROS, whereas the fast speed of the signaling response cause by P_i treatment makes this mechanism a less plausible explanation. In addition to ROS, other more specific cell surface molecules may play a part in the initial sensing of crystals. These could include scavenger receptors and toll-like receptors, which have known roles in detecting foreign materials in the immune system.

CHAPTER FIVE

Consequences of High Phosphate Diet Feeding

In the Kidney

5.1 Introduction

We have demonstrated using cell culture experiments that cells respond rapidly to elevated P_i concentrations in their extracellular environment. These responses include activation of cell signaling (MAP kinase pathway activation), rapid transcription factor activation and production (CREB activation and EGR1 production as shown by Yamazaki et al.), and osteopontin protein production over a longer time frame. In the course of investigating the mechanism by which P_i affects cells, we have found that elevation of extracellular P_i concentration results in the formation of calcium phosphate particles when sufficient calcium is present. We believe these particles are the stimulus that provokes the cellular responses we have observed, which may be a generalized response to mineral particles of endogenous or exogenous origin (see Chapter 4). If this response is indeed a general one, knowledge gained about cellular responses to one type of particle could potentially be applied toward managing the responses to other types of particles in related pathological conditions.

The ultimate goal of these experiments is to understand how high extracellular P_i leads to pathological changes in tissues and organs. There exists strong clinical evidence

indicating a correlation between high serum P_i concentrations and these adverse consequences, but a detailed understanding of why high P_i might be harmful is lacking. There are several possible approaches to modeling the effects of hyperphosphatemia. One approach is to observe the effects of P_i treatment on cells directly, as we have done in our culture studies presented above. However, it is also critical to expose tissues and organs to high extracellular P_i in the whole organism to observe how particular tissues and organs are affected, and determine if some locations in the organism are particularly sensitive. Mice lacking the Klotho protein or FGF23 hormone represent models of hyperphosphatemia because these mice fail to eliminate adequate amounts of P_i in the kidney. Alternatively, hyperphosphatemia can theoretically be produced in adult mice in any situation where P_i intake substantially exceeds the capacity of the animal to excrete that P_i load. This may arise when normal kidney function is compromised, or when P_i intake is much greater than normal.

Mouse Studies of High Dietary P_i Intake

High P_i feeding regimens have been used to model the excess P_i retention that can occur in kidney disease. However, animals with normal renal function increase urinary P_i excretion upon dietary P_i overload in an attempt to maintain serum P_i levels within normal range. Thus, high P_i feeding can result in increases in urinary P_i concentrations but not in serum P_i concentrations. To induce hyperphosphatemia, high P_i feeding treatment has usually been carried out as an adjunct to another perturbation to the kidney such as partial nephrectomy or ischemic injury to reduce the renal capacity to excrete P_i. This combination of treatments is considered more effective at producing hyperphosphatemia than either intervention alone. More recently, as P_i has gained

greater recognition as an independent risk factor for all-cause mortality, *in vivo* studies have been designed with a specific focus on the P_i contribution to pathology.

Eller et al. placed leptin receptor deficient *db/db* mice on a normal or high P_i diet, in combination with a uninephrectomy procedure (Eller et al., 2011). After the mice were fed either the normal or high P_i diet for 8 weeks, the authors found striking differences between diet groups. All mice fed the high P_i diet developed kidney calcifications that could be observed macroscopically on the surface of the kidney, while these were absent in the mice fed the normal diet. Crystal deposits were found in the lumen of kidney tubules, which were determined to be composed of hydroxyapatite (fluorine or hydroxyl-substituted calcium phosphate crystals). The mineral deposits were associated with deformities in tubule structure and fibrosis of kidney tissue. There was substantially more infiltration of tissue macrophages in the kidneys of mice fed the high P_i diet, as well as greater expression of inflammatory cytokines such as IFN-γ, IL-6, TNF-α and IL-10. High P_i fed mice had 2.5-fold greater serum concentration of osteopontin, and had metabolic phenotypes including weight loss, smaller fat stores and substantially lower fasting glucose levels (Eller et al., 2011). These results begin to identify some of the specific phenotypes that are attributable to dietary Pi overload, compared to mice receiving similar treatment (uninephrectomy and *db/db* background) that were not fed the high P_i diet.

A similar study attempted to define the contribution of high P_i load in the setting of impaired kidney function, but with a focus on evaluating the effects on vascular tissue (El-Abbadi et al., 2009). Mice with a wild-type but calcification-prone background (DBA2) underwent a two-step renal ablation procedure that involved partial cauterization

of one kidney and complete removal of the other kidney, producing uremic symptoms in these mice. After this renal ablation, mice were put on either a normal or high P_i diet and serum parameters and vascular histology were evaluated. The amount of calcium deposited in the aorta was greater only in mice fed the high P_i diet compared to normal diet or sham-operated mice. The same was also found to be true in mice that received a less severe renal ablation procedure ('moderately uremic' mice). These results were confirmed by histological examination and alizarin red staining for mineral. The combination of kidney ablation and high P_i diet resulted in the formation of mineral in large blood vessels, while such deposits were not observed in mice receiving kidney ablation and normal diet. Serum concentrations of FGF23 and osteopontin were also elevated in the moderately uremic mice receiving high P_i diet compared to those receiving normal diet. Osteopontin could also be detected in blood vessels at an early stage of pathological calcification (El-Abbadi et al., 2009). These two studies provide a foundation of evidence indicating that the P_i intake component of kidney disease has specific contributions to the resulting pathology. However, in both studies it is difficult to unambiguously determine the effect of P_i because the dietary experiments were carried out in combination with surgical renal ablation.

Tissue Fibrosis in Chronic Kidney Disease

The presence of histologically detectable mineral in the lumen of kidney tubules of mice fed the high P_i diet in the study by Eller et al. and the associated increase in inflammatory cytokines is notable because these molecules may contribute to tissue fibrosis, which is observed in chronic kidney disease. A similar process may be at work in the development of lung fibrosis caused by asbestos inhalation. Interaction with inorganic particles

causes an inflammatory reaction which over time results in irreversible lung fibrosis, with the generation of ROS as a necessary intermediate step (Fubini and Hubbard, 2003). It is therefore possible that mineral deposits formed in the renal tubular lumen in conditions of excessive P_i retention contribute to tissue fibrosis in the kidney. It is notable that the *klotho* mouse, which is one model of excessive Pi retention, has significant vascular calcification in the kidney but does not develop kidney fibrosis. However, there is *impaired* P_i excretion in the kidneys of these mice, leading to an increase in serum Pi but not in urine P_i. In contrast, while there is typically *increased* urine P_i in the mice with functioning kidneys fed a high P_i diet. The two models of phosphate nephropathy achieved by high P_i feeding mentioned above and the *klotho* mouse may therefore represent mechanistically distinct paths that expose different types of cells to high extracellular P_i, explaining the differences observed in the kidneys of these mice.

Hallmarks of Fibrosis

Fibrosis is often described as a wound-healing process that is uncontrolled and continues beyond a stage that is appropriate for the damage that may have initiated it. A normal wound-healing response (for example, to epithelial tissue) begins with clotting of blood if necessary, release of inflammatory cytokines and growth factors, and recruitment of immune cells such as macrophages. Immune cells secrete cytokines such as TGF-β1, which affect cellular behavior in the tissue and recruit fibroblasts and myofibroblasts, which remodel the damaged tissue and produce new extracellular matrix (ECM). Epithelial cells proliferate, replacing cells that may have been lost due to damage. In fibrosis, however, there is excessive proliferation and activity of fibroblasts, which produce abundant ECM. This excess ECM has the effect of displacing parenchymal cells

in the fibrotic tissue, leading to overall functional decline (Wynn, 2007). In kidney fibrosis, for example, this can be manifested as areas of ECM that have displaced and reduced the number of tubular epithelial cells, resulting in decline of kidney function.

5.2 Methods

Animals and Diets

Wild-type C57BL/6 and 129S1SvImJ background mice were obtained from Jackson Laboratories (Bar Harbor, ME) or from the University of Texas Southwestern Medical Center Animal Resource Center (ARC) core facility. The experimental diets were obtained from Harlan Laboratories. The control diet contains 0.35% w/w inorganic phosphate and 0.6% w/w calcium. The 'high P_i diet' contains 2% w/w inorganic phosphate and 0.6% w/w calcium. All animal experiments were approved by the Institutional Animal Care and Use Committee at the University of Texas Southwestern Medical at Dallas.

Blood Analysis

Blood was collected immediately following animal euthanization and serum separated for analysis of ion concentrations and FGF23. Serum concentrations of inorganic phosphate and calcium were measured by the University of Texas Southwestern Medical Center at Dallas Mouse Metabolic Phenotyping Core using VITROS MicroSlide™ technology. Serum FGF23 was measured using the FGF23 ELISA kit from Kinos (Japan), which detects intact FGF23.

Immunohistochemistry

Standard immunohistochemistry techniques for paraffin embedded tissue sections were employed unless otherwise mentioned. Reagents were obtained from Sigma-Aldrich unless otherwise mentioned. Masson's Trichrome staining was performed on paraffin embedded kidney sections by the University of Texas Southwestern Medical Center Histology core facility.

TGF-β1 staining: mouse primary anti-TGF-β1 antibody was obtained from R&D Systems and diluted 1:40 in 1% BSA solution for antigen labeling. Secondary goat anti-mouse biotin-conjugated antibody (1:200 dilution) was obtained from Invitrogen and streptavidin-horseradish peroxidase was also obtained from Invitrogen.

Osteopontin staining: mouse anti-OPN antibody was obtained from Santa Cruz Biotechnology and diluted 1:100 for antigen labeling. Secondary anti-mouse horseradish peroxidase-conjugated antibody was obtained from Vector Laboratories.

Quantitative Reverse-Transcription Polymerase Chain Reaction (qPCR) Analysis

Kidney tissue samples were lysed using Trizol® reagent from Invitrogen and homogenized using Polytron homogenizer. Total RNA was isolated using an RNeasy RNA extraction kit from Qiagen. For cell culture studies, cells were lysed and purified using reagents from the RNeasy RNA extraction kit from Qiagen. RNA was then treated with DNAse (Invitrogen) and subjected to a reverse transcription reaction (reverse transcriptase obtained from Invitrogen) to produce sample cDNA. The qPCR reaction mixture consisted of sample cDNA, qPCR primers and qPCR reaction master mix containing SYBR green from Applied Biosystems. The qPCR reaction was run using an Applied Biosystems 7900 HT Sequence Detection System and data were obtained using SDS 2.3 software from Applied Biosystems. Data were analyzed using the ΔΔCt method. Primer sequences used for qPCR are listed according to species below.

Human:

Gene Name	Forward Primer	Reverse Primer
MCP-1	5′-GGCTCAGCCAGATGCAGTTAAC-	5′-GCCTACTCATTGGGATCATCTTG-3′
GAPDH	5′-GTCAGTGGTGGACCTGACCT-3′	5′-TGAGGAGGGGAGATTCAGTG-3′

Mouse:

Gene Name	Forward Primer	Reverse Primer
TGF-β1	5′-TTGCTTCAGCTCCACAGAGA-3′	5′-TGGTTGTAGAGGGCAAGGAC-3′
α-SMA	5′-CTGACAGAGGCACCACTGAA-3′	5′-CATCTCCAGAGTCCAGCACA-3′
p21	5′-TCTCAGGGCCGAAAACG-3′	5′-AATCTGCGCTTGGAGTGATAGA-3′
Collagen-1	5′-GAGCGGAGAGTACTGGATCG-3′	5′-GTTCGGGCTGATGTACCAGT-3′
Cyclophilin	5′-TGGAGAGCACCAAGACAGACA-3′	5′-TGCCGGAGTCGACAATGAT-3′
Osteopontin	5′-CCCGGTGAAAGTGACTGATT-3′	5′-TTCTTCAGAGGACACAGCATTC-3′

Rat:

Gene Name	Forward Primer	Reverse Primer
α-SMA	5′-TGTGCTGGACTCTGGAGATG-3′	5′-GAAGGAATAGCCACGCTCAG-3′
Collagen-1	5′-CAGGGAAGCCTCTTTCTCCT-3′	5′-ACGTCCTGGTGAAGTTGGTC-3′
Cyclophilin	5′-GTCTGCTTCGAGCTGTTTGC-3′	5′-TTCACCTTCCCAAAGACCAC-3′

Immunoblot Analysis

Cells were collected in cell lysis buffer (20 mM HEPES, 100 mM NaCl, 1.5% Triton-X100, 15 mM NaF, 20 mM phosphatase inhibitor cocktail (Sigma), protease inhibitor mix (Roche), 1 mM EDTA and 20 mM sodium pyrophosphate) and centrifuged for 10 minutes at 13,000 rpm. Supernatants were collected and SDS sample buffer was added before boiling samples for 5 minutes. Protein samples were subjected to SDS-polyacrylamide gel electrophoresis (SDS-PAGE) and proteins were then transferred to nitrocellulose membranes. Membranes were incubated in blocking buffer (2% milk, 0.05% v/v Tween 20 in TBS) then incubated with primary antibodies. The phospho-ERK1/2, and total ERK1/2 antibodies were obtained from Cell Signaling Technologies. All antibodies were diluted at a ratio of 1:1000. Membranes were washed in a TBS-Tween solution and then incubated with appropriate secondary antibodies conjugated with horseradish peroxidase (GE Healthcare). Blots were developed using SuperSignal West Dura Extended Duration Substrate from Thermo Scientific.

Light Microscopy and Microphotography

Microscopy images were obtained using a Leica Microsystems DM IL inverted microscope. A SPOT-idea™ digital camera was used to capture images in conjunction with SPOT Advanced Plus software.

Cell Viability Assay

Cells were trypsinized and resuspended in PBS solution. An equal amount of 0.4% w/v trypan blue solution (Sigma-Aldrich) was then added to the cell solution and the combined solution was incubated for 10 minutes. After incubation, cells were delivered onto a hemocytometer and viable (non-staining) and non-viable (staining) cells were counted. Viability was calculates as: (total # of cells counted – # of staining cells)/(total # of cells counted) X 100 = % viability.

Calciprotein Particle (CPP) Generation

CPPs were synthesized by combining 10 mM NaP_i and 5 mM $CaCl_2$ in DMEM containing 10 % FBS for 72 hours at 37°C. After incubation, the solution was spun at 16,400 x g for 2 hours, and pellets were resuspended in 1 mL DMEM.

Cell Culture

HUVEC endothelial cells and NRK kidney cells were obtained from American Type Culture Collection (ATCC). Cells were cultured in 10 cm dishes and experiments were performed in 12 well plates purchased from Corning-Costar. Cells were maintained using Dulbecco's Modified Eagle Medium (DMEM) supplemented with 10% fetal bovine serum (FBS) and antibiotics (penciling and streptomycin, 100 U/ml and 100 µg/ml respectively), all obtained from Life Technologies, Gibco Brand.

5.3 Results

The studies by Eller et al. and El-Abbadi et al. utilizing a high P_i diet in conjunction with some form of renal ablation suggest that the excess P_i load has adverse effects in the kidney and vascular tissue (El-Abbadi et al., 2009; Eller et al., 2011). We wished to determine the effects of the high P_i diet alone without the additional experimental renal ablation and uremia that can develop as a consequence. To test the effects of high P_i diet alone, we designed a feeding regimen using wild-type mice and used no other experimental renal ablation procedures. Feeding treatments of this type, without additional renal ablation or mutant genetic background, are not typically used to model kidney diseases (with the exception of ethylene glycol feeding to model hyperoxaluria) because the pathological effects are not severe enough to be consistently useful for experimental evaluation. However, in other experiments in the laboratory designed to study the effects of high P_i diet on female fertility, we found consistent phenotypic changes caused by high P_i feeding. We fed adult 129 background mice (12 weeks of age) a diet containing 2% by weight P_i or a control diet that contained 0.35% by weight P_i for 12 weeks. At the end of the treatment period, mice we sacrificed and we evaluated serum and urine parameters, kidney histology and changes in kidney gene expression (experiments presented in Figures 5-1 through 5-4 were performed by Kazuhiro Shiizaki in the Kuro-o laboratory). As shown in Figure 5-1, blood concentration of FGF23 rose more than several-fold in mice fed the high P_i diet compared to normal diet controls by the end of the treatment period. Urine P_i also rose five-fold in mice receiving high P_i diet versus control diet (Figure 5-1). Blood serum concentration of P_i displayed a trend toward increase in mice receiving high P_i diet, although the effect was not

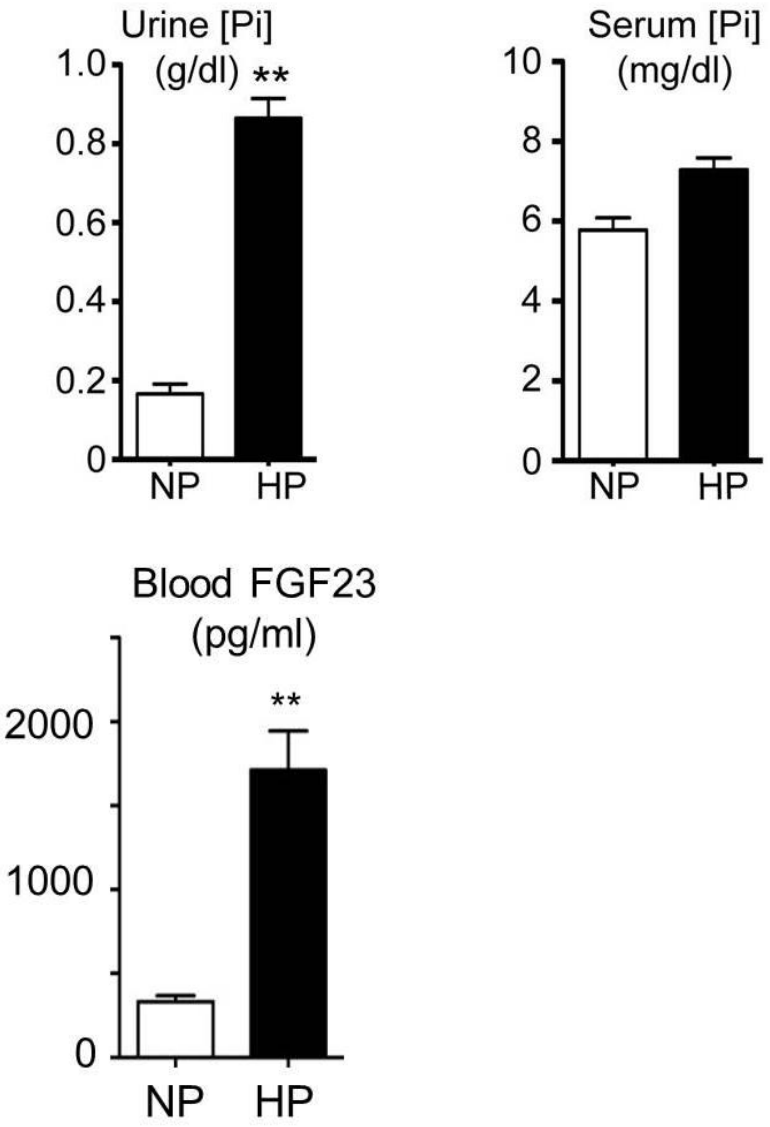

Figure 5-1: Serum measurements at the end of high P_i feeding treatment period. Wild-type 129 background mice were fed either normal control diet (NP) or high P_i diet (HP) for 12 weeks. Serum was collected at the end of the treatment period and FGF23 was measured by ELISA and calcium and P_i ions were measured using a VITROS chemical analyzer. Error bars represent standard error about the mean (* = $p < 0.05$).

statistically significant. These measurements clearly indicate that the high P_i diet causes compensatory changes in the FGF23 hormone axis resulting in increased P_i excretion in urine, and that these changes were mostly though not completely effective in maintaining normal serum P_i levels.

We next examined structural changes in the kidney by employing Masson's trichrome stain to kidney sections taken from mice fed control or high P_i diet. This staining mixture labels cytoplasm pink and connective tissue is stained blue. Unexpectedly, we found that mice fed the high P_i diet consistently developed tubulointerstitial fibrosis regions in the kidney cortex while mice fed the normal diet never developed these fibrotic regions (compare Figures 5-2a and 5-2b). A higher-magnification view is presented in Figure 5-3a. The interstitial fibrosis was observed primarily around proximal tubules. The proximal tubules surrounded by fibrotic tissues and infiltrated cells were characterized by bright nuclei and weak acidophilic staining in the cytoplasm (Figure 5-3a). TGF-β1 is a cytokine believed to play a key causative role in the development of tissue fibrosis (Wynn, 2007). We used immunohistochemical (IHC) staining to determine if there was an increase in the expression of TGF-β1 in the kidneys of mice fed high P_i diet. As shown in Figure 5-3b, we found substantial TGF-β1 staining in fibrotic areas in the kidneys of mice fed high P_i diet, but this staining was absent in the control diet samples. There was strong overlap of the fibrotic areas and TGF-β1 staining, where both tubular and interstitial cells expressed TGF-β1 while adjacent tubular cells in non-fibrotic areas did not express TGF-β1. We also examined the expression of osteopontin (OPN) using IHC staining. We demonstrated earlier that

a.

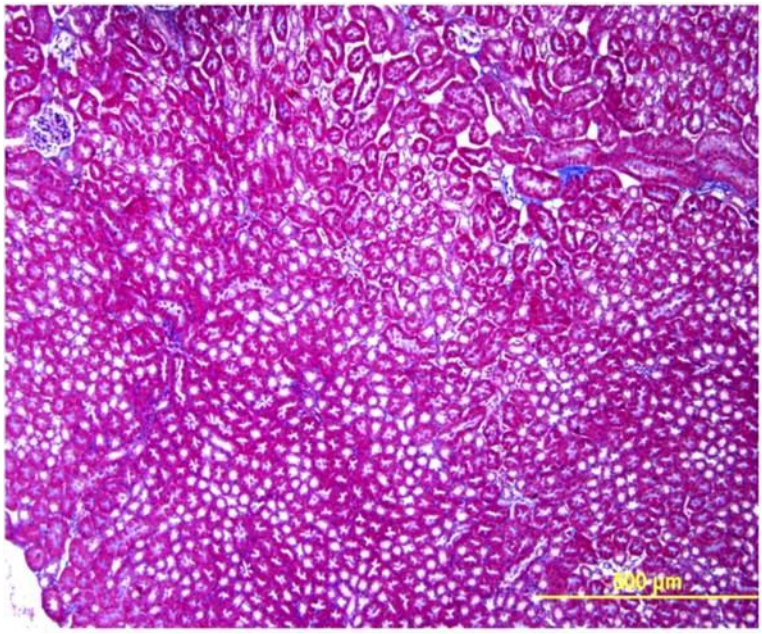

b.

Figure 5-2: Histology of kidneys from mice fed control or high P_i diet.
Wild-type 129 background mice were fed either normal control diet (NP, panel **a**) or high P_i diet (HP, panel **b**) for 12 weeks. Sections were taken from kidney cortices of each treatment group and paraffin embedded, then treated with Masson's trichrome stain. Scale bars represent 500 µm.

OPN is a P_i-responsive gene in cell culture studies, but it is not known if high P_i diet feeding has a similar effect on kidney cells *in vivo*. We found that like TGF-β1, OPN was also induced selectively in tubule cells located in fibrotic regions of kidneys from mice fed a high P_i diet, but OPN staining was largely absent outside fibrotic regions or in the kidneys of mice fed the control diet (Figure 5-3c). High P_i feeding therefore appears to replicate the effect of high extracellular Pi on OPN induction seen in our cell culture studies, though the mechanism of how this happens could be different *in vivo*.

We further evaluated gene expression changes in the kidney by performing quantitative reverse-transcription polymerase chain reaction (qPCR) using tissue samples obtained at four time points during the treatment period from the kidneys of mice fed the high P_i diet or the control diet. We chose to measure expression of four genes known to be involved in the development of fibrosis: TGF-β1, p21, collagen-1 and α-SMA. The p21 tumor suppressor gene is induced by TGF-β1 signaling and in part mediates cell senescence caused by TGF-β1 exposure (Datto et al., 1995); α-SMA is an actin isoform that is expressed in smooth muscle and myofibroblasts which may be present in fibrotic tissue. We found that by 8 weeks after beginning the high P_i diet treatment, the mRNA expression all four of these fibrosis-associated genes was significantly elevated and continued to rise until the end of the experiment at 12 weeks (Figure 5-4). Both histological examination and analysis of gene expression therefore support the novel conclusion that the high P_i diet by itself can cause fibrotic changes in the kidneys of the mouse. This conclusion is notable because mice with unimpaired kidney function are generally thought to be capable of adequately excreting an elevated P_i load, which only poses a problem to animals with impaired kidney function. These results suggest that

a. Masson's trichrome stain

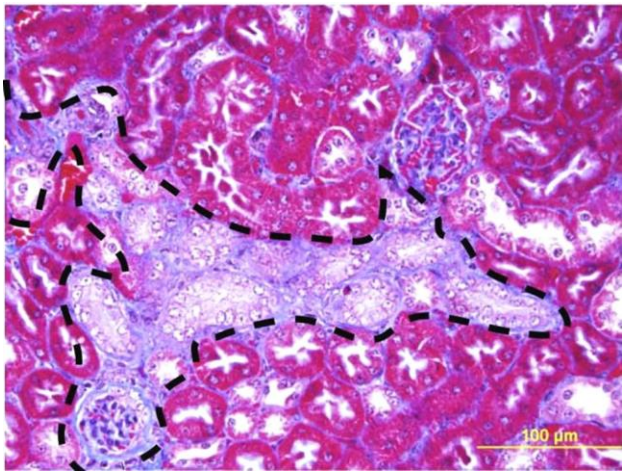

b. TGF-β

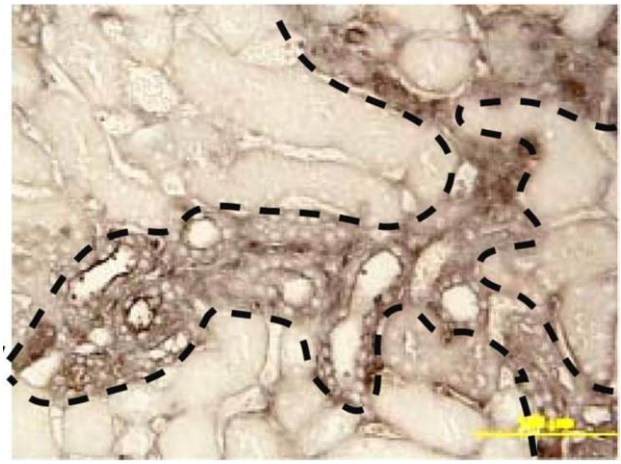

c. Osteopontin

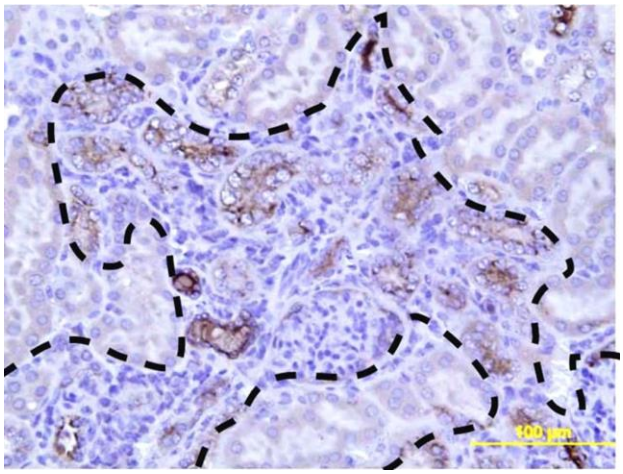

Figure 5-3: Immunohistochemistry of fibrotic kidney tissue in mice fed high P_i diet.
Kidney sections from adult wild-type mice fed a high P_i diet for 12 weeks were treated with Masson's trichrome stain (**a.**) or subjected to immunohistochemical staining for TGF-β (**b.**) or osteopontin (**c.**). Outlined areas represent fibrotic tissue. Scale bars represent 100 µm.

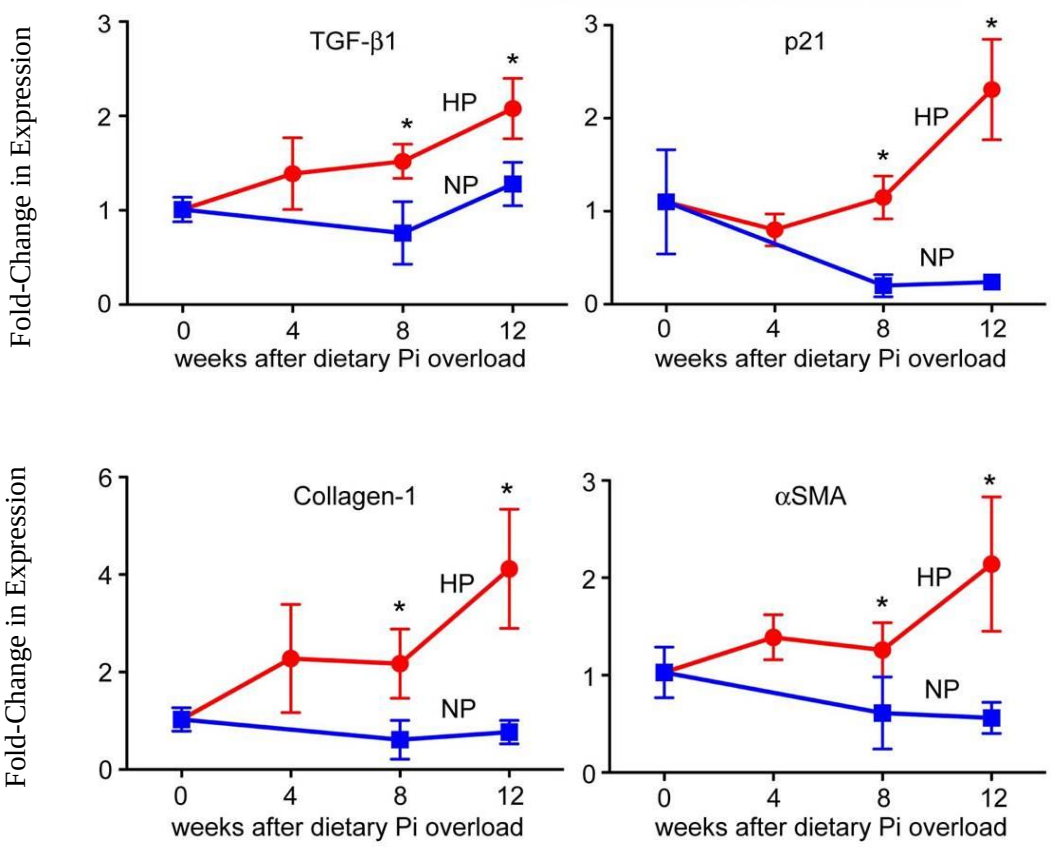

Figure 5-4: qPCR analysis of changes in gene expression in the kidney over the course of high P_i diet treatment.

Kidney tissue was collected from wild type mice fed control diet (blue squares) or high P_i diet (red circles) and subjected to qPCR analysis to quantify the expression of selected genes. Tissue was collected at the beginning of feeding treatment (t = 0) and at 4 week-intervals thereafter until 12 weeks, at which time the expression of TGF-β, p21, collagen-1α and α-SMA was measured. Error bars represent standard error about the mean (* = $p < 0.05$).

high dietary P_i could be harmful to otherwise healthy animals with unimpaired kidney function.

We performed an additional study of high P_i diet feeding in mice, both to replicate our previous findings and to examine the relationship between changes in gene expression in the kidney and changes in blood serum concentrations of P_i and calcium. We fed wild-type C57BL/6 mice aged 4.5 weeks with control diet supplied by the animal resource center (containing 0.35% Pi) or high P_i diet containing 2% P_i by weight. The treatment period lasted for 6 weeks, after which body weight, serum P_i and calcium, and kidney expression of OPN were measured. The body weight of mice fed the high P_i diet was significantly reduced compared to normal diet controls by the end of the treatment period (Figure 5-5a), indicating the physiological impact of excessive P_i load despite unimpaired kidney function at the beginning of the experiment. Measurement of serum calcium and P_i, however, indicated that were no significant changes in the concentrations of these ions caused by the high P_i diet (Figure 5-5b and 5-5c) after 6 weeks. Measurement of OPN expression in the kidney by qPCR showed a threefold increase in the kidneys of mice fed the high P_i diet compared to normal diet controls (Figure 5-5d). These data reveal a notable discrepancy: indicators of pathological consequences of high P_i feeding, such as lowered body weight and induction of OPN in the kidney, appear *before* there is a significant change in serum calcium or P_i ion concentrations. This result has implications for the use of monitoring of these serum ion parameters in evaluating risk of kidney pathology prospectively. In contrast, substantial kidney damage may occur before changes in these ions can be detected.

Since high P_i feeding alone appeared sufficient to cause kidney fibrosis, we hypothesized that high dietary P_i load results in a compensatory increase in P_i excretion, causing an increase in P_i concentration in the tubule lumen. This high P_i concentration in

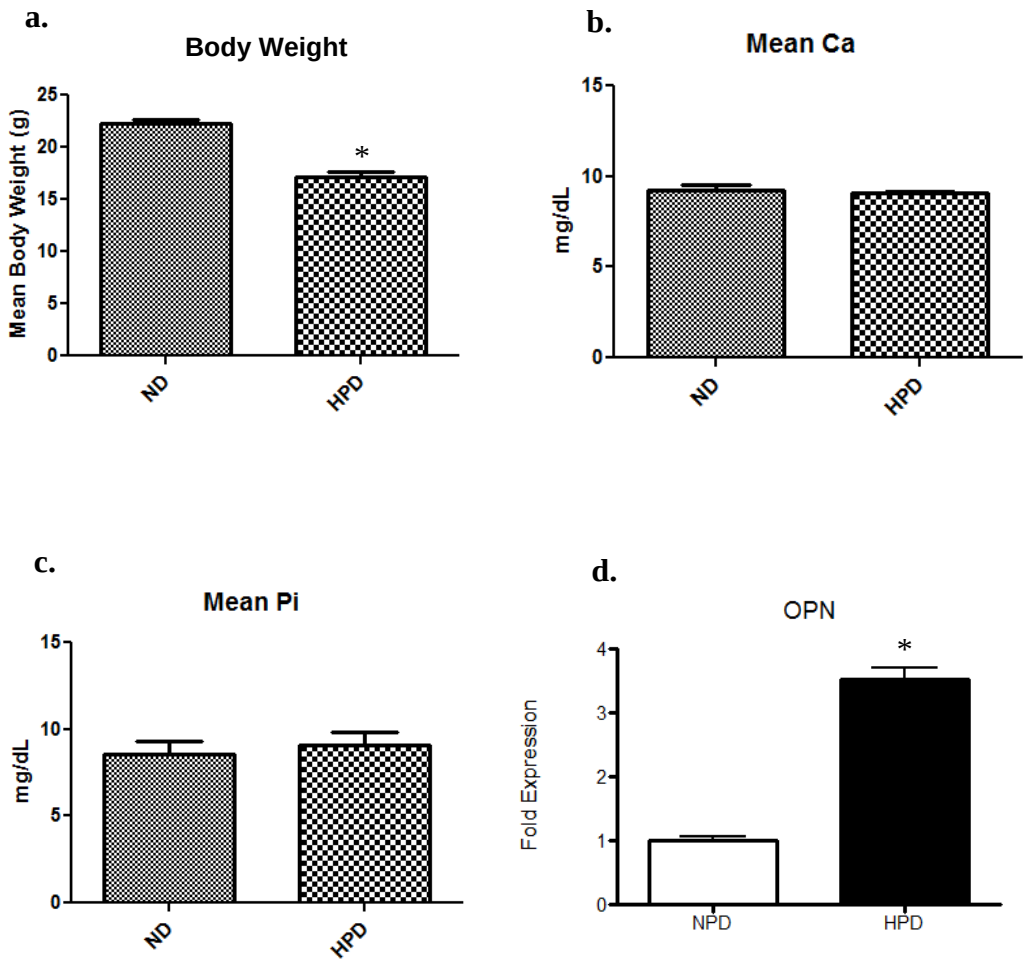

Figure 5-5: Changes in body weight, serum parameters and kidney OPN expression in C57BL/6 mice fed control or high P_i diet.
Wild-type C57BL/6 mice aged 4.5 weeks were fed either a control diet (ND) or a high P_i diet (HPD) for 6 weeks. At the end of the treatment period, body weight was measured (**a.**) as well as serum calcium (**b.**) and serum P_i (**c.**). Kidney tissue was isolated at the end of the treatment period and osteopontin expression was quantified using qPCR (**d.**). Error bars represent standard error about the mean (* = $p < 0.05$).

the tubule lumen results in the formation of calcium phosphate particles which affect cellular behavior. It was not clear, however, if high P_i treatment causes an increase in pro-fibrotic gene expression. To determine if such an effect exists, we synthesized calcium phosphate particles in serum-containing DMEM (calciprotein particles, CPPs) for treatments on the rat kidney cell line NRK. NRK cells were treated with 1.5 µl/ml CPPs (equivalent to 0.15 mM phosphate) for 48 hours, after which RNA was collected for qPCR analysis of various genes indicative of fibrotic transformation. We found that CPP treatment caused a significant increase in both α-SMA and collagen-1 in NRK cells (Figure 5-6). The interaction of calcium phosphate precipitates with tubule cells in the kidney may therefore be an early step in the development of fibrosis caused by high dietary P_i load.

Finally, we assessed the effect of calcium phosphate particles on vascular tissue. As demonstrated by El-Abbadi et al., excessive dietary P_i has adverse effects on vascular cells (El-Abbadi et al., 2009). We performed cell culture experiments to determine if CPPs have direct adverse effects on endothelial cells. We first treated cells of the human endothelial cell line HUVEC with 8 mM P_i buffer or 3 µl/ml CPPs for 20 minutes and evaluated activation of cell signaling. We found that both treatments acutely activated the ERK1/2 kinases after 20 minutes of treatment (Figure 5-7), suggesting that these endothelial cells are also responsive to calcium phosphate particles. When we attempted to perform longer-term experiments with CPPs on HUVEC cells, however, we found that CPPs had a strong negative effect on cell viability. When HUVEC cells incubated in serum-containing DMEM were treated with 3 µl/ml CPPs for 48 hours, a large amount of cell death occurred (compare Figures 5-8a and 5-8b). We performed viability assays to

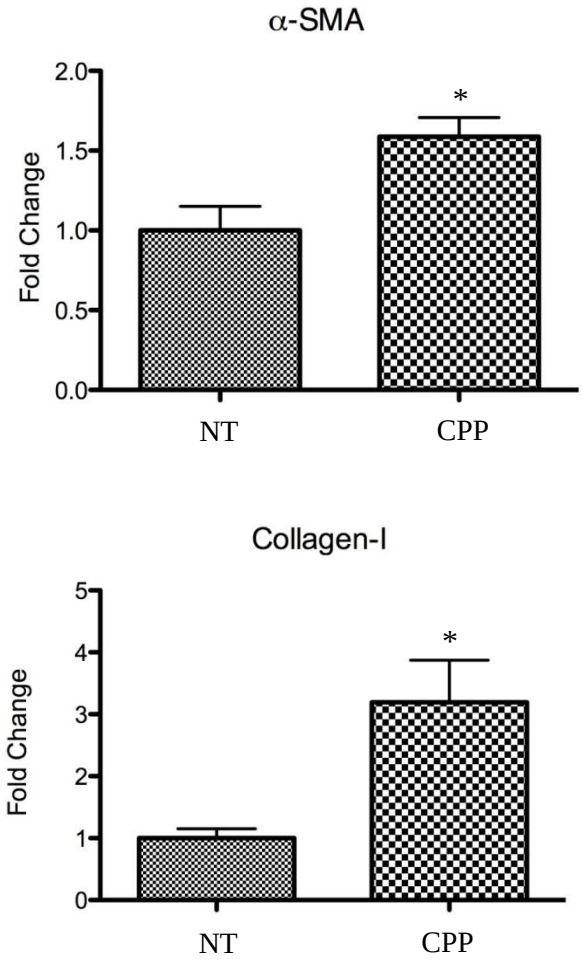

Figure 5-6: Changes in α-SMA and collagen-1α expression in NRK cells following treatment with CPPs.
NRK cells incubated in DMEM with 10% FBS were incubated with 1.5 µl/ml CPP (CPP) or no treatment (NT) for 48 hours. After the treatment period, RNA was isolated and expression of α-SMA and collagen-1α was measured by qPCR. Each treatment group was represented by 3 independent replicates. Error bars represent standard error about the mean (* = $p < 0.05$).

quantify the amount of cell death caused by treatment with P_i buffer or CPPs. Using trypan blue staining to label dead or dying cells, we found that HUVEC cells treated for 48 hours with 8 mM P_i buffer exhibited a trend toward lower viability (though not statistically significant) and cells treated with 3 µl/ml CPPs had significantly reduced viability (Figure 5-9a). In a dose-dependency study, we found that treatment of HUVEC cells with 2 µl/ml or 3 µl/ml CPPs for 48 hours significantly reduced cell viability, while treatment with 1 µl/ml CPPs did not (Figure 5-9b). It therefore appears that these endothelial cells are particularly sensitive to CPP treatment, because other cell lines (such as NRK) did not exhibit this decline in viability as a result of CPP treatment. We examined changes in gene expression that may be occurring over time in HUVEC cells following treatment with CPPs. We treated HUVEC cells with a lower dose of CPPs (2 µl/ml) for 12, 24 or 48 hours in serum-containing DMEM and evaluated changes in gene expression by qPCR. While we did not observe changes in OPN expression (OPN mRNA was not detectable in our samples), the expression of the chemokine MCP-1 rose significantly in all time points (Figure 5-10). MCP-1 has chemoattractant properties towards monocytes/macrophages and mediates inflammatory responses. Oxalate crystal treatment causes an increase in MCP-1 expression in NRK cells (Umekawa et al., 2005). Stimulation with calcium phosphate particles therefore appears to provoke an inflammatory response from endothelial cells in culture as well as kidney cells.

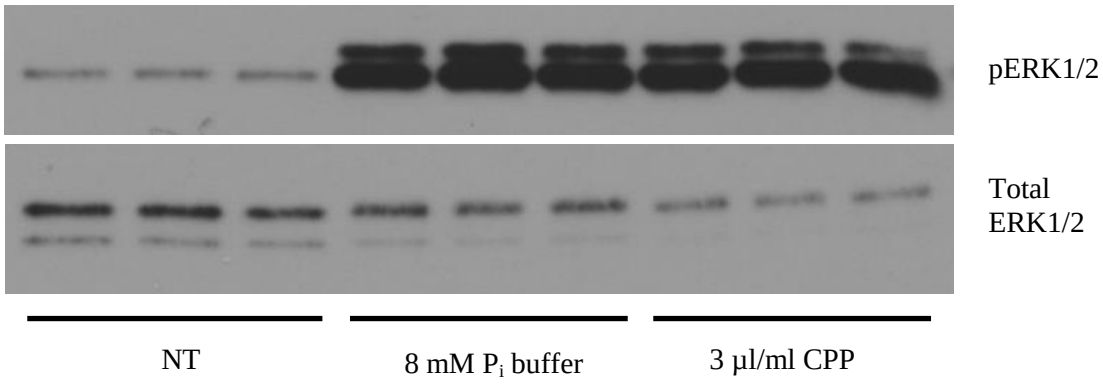

Figure 5-7: Activation of cell signaling in HUVEC cells by P_i buffer and CPP treatment.
HUVEC cells were starved of serum for 45 minutes prior to treatment with 8 mM P_i buffer or 3 µl/ml CPPs for 20 minutes. After the treatment period, cells were lysed and proteins were subjected to SDS-PAGE, then immunoblotted for activated ERK1/2 (p-ERK1/2) as well as total ERK1/2 protein. Three lanes in each treatment group represent 3 independent culture well samples.

a.

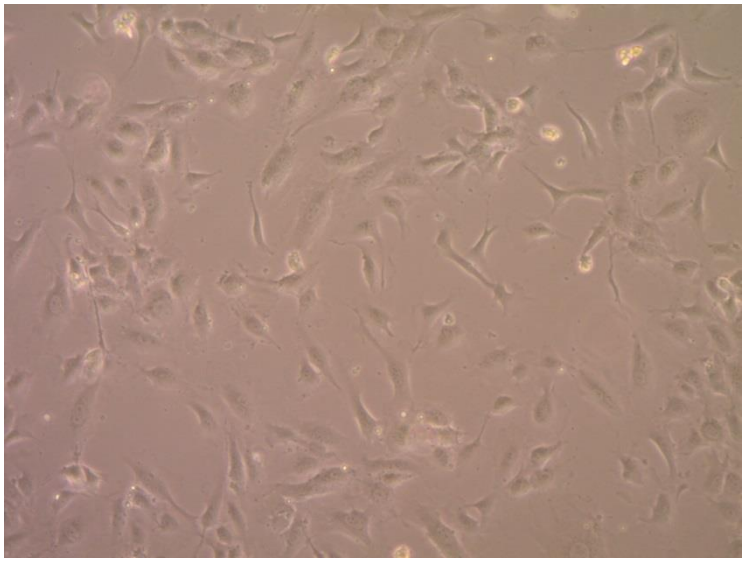

b.

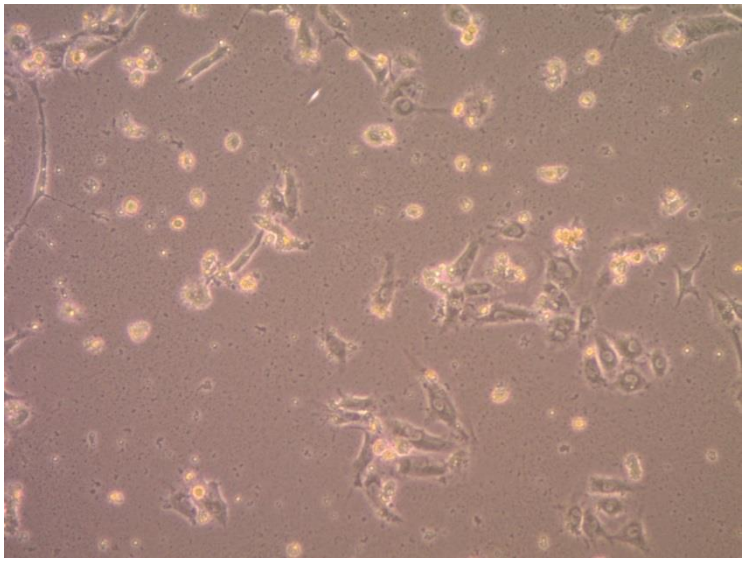

Figure 5-8: Treatment of HUVEC cells with CPPs affects cell viability.
HUVEC cells were culture in DMEM containing 10% FBS for 48 hours without (**a.**) or with (**b.**) the addition of 3 µl/ml CPP. Images were taken at 100X total magnification.

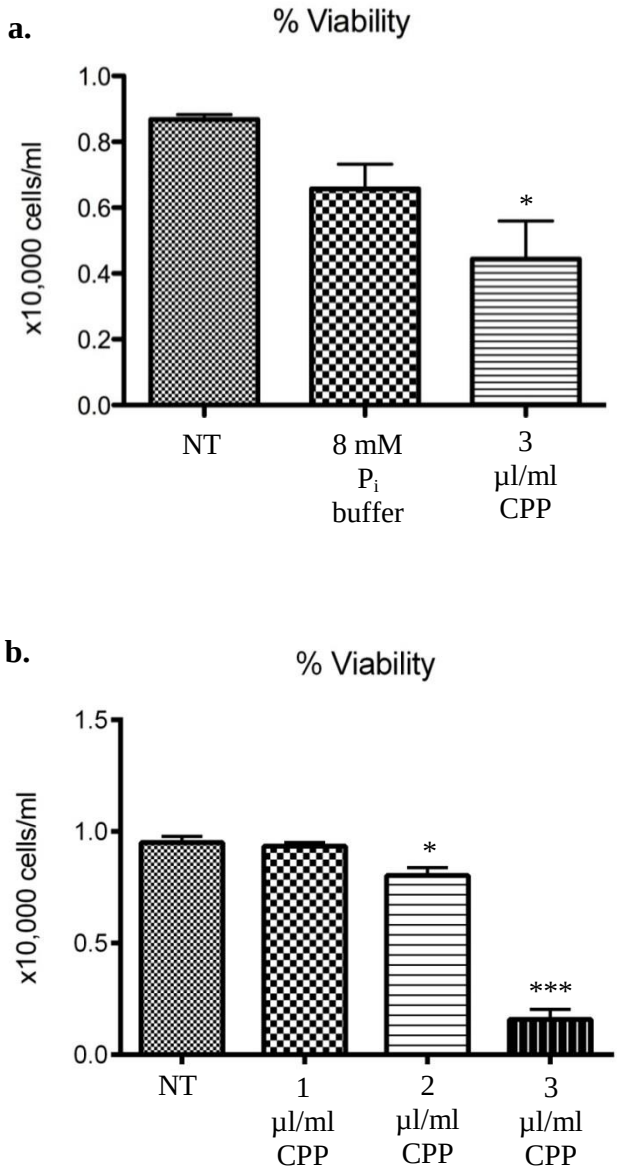

Figure 5-9: CPP treatment effect on HUVEC cell viability.
HUVEC cells were incubated in DMEM containing 10% FBS and treated with P_i buffer or CPPs for 48 hours. Cells were treated with either a single dose of P_i buffer and CPPs (**a.**) or a range of CPP doses (**b.**). Each treatment group is represented by 3 experimental replicates. Cell viability was assessed using trypan blue staining. Error bars represent standard error about the mean (* = $p< 0.05$; *** = $p<0.0005$).

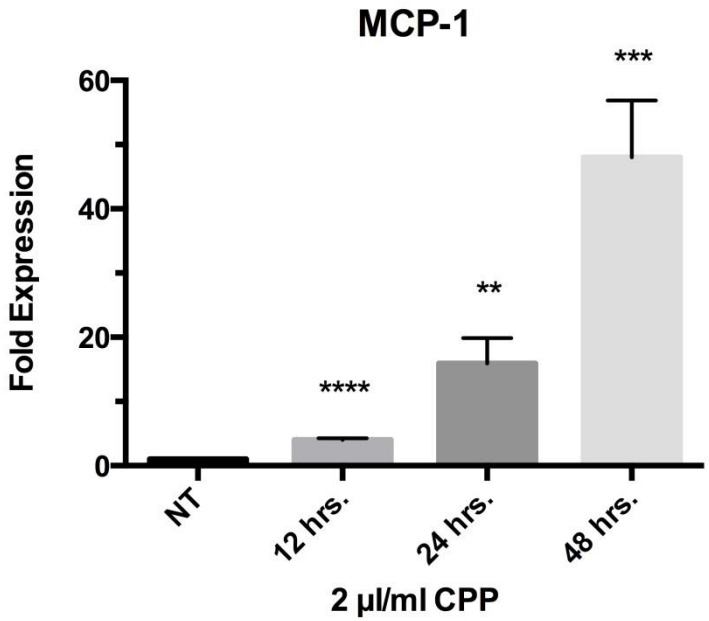

Figure 5-10: **Change in MCP-1 gene expression over time with CPP treatment.** HUVEC cells were incubated in DMEM containing 10% FBS and treated with 2 µl/ml or received no treatment (NT) for the indicated treatment lengths. After the treatment period, RNA was isolated and expression of MCP-1 was measured by qPCR. Each treatment group was represented by 3 independent replicates. Error bars represent standard error about the mean (** = $p< 0.005$; *** = $p<0.001$; **** = $p<0.0001$).

5.4 Discussion

The overall purpose of the experiments presented here is to gain an understanding of how excess retention of P_i in mammals leads to pathological consequences. By performing cell-culture experiments, we confirmed that high concentrations of P_i indeed provoke a signaling response in bone cells and fibroblasts, but only in the presence of calcium. We thus identified calcium phosphate particles as the agents responsible for changes in cellular behavior, while high extracellular P_i by itself may have relatively little effect on cells. In the experiments presented in this chapter, we attempted to extend the findings from the cell culture studies into an *in vivo* setting using wild-type mice. Specifically, we were interested in determining the effects of excessive P_i retention on the kidneys and the vasculature, which are tissues of critical importance in the pathology of CKD. Previous *in vivo* studies from other laboratories have provided evidence that challenge with a diet containing higher than normal P_i content exacerbates the pathologies of kidney disease models (El-Abbadi et al., 2009; Eller et al., 2011). However, in both of these studies the high P_i diet was used in combination with multiple conditions and interventions that alone compromise kidney function and overall health. These included uninephrectomy, cauterization of the remaining kidney, and genetic backgrounds that tended to worsen the impact of renal ablation (DBA/2 genetic background or leptin receptor deficiency). We therefore performed high P_i diet feeding experiments on wild-type mice to determine if excess P_i retention caused biological changes despite initially normal kidney function.

After treatment with high P_i diet for 12 weeks, wild-type 129 background mice showed changes in serum FGF23 concentration and urine P_i excretion that indicated

adjustment to the increased dietary P_i load, and serum P_i concentration was not significantly changed. These results made the finding of histological changes in the kidneys of these mice surprising. Wild-type mice fed the high P_i diet developed interstitial fibrosis in their kidneys, with increased expression of TGF-β1 and OPN in fibrotic regions. Analysis of gene expression in the kidney by qPCR also revealed increased expression of collagen-1α and α-SMA, which are proteins associated with tissue fibrosis. In a follow-up dietary experiment, wild-type C57BL/6 mice were fed a high P_i diet for 6 weeks. At the end of the treatment period, mice receiving the high P_i diet weighed significantly less than controls and had threefold greater OPN expression in their kidneys, despite having identical serum calcium and P_i concentrations as mice fed the control diet. Together, these dietary experiments indicate that excess P_i by itself does indeed have adverse effects *in vivo* in mice with initially intact kidney function. This was a surprising result because we and others presumed that the healthy kidney would be able to adequately clear the excess P_i present in the diet. Instead, the high P_i diet clearly had broad physiological effects, as evidenced by the weight loss, despite compensatory increases in P_i excretion. The lack of change in serum concentrations of calcium and P_i is also notable. An intuitive assumption is that high dietary P_i would not have adverse effects if serum P_i concentration has not increased, because the kidneys have adequately disposed of the excess and cells and tissues outside the kidney are therefore not chronically exposed to higher P_i concentrations. However, the presence of kidney fibrosis indicates that the high P_i diet does have biological effects despite normal serum P_i concentrations. One possible conclusion from these data is that serum measurements of P_i do not give a comprehensive or reliable indication of the total P_i load experienced

by the animal. Excess P_i may be accumulating inside cells, bones or soft tissues while the serum concentration of P_i remains unchanged.

Finally, we evaluated the effects of calcium phosphate-containing nanoparticles (CPPs) on kidney and vascular cells, to see if certain aspects of the *in vivo* responses to high P_i diet could be replicated in cell culture. We found that CPP treatment increased the expression of the fibrosis-associated genes α-SMA and collagen-1α in NRK cells. We also found that these particles had detrimental effects on the viability of endothelial cells in culture, and increased the expression of the inflammatory cytokine MCP-1 in these cells. It therefore appears that some of the key effects of the high P_i diet on sensitive tissues can be reproduced in cell culture, indicating that these effects are a direct consequence of particle exposure.

CHAPTER SIX

Summary and Outlook

6.1 Meeting the Challenges of Phosphate Homeostasis in Vertebrates

Phosphorus, typically in the form of phosphate, is an essential chemical component of known living organisms. Unicellular organisms such as bacteria and yeast have evolved sophisticated systems to acquire phosphate from the environment, sense the abundance or scarcity of phosphate and mount an appropriate response to conserve phosphate if necessary. In vertebrates, phosphate homeostasis is intimately integrated with fluxes of calcium and phosphate into and from bone, which serves as a store for the majority of total body calcium and phosphate. Phosphate and calcium are acquired in the diet and first flow through the intestine before entering the other major pools, such as blood serum, soft tissues and bone. The critical organ for maintaining phosphate homeostasis for the organism as a whole is the kidney, where reabsorption and excretion of phosphate and other ions can be adjusted based on scarcity or excess in the diet. To coordinate the flow of phosphate among the discrete pools within the body, several interconnected hormonal systems act on intestine, kidney and bone to ensure an adequate supply of these mineral ions to tissues throughout the body. Parathyroid hormone (PTH) liberates calcium and phosphate from bone and has phosphaturic effects in the kidney, while active vitamin D (calcitriol) increases intestinal absorption of calcium and

phosphate and downregulates PTH production in the parathyroid glands. The novel phosphaturic hormone FGF23 is produced in bone and acts on the kidney to increase phosphate excretion and reduce production of calcitriol. While calcitriol is known to increase FGF23 expression in bone, exactly how FGF23 expression is normally regulated to ensure long-term phosphate homeostasis remains less well understood than the consequences of complete FGF23 absence or abnormal excess. One current hypothesis is that mineralization activity or mineral content in the bone is sensed by osteocytes or osteoblasts, which adjust their production of FGF23 (Martin et al., 2012). The normal physiological regulation of FGF23 remains an area of active research interest, as does possible pathological effects of FGF23 excess.

6.2 Examining the Effects of Excess Extracellular Phosphate

When vertebrate phosphate homeostasis is not maintained, there can be adverse consequences such as deficiencies in structure and function of bone due to hypophosphatemia or deposition of mineral in soft tissues due to hyperphosphatemia. Mice lacking the Klotho protein, a co-receptor for FGF23, exhibit hyperphosphatemia and develop a wide array of pathological phenotypes including soft tissue calcifications. We endeavored to understand in greater detail what effects excess extracellular phosphate may have on cells, tissues and the organism as a whole. The effects of phosphate had been studied in some contexts previously, such as modeling bone mineralization or pathological mineral deposition, and we used this knowledge as a foundation for our studies. Treatment of osteoblasts or fibroblasts with high extracellular phosphate (typically 8 mM or greater, compared to 1 mM in typical cell culture media) resulted in the activation of the MAP kinases ERK1 and ERK2 as well as the transcription factor CREB. This activation of cellular signaling was dependent on the presence of extracellular calcium but not extracellular sodium. This evidence does not support the hypothesis that sodium-dependent

phosphate uptake is critical for the observed effect. Similar effects were observed for pyrophosphate treatment, except lower concentrations of pyrophosphate were required (500 μM). Since the induction of cell signaling by pyrophosphate also required extracellular calcium, we hypothesized that these two ions affected cells by a common mechanism. Indeed, we found that the concentrations of phosphate or pyrophosphate that produced a cellular response were consistently also concentrations that resulted in precipitate formation in a calcium-dependent manner. Agents that prevented precipitate formation also prevented activation of cell signaling by either phosphate or pyrophosphate. These findings were also extended to the induction of the phosphate-responsive gene osteopontin. Experimental conditions that prevented precipitate formation also blocked the induction of osteopontin gene expression by either agent.

These findings may be generalized to certain other ionic precipitates, since we found that oxalate treatment also activated similar cell signaling pathways and induced osteopontin expression. This led us to speculate on the mechanism by which chemically diverse particles or precipitates might provoke cellular responses. Studies of the interactions of cells with other such particles, such as asbestos, suggest that production of reactive oxygen species (ROS) could be a necessary intermediate event after cells are initially contacted by particles. We found that phosphate, like hydrogen peroxide treatment, activated the scaffolding protein FRS2α in the absence of natural FGF ligands, a result that has been independently verified (Yamazaki et al., 2010). Direct measurement of ROS also suggested that phosphate treatment increases cellular ROS. Recent research has shown that ROS are necessary for normal FGF signaling and that excessive ROS can lead to FGF signaling in the absence of native FGF ligands (Rhee, 2006). Collectively, our data concerning ROS support a model in which particle interactions with cells produce ROS, which in turn lead to activation of FGF receptor tyrosine kinase activity and

subsequent cell signaling, including activation of FRS2α and ERK1/2. This hypothesis was supported by the additional finding that co-treatment with a receptor-tyrosine kinase inhibitor prevented the activation of cellular signaling by phosphate treatment. It is not clear at this time why particles may result in increased cellular ROS, regardless of the exact chemical nature of the particles.

Lastly, we examined the effects of high dietary phosphate on wild-type mice with initially normal kidney function. Feeding adult mice with a high phosphate diet for 12 weeks resulted in elevated blood FGF23, elevated urine phosphate and a trend toward elevated serum phosphate, though this last change was not statistically significant. Unexpectedly, we found that mice receiving the high phosphate diet developed tubulointerstitial fibrosis in their kidneys. Analysis of gene expression showed that potential markers of fibrosis, such as TGFβ1 and collagen-1α, were also elevated. These results demonstrate the potentially harmful effects of excessive dietary phosphate, even in animals with initially normal kidney function. In a second dietary experiment, we fed wild-type adult mice a high phosphate diet for 6 weeks. At the end of the experimental feeding period, mice on high phosphate diet weighed significantly less than mice on control diet and expressed three-fold greater osteopontin in their kidneys. These differences arose despite no differences in serum calcium or phosphate between the two groups at the end of the experiment. This result suggests that measurements of serum calcium or phosphate alone may not accurately convey the true burden of an excess of either of these ions, and the effects that such excess may have. We performed cell culture experiments on kidney cells and endothelial cells to evaluate whether treating cells directly with phosphate could replicate some of the pathological effects of the high phosphate diet. We found that kidney cells treated with high phosphate increased their expression of α-SMA and collagen-1α, which match

the changes observed *in vivo*. We also found that viability of endothelial cells was adversely affected by treatment with calcium phosphate particles and that cells expressed more of the cytokine MCP-1 after such treatment.

The research presented here supports the notion of 'phosphotoxicity', in which failure to manage and dispose of excess phosphate leads to pathological changes in cells and tissues which encompass more than macroscopically or radiologically observable tissue calcifications. Our *in vitro* studies suggest that the agent responsible for these effects is not the phosphate ion *per se* but calcium phosphate precipitates. An *in vivo* equivalent of these precipitates may be calciprotein particles, which have recently received more attention as potential pathological substances (see below). Future research should seek to confirm the existence and effects of such particles, and to develop ways to prevent them from developing or reduce the harm they may cause.

6.3 Calciprotein Particles as Indicators of Disease Burden

Although human serum contains concentrations of calcium and phosphate that approach their mutual solubility limit, incompletely understood mechanisms appear to maintain the solubility of these ions even when the phosphate concentration rises above normal. The high protein content of serum likely plays a major role in preventing the precipitation of inorganic ions, either by sequestering the ions or by preventing ionic crystals from growing after they have formed. Two serum proteins that are probably major contributors to this inhibitory activity are the abundant liver-derived proteins albumin and fetuin-A (Herrmann et al., 2012a). Fetuin-A is a serum glycoprotein with multiple phosphorylation sites and is enriched in bone tissue where it strongly binds to mineral. Several lines of evidence indicate that fetuin-A also binds mineral precipitates that may form in the serum and help prevent pathological calcification. When

expression of fetuin-A was eliminated in mice of the calcification-prone DBA/2 background, severe ectopic calcifications formed in soft tissues including the kidney and vascular tissues (Schäfer et al., 2003). This result is in agreement with the growing consensus that protein inhibitors are necessary to prevent ectopic mineralization even when serum mineral ion concentrations are normal (Murshed et al., 2004; Murshed et al., 2005).

A second piece of evidence suggesting fetuin-A inhibits mineral growth is that it can be found in calciprotein particles (CPPs) isolated from blood. These small (200 nm diameter) particles typically contain calcium, phosphate and proteins such as fetuin-A, and have been alternatively named fetuin-mineral complexes. In a rat model of adenine-induced renal failure, CPPs could be isolated from the blood of rats with compromised renal function but not from the blood of healthy controls (Matsui et al., 2009). The serum amount of fetuin-A was lower in the adenine-treated rats, but CPPs were found to contain abundant fetuin-A. A proposed explanation for these findings is that phosphate is not sufficiently cleared in animals with renal failure, leading to phosphate accumulation in blood. As the concentration of this ion rises, precipitation with calcium begins to occur but is slowed by the binding of fetuin-A and other serum proteins. The presence of CPPs in blood therefore serves as an indicator of an excessive phosphate load.

In accordance with this model, several clinical studies have found a negative relationship between serum fetuin-A levels and adverse clinical outcomes such as cardiovascular mortality (Ketteler et al., 2003; Stenvinkel et al., 2005; Wang et al., 2005). This is presumably because free serum fetuin-A is consumed in the process of CPP formation when serum is near saturation for calcium and phosphate. Hamano et al. found further clinical evidence to support this idea by studying serum concentrations of fetuin-A in patients with diabetes or chronic kidney disease (Hamano et al., 2010). Importantly, the authors centrifuged the serum samples and found pellets

only in the samples from chronic kidney disease and not healthy controls. These pellets contained fetuin-A, and measurement of serum fetuin-A could therefore be subdivided into supernatant and pellet fractions of fetuin-A. After centrifugation, the supernatant concentration of fetuin-A was lower than the total serum concentration of fetuin-A before centrifugation. This suggests that a substantial fraction of total fetuin-A is in CPPs, which were separated from total serum by the centrifugation process. This separation did not occur in the serum from healthy subjects. This was an important refinement of fetuin-A measurement because it more accurately reflects the amount of free fetuin-A in serum, which correlates negatively with morbidity. Disease burden was also correlated with the capacity of serum to prevent CPP formation. Pasch et al. obtained serum samples from normal subjects, chronic kidney disease patients and from mice deficient in fetuin-A and used an *in vitro* assay to evaluate the propensity of each to form CPPs after adding excess calcium and phosphate (Pasch et al., 2012). The authors found that serum from the latter two groups formed CPPs more quickly than serum form the normal controls. These results suggest that the serum from patients with reduced kidney function has a lower capacity to inhibit calcification or CPP formation, possibly because this capacity has already been used over the progression of chronic kidney disease.

6.4 Outlook and Future Studies

The discovery of CPPs in serum of patients with chronic kidney disease may reflect the findings we have obtained using *in vitro* experiments. It appears that high extracellular phosphate affects cell behavior by first forming insoluble particles containing calcium, phosphate and potentially proteins present in the cell media, which then interact with cells. Similarly, in patients experiencing hyperphosphatemia due to compromised renal function, CPPs may form as a defensive measure to prevent the accumulation of large particles composed of inorganic ions.

These CPPs may then interact with cells and tissues and affect their behavior. Indeed, we found that synthetic CPPs adversely affected the viability of cultured endothelial cells (Figures 5-8, 5-9 and 5-10). It remains to be determined of CPPs formed *in vivo* can also have these deleterious effects if they accumulate and interact with cells. More studies must be performed to understand how and when these CPPs are formed *in vivo*. Herrmann et al. have presented evidence that CPPs can be cleared by liver macrophages in a scavenger receptor-A dependent manner (Herrman et al., 2012b). With improved detection methods, measurement of CPPs may in the future have prognostic and diagnostic value when evaluating patients with compromised renal function (Pasch et al., 2012). If it is determined that a patient's serum is at particular risk for CPP formation and calcification, a special effort may be used to control the intake of phosphate.

We began our studies with the aim of gaining a more detailed understanding of how hyperphosphatemia causes diverse pathological effects. Our findings suggest that phosphate becomes dangerous after forming insoluble particles with calcium and proteins. These can take the form of large-scale tissue calcifications or as much smaller CPPs in blood. The task for future investigations is to determine ways to aid the clearance of these particles and prevent mineral deposition in tissues and the attendant adverse effects for the patient.

Bibliography

Addison, W.N., F. Azari, E.S. Sorensen, M.T. Kaartinen, and M.D. McKee. 2007. Pyrophosphate inhibits mineralization of osteoblast cultures by binding to mineral, up-regulating osteopontin, and inhibiting alkaline phosphatase activity. *The Journal of Biological Chemistry*. 282:15872-15883.

Adeney, K.L., D.S. Siscovick, J.H. Ix, S.L. Seliger, M.G. Shlipak, N.S. Jenny, and B.R. Kestenbaum. 2009. Association of serum phosphate with vascular and valvular calcification in moderate CKD. *Journal of the American Society of Nephrology : JASN*. 20:381-387.

Aihara, K., K.J. Byer, and S.R. Khan. 2003. Calcium phosphate-induced renal epithelial injury and stone formation: Involvement of reactive oxygen species. *Kidney International*. 64:1283-1291.

Anderson, H.C. 2007. The role of matrix vesicles in physiological and pathological calcification. *Current Opinion in Orthopaedics*. 18:428-433.

Aslan, D., M.D. Andersen, L.B. Gede, T.K. de Franca, S.R. Jorgensen, P. Schwarz, and N.R. Jorgensen. 2012. Mechanisms for the bone anabolic effect of parathyroid hormone treatment in humans. *Scandinavian Journal of Clinical and Laboratory Investigation*. 72:14-22.

Beck, G.R., Jr., and N. Knecht. 2003. Osteopontin regulation by inorganic phosphate is ERK1/2-, protein kinase C-, and proteasome-dependent. *The Journal of Biological Chemistry*. 278:41921-41929.

Beck, G.R., Jr., B. Zerler, and E. Moran. 2000. Phosphate is a specific signal for induction of osteopontin gene expression. *Proceedings of the National Academy of Sciences of the United States of America*. 97:8352-8357.

Beck Jr, G.R., E.C. Sullivan, E. Moran, and B. Zerler. 1998. Relationship between alkaline phosphatase levels, osteopontin expression, and mineralization in differentiating MC3T3-E1 osteoblasts. *Journal of Cellular Biochemistry*. 68:269-280.

Bergwitz, C., and H. Jüppner. 2011. Phosphate Sensing. *Advances in Chronic Kidney Disease*. 18:132-144.

Berndt, T., and R. Kumar. 2007. Phosphatonins and the regulation of phosphate homeostasis. *Annual Review of Physiology*. 69:341-359.

Boskey, A.L., M. Maresca, W. Ullrich, S.B. Doty, W.T. Butler, and C.W. Prince. 1993. Osteopontin-hydroxyapatite interactions in vitro: Inhibition of hydroxyapatite formation and growth in a gelatin-gel. *Bone and Mineral*. 22:147-159.

Boskey, A.L., and R. Roy. 2008. Cell culture systems for studies of bone and tooth mineralization. *Chemical Reviews*. 108:4716-4733.

Boskey, A.L., L. Spevak, E. Paschalis, S.B. Doty, and M.D. McKee. 2002. Osteopontin deficiency increases mineral content and mineral crystallinity in mouse bone. *Calcified Tissue International*. 71:145-154.

Bringhurst, R.F., Demay, M.B. and H.M. Kronenberg. 2011. "Hormones and Disorders of Mineral Metabolism." Chap. 28 In Williams Textbook of Endocrinology, 12th Edition, edited by Kenneth S. Polonsky Shlomo Melmed, P. Reed Larsen, Henry M. Kronenberg, 1237-304: Elsevier.

Brownstein, C.A., F. Adler, C. Nelson-Williams, J. Iijima, P. Li, A. Imura, Y.-i. Nabeshima, M. Reyes-Mugica, T.O. Carpenter, and R.P. Lifton. 2008. A translocation causing increased α-Klotho level results in hypophosphatemic rickets and hyperparathyroidism. *Proceedings of the National Academy of Sciences of the United States of America*. 105:3455-3460.

Buder-Hoffmann, S.A., A. Shukla, T.F. Barrett, M.B. MacPherson, K.M. Lounsbury, and B.T. Mossman. 2009. A protein kinase Cdelta-dependent protein kinase D pathway modulates ERK1/2 and JNK1/2 phosphorylation and Bim-associated apoptosis by asbestos. *The American Journal of Pathology*. 174:449-459.

Cai, Q., S.F. Hodgson, P.C. Kao, V.A. Lennon, G.G. Klee, A.R. Zinsmiester, and R. Kumar. 1994. Inhibition of Renal Phosphate Transport by a Tumor Product in a Patient with Oncogenic Osteomalacia. *New England Journal of Medicine*. 330:1645-1649.

Carpenter, G. 1999. Employment of the epidermal growth factor receptor in growth factor-independent signaling pathways. *Journal of Cell Biology*. 146:697-702.

Cha, S.-K., B. Ortega, H. Kurosu, K.P. Rosenblatt, M. Kuro-o, and C.-L. Huang. 2008. Removal of sialic acid involving Klotho causes cell-surface retention of TRPV5 channel via binding to galectin-1. *Proceedings of the National Academy of Sciences of the United States of America*. 105:9805-9810.

Chaturvedi, L.S., S. Koul, A. Sekhon, A. Bhandari, M. Menon, and H.K. Koul. 2002. Oxalate selectively activates p38 mitogen-activated protein kinase and c-Jun N-terminal kinase signal transduction pathways in renal epithelial cells. *The Journal of Biological Chemistry*. 277:13321-13330.

Chefetz, I., R. Heller, A. Galli-Tsinopoulou, G. Richard, B. Wollnik, M. Indelman, F. Koerber, O. Topaz, R. Bergman, E. Sprecher, and E. Schoenau. 2005. A novel homozygous missense mutation in FGF23 causes Familial Tumoral Calcinosis associated with disseminated visceral calcification. *Human Genetics*. 118:261-266.

Chen, Z., T.B. Gibson, F. Robinson, L. Silvestro, G. Pearson, B.-e. Xu, A. Wright, C. Vanderbilt, and M.H. Cobb. 2001. MAP Kinases. *Chemical Reviews*. 101:2449-2476.

Cheung, H.S., J.D. Sallis, and J.A. Struve. 1996. Specific inhibition of basic calcium phosphate and calcium pyrophosphate crystal-induction of metalloproteinase synthesis by phosphocitrate. *Biochimica et Biophysica Acta - Molecular Basis of Disease*. 1315:105-111.

Chung, C.H., E.E. Golub, E. Forbes, T. Tokuoka, and I.M. Shapiro. 1992. Mechanism of action of β-glycerophosphate on bone cell mineralization. *Calcified Tissue International*. 51:305-311.

Datto, M.B., Y. Li, J.F. Panus, D.J. Howe, Y. Xiong, and X.F. Wang. 1995. Transforming growth factor β induces the cyclin-dependent kinase inhibitor p21 through a p53-independent mechanism. *Proceedings of the National Academy of Sciences of the United States of America*. 92:5545-5549.

Econs, M.J., and M.K. Drezner. 1994. Tumor-Induced Osteomalacia -- Unveiling a New Hormone. *New England Journal of Medicine*. 330:1679-1681.

Econs, M.J., P.T. McEnery, F. Lennon, and M.C. Speer. 1997. Autosomal dominant hypophosphatemic rickets is linked to chromosome 12p13. *Journal of Clinical Investigation*. 100:2653-2657.

El-Abbadi, M.M., A.S. Pai, E.M. Leaf, H.Y. Yang, B.A. Bartley, K.K. Quan, C.M. Ingalls, H.W. Liao, and C.M. Giachelli. 2009. Phosphate feeding induces arterial medial calcification in uremic mice: role of serum phosphorus, fibroblast growth factor-23, and osteopontin. *Kidney International*. 75:1297-1307.

Eller, P., K. Eller, A.H. Kirsch, J.J. Patsch, A.M. Wolf, A. Tagwerker, U. Stanzl, R. Kaindl, V. Kahlenberg, G. Mayer, J.R. Patsch, and A.R. Rosenkranz. 2011. A murine model of phosphate nephropathy. *The American Journal of Pathology*. 178:1999-2006.

El-Maadawy, S., M.T. Kaartinen, T. Schinke, M. Murshed, G. Karsenty, and M.D. McKee. 2003. Cartilage Formation and Calcification in Arteries of Mice Lacking Matrix Gla Protein. *Connective Tissue Research.* 44:272-278.

Erb, T.J., P. Kiefer, B. Hattendorf, D. Günther, and J.A. Vorholt. 2012. GFAJ-1 Is an Arsenate-Resistant, Phosphate-Dependent Organism. *Science*. 337:467-470.

Farrow, E.G., and K.E. White. 2010. Recent advances in renal phosphate handling. *Nature Reviews Nephrology*. 6:207-217.

Fedarko, N.S., A. Jain, A. Karadag, M.R. Van Eman, and L.W. Fisher. 2001. Elevated serum bone sialoprotein and osteopontin in colon, breast, prostate, and lung cancer. *Clinical Cancer Research*. 7:4060-4066.

Fleisch, H.A., R.G. Russell, S. Bisaz, R.C. Mühlbauer, and D.A. Williams. 1970. The inhibitory

effect of phosphonates on the formation of calcium phosphate crystals in vitro and on aortic and kidney calcification in vivo. *European Journal of Clinical Investigation*. 1:12-18.

Fubini, B., and A. Hubbard. 2003. Reactive oxygen species (ROS) and reactive nitrogen species (RNS) generation by silica in inflammation and fibrosis. *Free Radical Biology and Medicine*. 34:1507-1516.

George, A., and A. Veis. 2008. Phosphorylated proteins and control over apatite nucleation, crystal growth, and inhibition. *Chemical Reviews*. 108:4670-4693.

Giachelli, C.M. 2009. The emerging role of phosphate in vascular calcification. *Kidney International*. 75:890-897.

Goetz, R., A. Beenken, O.A. Ibrahimi, J. Kalinina, S.K. Olsen, A.V. Eliseenkova, C. Xu, T.A. Neubert, F. Zhang, R.J. Linhardt, X. Yu, K.E. White, T. Inagaki, S.A. Kliewer, M. Yamamoto, H. Kurosu, Y. Ogawa, M. Kuro-o, B. Lanske, M.S. Razzaque, and M. Mohammadi. 2007. Molecular insights into the klotho-dependent, endocrine mode of action of fibroblast growth factor 19 subfamily members. *Molecular and Cellular Biology*. 27:3417-3428.

Golub, E.E., and K. Boesze-Battaglia. 2007. The role of alkaline phosphatase in mineralization. *Current Opinion in Orthopaedics*. 18:444-448.

Goodman, W.G., and L.D. Quarles. 2008. Development and progression of secondary hyperparathyroidism in chronic kidney disease: lessons from molecular genetics. *Kidney International*. 74:276-288.

Hamano, T., I. Matsui, S. Mikami, K. Tomida, N. Fujii, E. Imai, H. Rakugi, and Y. Isaka. 2010. Fetuin-mineral complex reflects extraosseous calcification stress in CKD. *Journal of the American Society of Nephrology : JASN*. 21:1998-2007.

Herrmann, M., A. Kinkeldey, and W. Jahnen-Dechent. 2012a. Fetuin-A Function in Systemic Mineral Metabolism. *Trends in Cardiovascular Medicine*. 22:197-201.

Herrmann, M., C. Schafer, A. Heiss, S. Graber, A. Kinkeldey, A. Buscher, M.M. Schmitt, J. Bornemann, F. Nimmerjahn, M. Herrmann, L. Helming, S. Gordon, and W. Jahnen-Dechent. 2012b. Clearance of fetuin-A--containing calciprotein particles is mediated by scavenger receptor-A. *Circulation Research*. 111:575-584.

Ho, A.M. 2000. Role of the Mouse ank Gene in Control of Tissue Calcification and Arthritis. *Science*. 289:265-270.

Hofer, A.M., and E.M. Brown. 2003. Extracellular calcium sensing and signalling. *Nature Reviews Molecular Cell Biology*. 4:530-538.

Hruska, K., S. Mathew, R. Lund, Y. Fang, and T. Sugatani. 2011. Cardiovascular risk factors in chronic kidney disease: does phosphate qualify? *Kidney International Supplement*:S9-13.

Hruska, K.A., S. Mathew, R. Lund, P. Qiu, and R. Pratt. 2008. Hyperphosphatemia of chronic kidney disease. *Kidney International*. 74:148-157.

Hsieh, Y.J., and B.L. Wanner. 2010. Global regulation by the seven-component Pi signaling system. *Current Opinion in Microbiology*. 13:198-203.

Hu, M.C., M. Shi, J. Zhang, J. Pastor, T. Nakatani, B. Lanske, M.S. Razzaque, K.P. Rosenblatt, M.G. Baum, M. Kuro-o, and O.W. Moe. 2010. Klotho: a novel phosphaturic substance acting as an autocrine enzyme in the renal proximal tubule. *FASEB Journal : Official publication of the Federation of American Societies for Experimental Biology*. 24:3438-3450.

Hunter, G.K., C.L. Kyle, and H.A. Goldberg. 1994. Modulation of crystal formation by bone phosphoproteins: Structural specificity of the osteopontin-mediated inhibition of hydroxyapatite formation. *Biochemical Journal*. 300:723-728.

Hutchison, A.J. 2009. Oral phosphate binders. *Kidney International*. 75:906-914.

Imura, A., A. Iwano, O. Tohyama, Y. Tsuji, K. Nozaki, N. Hashimoto, T. Fujimori, and Y.I. Nabeshima. 2004. Secreted Klotho protein in sera and CSF: Implication for post-translational cleavage in release of Klotho protein from cell membrane. *FEBS Letters*. 565:143-147.

Jono, S., M.D. McKee, C.E. Murry, A. Shioi, Y. Nishizawa, K. Mori, H. Morii, and C.M. Giachelli. 2000. Phosphate Regulation of Vascular Smooth Muscle Cell Calcification. *Circulation Research*. 87:e10-e17.

KDIGO Working Group. 2009. KDIGO clinical practice guidelines for the prevention, diagnosis, evaluation, and treatment of Chronic Kidney Disease-Mineral and Bone Disorder (CKD-MBD). *Kidney International Supplement*:S1-130.

Ketteler, M., P. Bongartz, R. Westenfeld, J.E. Wildberger, A.H. Mahnken, R. Böhm, T. Metzger, C. Wanner, W. Jahnen-Dechent, and J. Floege. 2003. Association of low fetuin-A (AHSG) concentrations in serum with cardiovascular mortality in patients on dialysis: A cross-sectional study. *Lancet*. 361:827-833.

Khan, S.R. 2004. Crystal-induced inflammation of the kidneys: results from human studies, animal models, and tissue-culture studies. *Clinical and Experimental Nephrology*. 8:75-88.

Kiela, P.R., and F.K. Ghishan. 2009. Recent advances in the renal-skeletal-gut axis that controls phosphate homeostasis. *Laboratory Investigation: a journal of technical methods and pathology*. 89:7-14.

Kleinman, J.G., J.A. Wesson, and J. Hughes. 2004. Osteopontin and calcium stone formation. *Nephron Physiology*. 98:p43-47.

Knebel, A., H.J. Rahmsdorf, A. Ullrich, and P. Herrlich. 1996. Dephosphorylation of receptor tyrosine kinases as target of regulation by radiation, oxidants or alkylating agents. *EMBO Journal*. 15:5314-5325.

Koul, H.K., M. Menon, L.S. Chaturvedi, S. Koul, A. Sekhon, A. Bhandari, and M. Huang. 2002. COM crystals activate the p38 mitogen-activated protein kinase signal transduction pathway in renal epithelial cells. *The Journal of Biological Chemistry*. 277:36845-36852.

Kuro-o, M., Y. Matsumura, H. Aizawa, H. Kawaguchi, T. Suga, T. Utsugi, Y. Ohyama, M. Kurabayashi, T. Kaname, E. Kume, H. Iwasaki, A. Iida, T. Shiraki-Iida, S. Nishikawa, R. Nagai, and Y.I. Nabeshima. 1997. Mutation of the mouse klotho gene leads to a syndrome resembling ageing. *Nature*. 390:45-51.

Kurosu, H., Y. Ogawa, M. Miyoshi, M. Yamamoto, A. Nandi, K.P. Rosenblatt, M.G. Baum, S. Schiavi, M.C. Hu, O.W. Moe, and M. Kuro-o. 2006. Regulation of fibroblast growth factor-23 signaling by klotho. *The Journal of Biological Chemistry*. 281:6120-6123.

Larsson, T., X. Yu, S.I. Davis, M.S. Draman, S.D. Mooney, M.J. Cullen, and K.E. White. 2005. Rapid communication: A novel recessive mutation in fibroblast growth factor-23 causes familial tumoral calcinosis. *Journal of Clinical Endocrinology and Metabolism*. 90:2424-2427.

Lau, W.L., A. Pai, S.M. Moe, and C.M. Giachelli. 2011. Direct effects of phosphate on vascular cell function. *Advances in Chronic Kidney Disease*. 18:105-112.

Lee, Y.S., K. Huang, F.A. Quiocho, and E.K. O'Shea. 2008. Molecular basis of cyclin-CDK-CKI regulation by reversible binding of an inositol pyrophosphate. *Nature Chemical Biology*. 4:25-32.

Lee, Y.S., S. Mulugu, J.D. York, and E.K. O'Shea. 2007. Regulation of a cyclin-CDK-CDK inhibitor complex by inositol pyrophosphates. *Science*. 316:109-112.

Lemmon, M.A., and J. Schlessinger. 2010. Cell signaling by receptor tyrosine kinases. *Cell*. 141:1117-1134.

Lieske, J.C., M.S. Hammes, J.R. Hoyer, and F.G. Toback. 1997. Renal cell osteopontin production is stimulated by calcium oxalate monohydrate crystals. *Kidney International*. 51:679-686.

Lieske, J.C., H. Swift, T. Martin, B. Patterson, and F.G. Toback. 1994. Renal epithelial cells rapidly bind and internalize calcium oxalate monohydrate crystals. *Proceedings of the National Academy of Sciences of the United States of America*. 91:6987-6991.

Liu, G., P. Cheresh, and D.W. Kamp. 2013. Molecular basis of asbestos-induced lung disease. *Annual Review of Pathology*. 8:161-187.

Liu, S., W. Tang, J. Zhou, J.R. Stubbs, Q. Luo, M. Pi, and L.D. Quarles. 2006. Fibroblast growth factor 23 is a counter-regulatory phosphaturic hormone for vitamin D. *Journal of the American Society of Nephrology : JASN*. 17:1305-1315.

Liu, S., L. Vierthaler, W. Tang, J. Zhou, and L.D. Quarles. 2008. FGFR3 and FGFR4 do not mediate renal effects of FGF23. *Journal of the American Society of Nephrology : JASN*. 19:2342-2350.

Luo, G., P. Ducy, M.D. McKee, G.J. Pinero, E. Loyer, R.R. Behringer, and G. Karsenty. 1997. Spontaneous calcification of arteries and cartilage in mice lacking matrix GLA protien. *Nature*. 386:78-81.

Martin, A., V. David, and L. Darryl Quarles. 2012. Regulation and function of the FGF23/klotho endocrine pathways. *Physiological Reviews*. 92:131-155.

Martínez, V.G., S.K. Moestrup, U. Holmskov, J. Mollenhauer, and F. Lozano. 2011. The conserved scavenger receptor cysteine-rich superfamily in therapy and diagnosis. *Pharmacological Reviews*. 63:967-1000.

Matsui, I., T. Hamano, S. Mikami, N. Fujii, Y. Takabatake, Y. Nagasawa, N. Kawada, T. Ito, H. Rakugi, E. Imai, and Y. Isaka. 2009. Fully phosphorylated fetuin-A forms a mineral complex in the serum of rats with adenine-induced renal failure. *Kidney International*. 75:915-928.

Matsumura, Y., H. Aizawa, T. Shiraki-Iida, R. Nagai, M. Kuro-o, and Y.I. Nabeshima. 1998. Identification of the human klotho gene and its two transcripts encoding membrane and secreted klotho protein. *Biochemical and Biophysical Research Communications*. 242:626-630.

McCarthy, G.M., J.A. Augustine, A.S. Baldwin, P.A. Christopherson, H.S. Cheung, P.R. Westfall, and R.I. Scheinman. 1998. Molecular mechanism of basic calcium phosphate crystal-induced activation of human fibroblasts: Role of nuclear factor κB, activator protein 1, and protein kinase C. *Journal of Biological Chemistry*. 273:35161-35169.

McCarthy, G.M., and H.S. Cheung. 2009. Point: Hydroxyapatite crystal deposition is intimately involved in the pathogenesis and progression of human osteoarthritis. *Current Rheumatology Reports*. 11:141-147.

McKee, M.D., and A. Nanci. 1995. Osteopontin at mineralized tissue interfaces in bone, teeth, and osseointegrated implants: Ultrastructural distribution and implications for mineralized tissue formation, turnover, and repair. *Microscopy Research and Technique*. 33:141-164.

Meng, T.C., T. Fukada, and N.K. Tonks. 2002. Reversible oxidation and inactivation of protein tyrosine phosphatases in vivo. *Molecular Cell*. 9:387-399.

Miyauchi, A., M. Fukase, M. Tsutsumi, and T. Fujita. 1988. Hemangiopericytoma-induced osteomalacia: Tumor transplantation in nude mice causes hypophosphatemia and tumor extracts inhibit renal 25-hydroxyvitamin D 1-hydroxylase activity. *Journal of Clinical Endocrinology and Metabolism*. 67:46-53.

Mizobuchi, M., D. Towler, and E. Slatopolsky. 2009. Vascular calcification: the killer of patients with chronic kidney disease. *Journal of the American Society of Nephrology : JASN*. 20:1453-1464.

Moe, S.M. and S.M. Sprague. 2012. "Chronic Kidney Disease-Mineral Bone Disorder." Chap. 54 In Brenner & Rector's the Kidney, 9th Edition, edited by Glenn M. Chertow Maarten W. Taal, Philip A. Marsden, Karl Skorecki, Alan S. Yu, Barry M. Brenner 2021-58: Elsevier.

Morishita, K., A. Shirai, M. Kubota, Y. Katakura, Y.I. Nabeshima, K. Takeshige, and T. Kamiya. 2001. The progression of aging in klotho mutant mice can be modified by dietary phosphorus and zinc. *Journal of Nutrition*. 131:3182-3188.

Muller, F., N.J. Mutch, W.A. Schenk, S.A. Smith, L. Esterl, H.M. Spronk, S. Schmidbauer, W.A. Gahl, J.H. Morrissey, and T. Renne. 2009. Platelet polyphosphates are proinflammatory and procoagulant mediators in vivo. *Cell*. 139:1143-1156.

Murshed, M., D. Harmey, J.L. Millan, M.D. McKee, and G. Karsenty. 2005. Unique coexpression in osteoblasts of broadly expressed genes accounts for the spatial restriction of ECM mineralization to bone. *Genes & Development*. 19:1093-1104.

Murshed, M., T. Schinke, M.D. McKee, and G. Karsenty. 2004. Extracellular matrix mineralization is regulated locally; different roles of two Gla-containing proteins. *The Journal of Cell Biology*. 165:625-630.

Nair, D., R.P. Misra, J.D. Sallis, and H.S. Cheung. 1997. Phosphocitrate inhibits a basic calcium phosphate and calcium pyrophosphate dihydrate crystal-induced mitogen-activated protein kinase cascade signal transduction pathway. *Journal of Biological Chemistry*. 272:18920-18925.

Nelson, D.L. and M.M. Cox. 2008. Lehninger Principles of Biochemistry. 5 ed.: W. H. Freeman and Company.

Orr, A.W., B.P. Helmke, B.R. Blackman, and M.A. Schwartz. 2006. Mechanisms of mechanotransduction. *Developmental Cell*. 10:11-20.

Palmer, S.C., A. Hayen, P. Macaskill, F. Pellegrini, J.C. Craig, G.J. Elder, and G.F.M. Strippoli.

2011. Serum levels of phosphorus, parathyroid hormone, and calcium and risks of death and cardiovascular disease in individuals with chronic kidney disease a systematic review and meta-analysis. *JAMA - Journal of the American Medical Association*. 305:1119-1127.

Pasch, A., S. Farese, S. Graber, J. Wald, W. Richtering, J. Floege, and W. Jahnen-Dechent. 2012. Nanoparticle-based test measures overall propensity for calcification in serum. *Journal of the American Society of Nephrology : JASN*. 23:1744-1752.

Pin, J.-P., T. Galvez, and L. Prézeau. 2003. Evolution, structure, and activation mechanism of family 3/C G-protein-coupled receptors. *Pharmacology & Therapeutics*. 98:325-354.

Pritzker, K.P.H. 2009. Counterpoint: Hydroxyapatite crystal deposition is not intimately involved in the pathogenesis and progression of human osteoarthritis. *Current Rheumatology Reports*. 11:148-153.

Reaves, M.L., S. Sinha, J.D. Rabinowitz, L. Kruglyak, and R.J. Redfield. 2012. Absence of Detectable Arsenate in DNA from Arsenate-Grown GFAJ-1 Cells. *Science*. 337:470-473.

Rhee, S.G. 2006. H_2O_2, a necessary evil for cell signaling. *Science*. 312:1882-1883.

Robinson, K.M., M.S. Janes, M. Pehar, J.S. Monette, M.F. Ross, T.M. Hagen, M.P. Murphy, and J.S. Beckman. 2006. Selective fluorescent imaging of superoxide in vivo using ethidium-based probes. *Proceedings of the National Academy of Sciences of the United States of America*. 103:15038-15043.

Sabbagh, Y., S.P. O'Brien, W. Song, J.H. Boulanger, A. Stockmann, C. Arbeeny, and S.C. Schiavi. 2009. Intestinal npt2b plays a major role in phosphate absorption and homeostasis. *Journal of the American Society of Nephrology : JASN*. 20:2348-2358.

Scatena, M., L. Liaw, and C.M. Giachelli. 2007. Osteopontin: a multifunctional molecule regulating chronic inflammation and vascular disease. *Arteriosclerosis, Thrombosis and Vascular Biology*. 27:2302-2309.

Schäfer, C., A. Heiss, A. Schwarz, R. Westenfeld, M. Ketteler, J. Floege, W. Müller-Esterl, T. Schinke, and W. Jahnen-Dechent. 2003. The serum protein α2–Heremans-Schmid glycoprotein/fetuin-A is a systemically acting inhibitor of ectopic calcification. *Journal of Clinical Investigation*. 112:357-366.

Schepers, M.S.J., E.S. Van Ballegooijen, C.H. Bangma, and C.F. Verkoelen. 2005. Oxalate is toxic to renal tubular cells only at supraphysiologic concentrations. *Kidney International*. 68:1660-1669.

Shanahan, C.M., M.H. Crouthamel, A. Kapustin, and C.M. Giachelli. 2011. Arterial calcification in chronic kidney disease: key roles for calcium and phosphate. *Circulation Research*. 109:697-711.

Sheng, X., M.D. Ward, and J.A. Wesson. 2005. Crystal surface adhesion explains the pathological activity of calcium oxalate hydrates in kidney stone formation. *Journal of the American Society of Nephrology : JASN*. 16:1904-1908.

Shimada, T., M. Kakitani, Y. Yamazaki, H. Hasegawa, Y. Takeuchi, T. Fujita, S. Fukumoto, K. Tomizuka, and T. Yamashita. 2004. Targeted ablation of Fgf23 demonstrates an essential physiological role of FGF23 in phosphate and vitamin D metabolism. *Journal of Clinical Investigation*. 113:561-568.

Shimada, T., S. Mizutani, T. Muto, T. Yoneya, R. Hino, S. Takeda, Y. Takeuchi, T. Fujita, S. Fukumoto, and T. Yamashita. 2001. Cloning and characterization of FGF23 as a causative factor of tumor-induced osteomalacia. *Proceedings of the National Academy of Sciences of the United States of America*. 98:6500-6505.

Sitara, D., M.S. Razzaque, M. Hesse, S. Yoganathan, T. Taguchi, R.G. Erben, H. Juppner, and B. Lanske. 2004. Homozygous ablation of fibroblast growth factor-23 results in hyperphosphatemia and impaired skeletogenesis, and reverses hypophosphatemia in Phex-deficient mice. *Matrix Biology : Journal of the International Society for Matrix Biology*. 23:421-432.

Speer, M.Y., H.Y. Yang, T. Brabb, E. Leaf, A. Look, W.L. Lin, A. Frutkin, D. Dichek, and C.M. Giachelli. 2009. Smooth muscle cells give rise to osteochondrogenic precursors and chondrocytes in calcifying arteries. *Circulation Research*. 104:733-741.

Steitz, S.A., M.Y. Speer, G. Curinga, H.Y. Yang, P. Haynes, R. Aebersold, T. Schinke, G. Karsenty, and C.M. Giachelli. 2001. Smooth Muscle Cell Phenotypic Transition Associated With Calcification: Upregulation of Cbfa1 and Downregulation of Smooth Muscle Lineage Markers. *Circulation Research*. 89:1147-1154.

Stenvinkel, P., K. Wang, A.R. Qureshi, J. Axelsson, R. Pecoits-Filho, P. Gao, P. Barany, B. Lindholm, T. Jogestrand, O. Heimbürger, C. Holmes, M. Schalling, and L. Nordfors. 2005. Low fetuin-A levels are associated with cardiovascular death: Impact of variations in the gene encoding fetuin. *Kidney International*. 67:2383-2392.

Stubbs, J.R., S. Liu, W. Tang, J. Zhou, Y. Wang, X. Yao, and L.D. Quarles. 2007. Role of hyperphosphatemia and 1,25-dihydroxyvitamin D in vascular calcification and mortality in fibroblastic growth factor 23 null mice. *Journal of the American Society of Nephrology: JASN*. 18:2116-2124.

Sundaresan, M., Z.X. Yu, V.J. Ferrans, K. Irani, and T. Finkel. 1995. Requirement for generation of H_2O_2 for platelet-derived growth factor signal transduction. *Science*. 270:296-299.

Szczepanska-Konkel, M., A.N.K. Yusufi, M. VanScoy, S.K. Webster, and T.P. Dousa. 1986. Phosphonocarboxylic acids as specific inhibitors of Na+-dependent transport of phosphate across renal brush border membrane. *Journal of Biological Chemistry*.

261:6375-6383.

Umekawa, T., K. Byer, H. Uemura, and S.R. Khan. 2005. Diphenyleneiodium (DPI) reduces oxalate ion- and calcium oxalate monohydrate and brushite crystal-induced upregulation of MCP-1 in NRK 52E cells. *Nephrology, Dialysis, Transplantation : Official Publication of the European Dialysis and Transplant Association - European Renal Association*. 20:870-878.

Umekawa, T., M. Iguchi, H. Uemura, and S.R. Khan. 2006. Oxalate ions and calcium oxalate crystal-induced up-regulation of osteopontin and monocyte chemoattractant protein-1 in renal fibroblasts. *BJU International*. 98:656-660.

Urakawa, I., Y. Yamazaki, T. Shimada, K. Iijima, H. Hasegawa, K. Okawa, T. Fujita, S. Fukumoto, and T. Yamashita. 2006. Klotho converts canonical FGF receptor into a specific receptor for FGF23. *Nature*. 444:770-774.

Van De Lest, C.H.A., and A.B. Vaandrager. 2007. Mechanism of cell-mediated mineralization. *Current Opinion in Orthopaedics*. 18:434-443.

Villa-Bellosta, R., and V. Sorribas. 2009. Phosphonoformic acid prevents vascular smooth muscle cell calcification by inhibiting calcium-phosphate deposition. *Arteriosclerosis, Thrombosis, and Vascular Biology*. 29:761-766.

Virkki, L.V., J. Biber, H. Murer, and I.C. Forster. 2007. Phosphate transporters: A tale of two solute carrier families. *American Journal of Physiology - Renal Physiology*. 293:F643-F654.

Wada, T., M.D. McKee, S. Steitz, and C.M. Giachelli. 1999. Calcification of Vascular Smooth Muscle Cell Cultures : Inhibition by Osteopontin. *Circulation Research*. 84:166-178.

Wang, A.Y.M., J. Woo, C.W.K. Lam, M. Wang, I.H.S. Chan, P. Gao, S.F. Lui, P.K.T. Li, and J.E. Sanderson. 2005. Associations of serum fetuin-A with malnutrition, inflammation, atherosclerosis and valvular calcification syndrome and outcome in peritoneal dialysis patients. *Nephrology Dialysis Transplantation*. 20:1676-1685.

Wesson, J.A. 2003. Osteopontin Is a Critical Inhibitor of Calcium Oxalate Crystal Formation and Retention in Renal Tubules. *Journal of the American Society of Nephrology*. 14:139-147.

Wesson, J.A., E.M. Worcester, J.H. Wiessner, N.S. Mandel, and J.G. Kleinman. 1998. Control of calcium oxalate crystal structure and cell adherence by urinary macromolecules. *Kidney International*. 53:952-957.

White, K.E., W.E. Evans, J.L.H. O'Riordan, M.C. Speer, M.J. Econs, B. Lorenz-Depiereux, M. Grabowski, T. Meitinger, and T.M. Strom. 2000. Autosomal dominant hypophosphataemic rickets is associated with mutations in FGF23. *Nature Genetics*. 26:345-348.

Williams, G., and J.D. Sallis. 1979. Structure--activity relationship of inhibitors of hydroxyapatite formation. *Biochemical Journal*. 184:181-184.

Wolfe-Simon, F., J.S. Blum, T.R. Kulp, G.W. Gordon, S.E. Hoeft, J. Pett-Ridge, J.F. Stolz, S.M. Webb, P.K. Weber, P.C.W. Davies, A.D. Anbar, and R.S. Oremland. 2011. A Bacterium That Can Grow by Using Arsenic Instead of Phosphorus. *Science*. 332:1163-1166.

Woo, H.A., S.H. Yim, D.H. Shin, D. Kang, D.Y. Yu, and S.G. Rhee. 2010. Inactivation of peroxiredoxin I by phosphorylation allows localized H_2O_2 accumulation for cell signaling. *Cell*. 140:517-528.

Wynn, T.A. 2007. Common and unique mechanisms regulate fibrosis in various fibroproliferative diseases. *The Journal of Clinical Investigation*. 117:524-529.

Yamazaki, M., K. Ozono, T. Okada, K. Tachikawa, H. Kondou, Y. Ohata, and T. Michigami. 2010. Both FGF23 and extracellular phosphate activate Raf/MEK/ERK pathway via FGF receptors in HEK293 cells. *Journal of Cellular Biochemistry*. 111:1210-1221.

Yang, X.C., and F. Sachs. 1989. Block of stretch-activated ion channels in Xenopus oocytes by gadolinium and calcium ions. *Science*. 243:1068-1071.

Yu, X., O.A. Ibrahimi, R. Goetz, F. Zhang, S.I. Davis, H.J. Garringer, R.J. Linhardt, D.M. Ornitz, M. Mohammadi, and K.E. White. 2005. Analysis of the biochemical mechanisms for the endocrine actions of fibroblast growth factor-23. *Endocrinology*. 146:4647-4656.